



UNIVERSITEIT VAN PRETORIA
UNIVERSITY OF PRETORIA
YUNIBESITHI YA PRETORIA

**INVESTIGATION INTO A SYSTEM THAT CAN DETECT
IMPROPER COMBUSTION IN A DIESEL ENGINE BEFORE
SIGNIFICANT DAMAGE CAN OCCUR**

by

Theo Lawrence Wilcocks

**Submitted in fulfilment of part of the requirements for the degree
of Master of Engineering
in the Faculty of Engineering and the Built Environment**

University of Pretoria

**Study leaders: Mr AJ Von Wielligh
& Prof NDL Burger**

October 2008



INVESTIGATION INTO A SYSTEM THAT CAN DETECT IMPROPER COMBUSTION IN A DIESEL ENGINE BEFORE SIGNIFICANT DAMAGE CAN OCCUR

By

Theo Lawrence Wilcocks

**Submitted in fulfilment of part of the requirements for the degree of Master of Engineering
in the Faculty of Engineering and the Built Environment**

University of Pretoria

**Study leaders: Mr AJ Von Wielligh
& Prof NDL Burger**

An alarming number of compression ignition (CI) engines in the transport, mining and heavy engineering environments have been failing due to combustion irregularities within their combustion chambers. It has been found that diesel fuels containing contaminants or diesel fuels with poor lubricity characteristics lead to stickiness of diesel injector needles, which badly affects injector spray patterns resulting in the phenomenon of “cold combustion”. This study has been undertaken to develop a technique for detecting and preventing the damage resulting from this deviation in the combustion of a diesel engine. The technique has been formulated with a view to being as non intrusive as possible, so as not to require major modification of an existing test engine to accommodate the technique. The practice of monitoring individual cylinder exhaust gas temperatures (EGTs) proved to be an effective way of determining whether potentially destructive combustion abnormalities were taking place within the diesel engine. By recording these temperatures at certain stages during the engine’s operation, taking their average, and comparing each one to this average it is also possible to isolate the location of the combustion abnormality. This method proved to be most effective at full loads and maximum fuel delivery where combustion temperatures are highest and the effects of poor combustion are most noticeable and potentially damaging. The second goal was to develop a small, portable electronic device that makes use of the monitoring technique developed and provides a visual and audible alarm to notify a vehicle operator or technician of a combustion fault within a diesel engine. A Combustion Monitoring System (CMS) prototype was developed and tested on a small naturally aspirated engine at the University of Pretoria’s engine testing facilities. The prototype met its primary goal of detecting simulated combustion abnormalities under a variety of test conditions. It is envisaged that the monitoring techniques applied in developing the CMS unit may eventually be incorporated into the powerful processing abilities of the modern diesel Engine Control Unit (ECU). In its current form the CMS prototype is a useful tool in sensing combustion related malfunctions within a diesel engine and preventing damage from occurring.



TABLE OF CONTENTS

1.0	CHAPTER I – INTRODUCTION	1
1.1	Problem Description.....	1
1.2	The Modern Compression Ignition (Diesel) Engine	1
1.3	The Effects of Improper Combustion.....	2
1.4	Current Engine Monitoring Techniques	3
1.5	The Scope of this Dissertation	4
2.0	CHAPTER II - THE COMBUSTION PROCESS IN DIESEL ENGINES	6
2.1	The Injection Systems in Diesel Engines	6
2.1.1	Fuel injection pumps.....	8
2.1.1.1	In-line injection pumps	8
2.1.1.2	Distributor or rotary-type fuel injection pumps.....	10
2.1.1.3	Single-barrel injection pumps.....	11
2.1.1.4	Unit fuel injectors	12
2.1.1.5	Common rail injection systems	14
2.2	Combustion Systems in Diesel Engines	16
2.2.1	Direct-injection engines	17
2.2.2	Indirect-injection engines.....	18
2.3	The Combustion Process in Diesel Engines	19
2.4	Spray Behaviour.....	20
2.4.1	Spray structure.....	20
2.4.2	Atomisation, evaporation and mixing.....	22
2.5	Improper Combustion.....	23
2.5.1	Causes of injection system malfunction	23
2.5.2	Resultant spray pattern due to malfunctioning injection system... 26	
2.5.3	Damage caused by a malfunctioning injection system.....	28
2.5.4	Piston damage due to overheating versus injector malfunction.... 34	
2.5.5	The difference between cold combustion and over-fuelling..... 39	
3.0	CHAPTER III – CURRENT INJECTION EQUIPMENT	
	PREVENTATIVE MAINTENANCE AND MONITORING TECHNIQUES	41
3.1	Traditional Condition Based Maintenance Techniques.....	41
3.1.1	Fuel cleanliness monitoring	41
3.1.2	Gravimetric methods.....	43
3.1.3	Particle Counters	44
3.2	Current Condition Based Maintenance Techniques.....	46
3.2.1	Engine signature analysis.....	46
3.2.1.1	Combustion pressure analysis	46
3.2.1.2	Vibration and ultrasonic data	49
3.2.1.3	Exhaust gas temperature measurement.....	53
4.0	CHAPTER IV - INVESTIGATION INTO THE EFFECTS THAT	
	DAMAGED INJECTORS HAVE ON EXHAUST GAS TEMPERATURE.....	55
4.1	Test Setup on University of Pretoria Dynamometer	55
4.1.1	Test Equipment.....	55
4.1.2	Experimental Setup.....	57
4.1.3	Experimental Procedure.....	61
4.1.3.1	Injector damage	62
4.1.3.2	Fuel blending	64



4.1.4	Results.....	64
4.1.4.1	Properly functioning injectors	64
4.1.4.2	Injector damage	69
4.1.4.3	Fuel blending	75
4.2	Caterpillar 3412 and 3512 Tests	81
4.2.1	Test setup	81
4.2.2	Test results	85
4.2.2.1	Caterpillar 3512 MEUI	85
4.2.2.2	Caterpillar 3412 HEUI.....	87
4.2.3	Findings.....	89
5.0	CHAPTER V – ELECTRONIC MONITORING AND DETECTION SYSTEM.....	90
5.1	System Requirements	90
5.1.1	Discussion of requirements	91
5.2	Development of the Combustion Monitoring System (CMS).....	94
5.2.1	Functional layout	95
5.2.2	Data capture and interfacing	102
5.2.3	Operation of the CMS prototype	105
5.3	Evaluation of the CMS prototype.....	110
5.3.1	Results at full load maximum fuel delivery	113
5.3.1.1	Discussion	118
5.3.2	Results at half load partial fuel delivery	119
5.3.2.1	Discussion	120
5.3.3	Results for engine rundown	121
5.3.3.1	Discussion	122
6.0	CHAPTER VI – CONCLUSION	123
6.1	Detecting Combustion Abnormalities within a Diesel Engine	123
6.2	CMS System	123
6.3	System Effectiveness and Limitations.....	124
6.4	Potential Applications	125



LIST OF TABLES

Table 3-1: Material found as particulates in diesel fuel (Abraham 2001:1).....	41
Table 3-2: Test methods for the determination of diesel cleanliness (Abraham 2001:2).....	43
Table 4-1: Table of engine speed vs. EGT standard deviations for half and full load conditions over multiple dynamometer runs.....	66
Table 4-2: Table of EGT standard deviations for quarter and half load conditions on the Cat 3512 MEUI engine	86
Table 4-3: Table of EGT standard deviations for left and right hand banks on the Cat 3412 HEUI engine	88
Table 5-1: CMS communications protocols.....	106
Table 5-2: Results with reference to Figure 5-17	113

LIST OF FIGURES

Figure 1-1: Photograph of damage caused to diesel engine piston due to ‘hot spot’ formation as a result of incorrect spray pattern. (Courtesy AJ von Wielligh & Associates).....	2
Figure 1-2: Damage caused to diesel engine piston flank due to washing away of the lubrication oil film from the cylinder liner. (Courtesy AJ von Wielligh & Associates)	3
Figure 2-1: Basic layout of diesel injection system. (Heywood 1988:519)The diesel fuel injection system consists of two core elements. The first is the injection pump of which several different types are available on the market.....	6
Figure 2-2: Photograph of a typical distributor type fuel-injection pump with electronic flow control. (Courtesy AJ von Wielligh & Associates)	7
Figure 2-3: Photograph of a disassembled multi-orifice diesel injector. On the left is the injector body or holder. On the lower right the nozzle needle can be seen and above it, the nozzle tip. (Courtesy AJ von Wielligh & Associates)	7
Figure 2-4: Typical mechanical in-line diesel fuel injector pump. (Heywood 1988:30).....	8
Figure 2-5: Helical control of fuel delivery by rotating plunger. (Heywood 1988:31)	9
Figure 2-6: Distributor-type diesel fuel pump. (Heywood 1988:32).....	10
Figure 2-7: A single-barrel injection pump. (Heywood 1988:519).....	11
Figure 2-8: A cutaway view of a cam operated, pintle type fuel injector. (Heywood 1988:520)....	12
Figure 2-9: Electronically controlled unit fuel injector. (Heywood 1988:521)	13
Figure 2-10: Common rail fuel injection system (GlobalDenso: 2001:13).....	15
Figure 2-11: Piezo-injector with coaxial-vario-nozzle (Robert Bosch GmbH: 2004:14).....	16
Figure 2-12: Common types of DI engine combustion systems. a) Quiescent chamber with multihole nozzle b) Bowl-in-piston chamber with swirl and multihole nozzle c) Bowl-in-piston chamber with swirl and single-hole nozzle. (Heywood 1988:494)	17
Figure 2-13: Two common types of small indirect-injection diesel engine combustion system: a) swirl pre-chamber b) turbulent pre-chamber. (Heywood 1988:495)	18
Figure 2-14: Sequence of photographs from high-speed cameras taken in a special direct injection engine. The sequence shows the combustion of a four-spray injector with counter clockwise swirl. (Heywood 1988:499).....	19
Figure 2-15: Schematic of diesel fuel spray defining its major parameters. (Heywood 1988:522)	21
Figure 2-16: Schematic of fuel spray makeup as it is injected radially into swirling air flow. (Heywood 1988:524).....	22
Figure 2-17: 60X magnification of the unscarred surface of a properly operating injector needle. (Courtesy AJ von Wielligh & Associates)	24
Figure 2-18: Score marks under 60X magnification of the needle in Figure 16a. (Courtesy AJ von Wielligh & Associates)	24
Figure 2-19: Example of injector needle damage. Note scoring marks on needle (Courtesy AJ von Wielligh & Associates)	25

Figure 2-20: Score marks under 100X magnification of the needle in Figure 2-19. (Courtesy AJ von Wielligh & Associates)	25
Figure 2-21: Scorch mark damage on injector pump plunger. (Courtesy AJ von Wielligh & Associates)	25
Figure 2-22: Expected spray pattern from a properly functioning injector. (Courtesy AJ von Wielligh & Associates)	26
Figure 2-23: Poor spray pattern from a malfunctioning injector. (Courtesy AJ von Wielligh & Associates)	27
Figure 2-24: Poor spray pattern from a malfunctioning multi-hole injector. (Courtesy AJ von Wielligh & Associates)	28
Figure 2-25: Schlieren photograph showing liquid-containing core (dark) in relation to vapour regions (Heywood 1988: 525).....	29
Figure 2-26: With reference to Figure 1-2 Seizing marks indicating unlubricated metal-to-metal contact between cylinder wall and piston. (Courtesy AJ von Wielligh & Associates)..	30
Figure 2-27: Corresponding seizing marks on cylinder wall. (Courtesy AJ von Wielligh & Associates)	30
Figure 2-28: Stribeck/Hersey/Gumbel curve relating friction coefficient to film thickness and surface roughness (Spikes, Olver 2005: 6).....	31
Figure 2-29: Boundary lubrication in a journal bearing (SKF International 2007: 28).....	32
Figure 2-30: Elasto-hydrodynamic lubrication for a rolling element bearing (SKF International 2007: 29)	32
Figure 2-31: Damage resulting from a deterioration of the lubrication film into the boundary lubrication regime between two surfaces forced together under normal load FN (SKF International 2007: 30)	33
Figure 2-32: Lubrication regimes existing at the various piston components that interface with the cylinder bore of an internal combustion engine during normal operation. (Esfahanian, Mohsen 1994).....	34
Figure 2-33: Piston skirt damage due to overheating (Waldhauer, Schilling, Schnaibol, Szopa: 2004: 26)	35
Figure 2-34: Illustration depicting damage zone on piston skirt due to overheating (Waldhauer, Schilling, Schnaibol, Szopa: 2004: 26)	36
Figure 2-35: Piston skirt damage due to an injector malfunction (Waldhauer, Schilling, Schnaibol, Szopa: 2004: 21).....	37
Figure 2-36: Illustration depicting damage zone on piston skirt due to a malfunctioning injector (Waldhauer, Schilling, Schnaibol, Szopa: 2004: 21).....	38
Figure 2-37: Picture of piston damage due to malfunctioning injector. The picture shows the exit point of a hole burnt through from the piston crown, out the side of the piston skirt. (Courtesy AJ von Wielligh & Associates)	39

Figure 3-1: Chemtrac Systems portable fuel/oil particle counter. (Courtesy Chemtrac Systems online catalogue 2004)	44
Figure 3-2: Light blocking sensor (left) compared to a light scattering sensor (right) (Hunt 2004: pg 1)	45
Figure 3-3: Wall mounted pressure transducer shown removed from its mounting location in the cylinder head, but directly positioned directly above it for clarity (mounting hole not visible in this picture) (Roth, Sobiesiak, Robertson & Yates 2002: pg2).....	46
Figure 3-4: Pressure vs. crank angle signature (P- θ) diagram (Goldwine, deBotton, Rivin & Sher 2004: pg 3)	47
Figure 3-5: Acceleration/time waveform (Goldwine, deBotton, Rivin & Sher 2004: pg 4)	50
Figure 3-6: Pressure trace overlayed with vibration trace (Goldwine, deBotton, Rivin & Sher 2004: pg 4)	51
Figure 3-7: Vibration signatures for the 9 pump elements of a medium speed 9 cylinder diesel engine. (O'Connel & Haller 2002: pg 11).....	52
Figure 4-1: Photograph of engine mounted on SuperFlow dynamometer.....	55
Figure 4-2: SF-901 dynamometer engine stand (SuperFlow Corporation 1992: 1-5).....	56
Figure 4-3: Photograph of thermocouples plugged directly into dynamometer sensor input panel	58
Figure 4-4: Photograph of thermocouple mounting points in exhaust manifold	59
Figure 4-5: Arrows in photograph indicate thermocouple positions on engine exhaust manifold ..	60
Figure 4-6: Photograph of thermocouple protruding into cylinder 4 outlet	60
Figure 4-7: Photograph of thermocouple protruding into cylinder 1 outlet	61
Figure 4-8: Photograph of wear damage induced on sealing face of injector needle to facilitate leakage at 20X magnification.....	62
Figure 4-9: The arrow on this photograph indicates a large vertical scratch purposely affected to facilitate seizing of the needle within the injector tip.....	63
Figure 4-10: A view of the needle damage captured under 100X magnification as indicated by the arrow. Note that small pieces of material were ripped out of the needle surface as it was forced to reciprocate within the needle.....	63
Figure 4-11: Exhaust gas temperature envelope for properly functioning injectors	64
Figure 4-12: Normal distribution across all four cylinders of EGTs for properly functioning injectors at 3 750 RPM.....	67
Figure 4-13: Histogram of measured temperature range distribution across all four cylinders for properly functioning injectors at 3 750 RPM	68
Figure 4-14: Exhaust gas temperature envelope for properly functioning injectors	69
Figure 4-15: Good and badly scratched injector comparison graph of EGT readings taken from the thermocouple mounted in cylinder 1 exhaust.....	70
Figure 4-16: Good and improperly sealing injector comparison graph of EGT readings taken from the thermocouple mounted in cylinder 1 exhaust.....	71

Figure 4-17: Good and badly scratched injector comparison graph of EGT readings taken from the thermocouple mounted in cylinder 2 exhaust.....	72
Figure 4-18: Good and improperly sealing injector comparison graph of EGT readings taken from the thermocouple mounted in cylinder 2 exhaust.....	72
Figure 4-19: Good and badly scratched injector comparison graph of EGT readings taken from the thermocouple mounted in cylinder 3 exhaust.....	73
Figure 4-20: Good and improperly sealing injector comparison graph of EGT readings taken from the thermocouple mounted in cylinder 3 exhaust.....	73
Figure 4-21: Good and badly scratched injector comparison graph of EGT readings taken from the thermocouple mounted in cylinder 4 exhaust.....	74
Figure 4-22: Good and improperly sealing injector comparison graph of EGT readings taken from the thermocouple mounted in cylinder 4 exhaust.....	74
Figure 4-23: Injector degradation graph of EGT readings taken from the thermocouple mounted in cylinder 1 exhaust.....	75
Figure 4-24: Injector degradation graph of EGT readings taken from the thermocouple mounted in cylinder 2 exhaust.....	76
Figure 4-25: Injector degradation graph of EGT readings taken from the thermocouple mounted in cylinder 3 exhaust.....	76
Figure 4-26: Injector degradation graph of EGT readings taken from the thermocouple mounted in cylinder 4 exhaust.....	77
Figure 4-27: Comparison of engine torque measured during run with fuel blend and average value measured during previous runs using good fuel and new injectors	78
Figure 4-28: Photograph of hand operated injector test bench.....	79
Figure 4-29: Injector number 4 spray pattern.....	80
Figure 4-30: Spray pattern of a new injector.....	80
Figure 4-31: Close-up photograph of damage on needle surface	80
Figure 4-32: 100X magnification of score mark on needle surface	81
Figure 4-33: Caterpillar 3512 V12 engine on which testing was conducted.....	82
Figure 4-34: Photograph of thermocouple mounted in CAT 3512 head	83
Figure 4-35: Photograph of the thermocouple protruding into the exhaust port on a stripped 3512 head	83
Figure 4-36: Photograph from below of thermocouples mounted adjacent to exhaust port in manifold of 3412	84
Figure 4-37: EGT readings taken from the head mounted thermocouples on the 3512 engine at quarter load.....	85
Figure 4-38: EGT readings taken from the head mounted thermocouples on the 3512 engine at full load.....	86
Figure 4-39: EGT readings taken from the manifold mounted thermocouples on the right hand bank of the 3412 engine	87

Figure 4-40: EGT readings taken from the manifold mounted thermocouples on the left hand bank of the 3412 engine 88

Figure 5-1: Photograph of the CMS prototype..... 95

Figure 5-2: Solid model of CMS prototype unit. 95

Figure 5-3: “Functional” printed circuit board diagram 96

Figure 5-4: “Display” printed circuit board diagram..... 97

Figure 5-5: Photograph of the CMS unit. Green LED indicates unit has power and is switched on. 98

Figure 5-6: Photograph of CMS display indicating that thermocouples have been connected to slots 1 to 4. 99

Figure 5-7: Photograph of CMS unit indicating a deviation in temperature on the no. 4 thermocouple from the average of the other three thermocouples. 100

Figure 5-8: Photograph of female miniature thermocouple input sockets..... 101

Figure 5-9: Photograph of CMS prototype right hand side panel. 101

Figure 5-10: Photograph of CMS prototype left hand side panel..... 102

Figure 5-11: Photograph of CMS and laptop interfacing. 103

Figure 5-12: CMS text file output to Hyper Terminal..... 104

Figure 5-13: CMS current settings displayed in Hyper Terminal window..... 107

Figure 5-14: Photograph of CMS prototype with laptop interface on SuperFlow dynamometer control panel..... 110

Figure 5-15: Photograph of engine thermocouple to CMS connections 111

Figure 5-16: CMS display upon thermocouple connection..... 112

Figure 5-17: Hyper Terminal display screen of temperature values 112

Figure 5-18: Graphic representation of CMS output values for properly functioning injectors at maximum fuel delivery, full load 114

Figure 5-19: Damaged injector test needle..... 115

Figure 5-20: Graphic representation of CMS output values for damaged injector in cylinder number 3..... 116

Figure 5-21: CMS visual alarm for EGT drop in cylinder number 3 116

Figure 5-22: Graphic representation of CMS output values for damaged injector in cylinder number 1..... 117

Figure 5-23: Graphic representation of CMS output values for damaged injector in cylinder number 2..... 117

Figure 5-24: Graphic representation of CMS output values for damaged injector in cylinder number 4..... 118

Figure 5-25: Graphic representation of CMS output values for properly functioning injectors at partial load..... 119

Figure 5-26: Graphic representation of CMS output values for damaged injector in cylinder number 3 at partial load..... 120

Figure 5-27: EGT results as engine cools down after full load run.....	121
Figure 6-1: Normal distributions at full throttle, throughout RPM range	127
Figure 6-2: Normal distribution at half throttle @ 3 750 RPM.....	127
Figure 6-3: Histogram of measured temperature range distribution across all four cylinders for properly functioning injectors at 1500 RPM.....	128
Figure 6-4: Histogram of measured temperature range distribution across all four cylinders for properly functioning injectors at 1750 RPM.....	128
Figure 6-5: Histogram of measured temperature range distribution across all four cylinders for properly functioning injectors at 2000 RPM.....	129
Figure 6-6: Histogram of measured temperature range distribution across all four cylinders for properly functioning injectors at 2250 RPM.....	129
Figure 6-7: Histogram of measured temperature range distribution across all four cylinders for properly functioning injectors at 2500 RPM.....	130
Figure 6-8: Histogram of measured temperature range distribution across all four cylinders for properly functioning injectors at 2750 RPM.....	130
Figure 6-9: Histogram of measured temperature range distribution across all four cylinders for properly functioning injectors at 3000 RPM.....	131
Figure 6-10: Histogram of measured temperature range distribution across all four cylinders for properly functioning injectors at 3250 RPM.....	131
Figure 6-11: Histogram of measured temperature range distribution across all four cylinders for properly functioning injectors at 3500 RPM.....	132
Figure 6-12: Histogram of measured temperature range distribution across all four cylinders for properly functioning injectors at 3750 RPM.....	132
Figure 6-13: Histogram of measured temperature range distribution across all four cylinders for properly functioning injectors at 4000 RPM.....	133
Figure 6-14: Display circuit board diagram	134
Figure 6-15: Functional circuit board diagram.....	135



LIST OF ABBREVIATIONS AND SYMBOLS

C	Celsius
CI	Compression ignition
CMS	Combustion Monitoring System
ECU	Electronic Control Unit
EGT	Exhaust Gas Temperature
F_N	Normal Force
F_R	Relative Force
F/A	Fuel/air equivalence ratio
HEUI	Hydraulically Operated Electronic Unit Injection
IP	Illuminating paraffin
kW	kilo watt
MEUI	Mechanically operated Electronic Unit Injection
N	Engine operating speed (Revolutions per Second)
Nm	Newton metre
P_i	Indicated engine power
ppm	Parts Per Million
Q_{HV}	Heating value of the fuel
RPM	Revolutions Per Minute
SI	Spark Ignition
LED	Light Emitting Diode
V_d	Displacement volume
•	
V_f	Fuel volume flow rate
mm	Millimetre
μm	Micro-metre
MPa	Mega Pascal
psi	Pounds Per Square Inch
UP	University Of Pretoria
$U\eta$	Film thickness
λ	Surface roughness
η_f	Fuel combustion efficiency



η_v	Engine volumetric efficiency
θ	Crank angle degrees
$\rho_{a,i}$	Indicated air density
ρ_f	Fuel density
σ	One standard deviation
1.6449σ	“90%” error deviation

1.0 CHAPTER I – INTRODUCTION

1.1 Problem Description

An alarming number of compression ignition (CI) engines have been failing due to combustion irregularities within their combustion chambers. These failures occur as a result of the incorrect delivery of fuel from their injection systems. A large number of these failures are occurring in the transport, mining and heavy engineering environments where large, powerful, expensive diesel engines are used to a large extent. Much of the damage caused by incorrect fuel combustion could be avoided, if the drivers were aware of such problems during the normal operation of the equipment. The need has thus arisen to develop a condition based maintenance technique to warn the machine operator of the start of injection equipment malfunction, hence preventing engine damage and subsequent costly rebuilds or replacements.

1.2 The Modern Compression Ignition (Diesel) Engine

Far from being regarded as the slow plodding workhorses of yesteryear, the modern generation of diesel engines are challenging spark ignition (petrol) engines for performance, efficiency, emissions and compactness in the passenger and commercial vehicle segment. In heavy industry, the vehicles and equipment used are almost exclusively powered by diesel engines. The developments that have allowed modern diesels to improve so radically include:

- Extensive use of turbo charging coupled with intercoolers to boost the torque and power per unit volume engine displacement.
- Extremely high injection pressures of around 200 Mega Pascal (Mpa) to maximise the quantity of fuel that can be atomised completely with the fresh charge air being drawn into the engine.
- Electronically controlled injection to allow the exact metering of fuel injected into each cylinder.
- Adjustable valve and injection timing to maximise volumetric efficiency of the engine across its operating range.

- Positioning of the top, sealing ring high up on the piston crown to reduce the formation of unburned hydrocarbons in the crevices between the piston and cylinder wall, thus reducing emissions.
- A reduction in the water volume size cooling the engine thus making it more compact.

In order for these developments to be implemented effectively, the tolerances between moving components, such as those found in the injection systems, have been reduced significantly over the last few generations of engines. Such close fits however make modern diesels appreciably less tolerant of fuel containing contaminants or fuel not possessing the necessary lubricity qualities.

1.3 The Effects of Improper Combustion

It has been found that diesel fuels containing contaminants or diesel fuels with poor lubricity characteristics lead to stickiness of diesel injector needles, which badly affects injector spray patterns. The poor spray patterns and fuel drops lead to melting of piston crown material as can be seen below in Figure 1-1.



Figure 1-1: Photograph of damage caused to diesel engine piston due to 'hot spot' formation as a result of incorrect spray pattern. (Courtesy AJ von Wielligh & Associates)



Figure 1-2: Damage caused to diesel engine piston flank due to washing away of the lubrication oil film from the cylinder liner. (Courtesy AJ von Wielligh & Associates)

This effect also results in the washing away of the lubrication film between the piston and cylinder liner materials, bringing about “dry rubbing” and extremely fast wear, resulting in seizing of the pistons within the cylinder liners. Piston damage resulting from this effect is shown in Figure 1-2 above.

The latest trend in newly developed diesel engines is that of individual injectors as sealed units that are replaced rather than serviced when wear is apparent. Examples of such units are the HEUI (High Pressure Electronically Controlled Unit Injectors) used on the 34 and 35 series Caterpillar engines. The cost of such unit injectors can range from R 1 500 per unit for the smaller passenger vehicle engines up to R 12 000 each on the large turbo diesels used in industry. Maintenance staff are thus reluctant to replace these injectors unnecessarily. In most cases no facilities exist, even at the local engine supplier, to test the injectors, once removed.

1.4 Current Engine Monitoring Techniques

At present some mining operations take oil samples on a daily basis to determine the condition of the lubricating oil. The oil samples are tested spectrographically

in a laboratory on site and results of the tests are usually available within one to two hours. Despite these measures, it often happens that several power kits, consisting of an injector, piston and sleeve, have to be replaced weekly. Unfortunately oil analysis can only indicate that damage is busy occurring or has already occurred within the engine.

Vehicle chassis dynamometers are also frequently used on site to monitor vehicle performance periodically. A drop in vehicle performance is a good indication of a defect. If the problem can be traced to the injectors the dilemma lies with trying to ascertain which injector is malfunctioning, as all the injectors seldom fail at once. This can be a time consuming operation on a large 12-cylinder engine and the excessive costs involved prohibit replacement of an entire set of injectors.

Visual spray pattern checks are possible on the older generation mechanical injectors, while the new generation electronically controlled unit injectors require a dedicated injector test bench to activate the injector once removed from the engine. As the tendency is for modern injectors to be regarded as ‘disposable’ items, test equipment is widely unavailable. This makes visual inspection of the injectors’ spray patterns virtually impossible.

On the vast majority of modern sophisticated diesels, the engines’ Electronic Control Units (ECU’s) monitor a number of engine operating parameters. Often the ECUs are equipped with data loggers that store the information from the various sensors over extended periods of time. The problem lies in the fact, that, in most cases only the engine supplier’s technicians have the equipment to download the acquired data. Even if the operator has access to this data it is very often misinterpreted or simply ignored. Therefore, malfunctions that could have been diagnosed beforehand are left to degenerate into catastrophic engine failures.

1.5 The Scope of this Dissertation

This study has been undertaken to develop a technique for determining any deviation in the combustion of a diesel engine beyond prescribed limits and build

a prototype device for applying the technique to the test engine. The device should be capable of warning the operator and the maintenance staff that incomplete combustion is taking place, which in turn, might lead to engine failure. They can then take the necessary steps to either replace the injector or rectify the problem. The technique would be formulated with a view to being as non intrusive as possible, so as not to require major modification of an existing test engine to accommodate the technique.

The databases of the mines, where experiments have been carried out, were used so as to compare the new, to existing methods such as contamination control or spectrographic analysis. By means of newly developed techniques, it is envisaged that maintenance staff can identify potential engine failures before any real damage occurs, thus improving reliability, decreasing running costs and extending production.

2.0 CHAPTER II - THE COMBUSTION PROCESS IN DIESEL ENGINES

2.1 The Injection Systems in Diesel Engines

In summary the combustion process in compression ignition (diesel) engines is brought about by the following fuel injection process: “Fuel is injected by the fuel injection system into the engine cylinder towards the end of the compression stroke, just before the desired start of combustion.” (Heywood 1988:491) A schematic of a typical fuel injection system is shown in

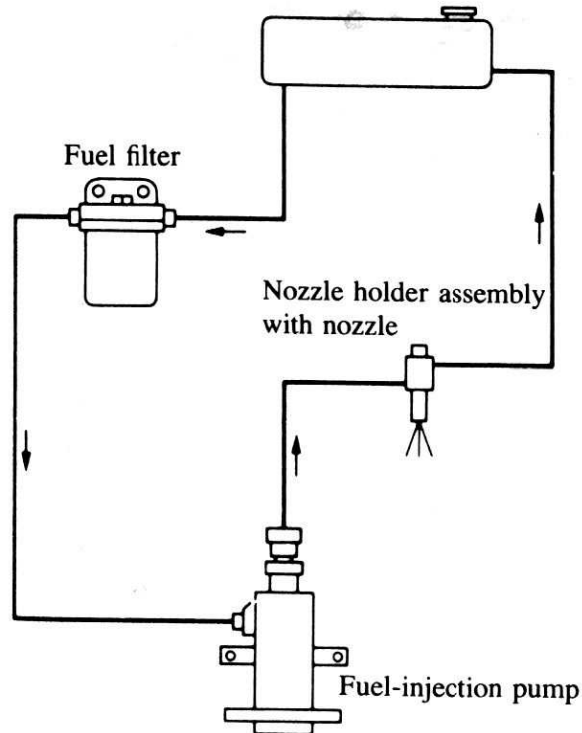


Figure 2-1: Basic layout of diesel injection system. (Heywood 1988:519)The diesel fuel injection system consists of two core elements. The first is the injection pump of which several different types are available on the market.

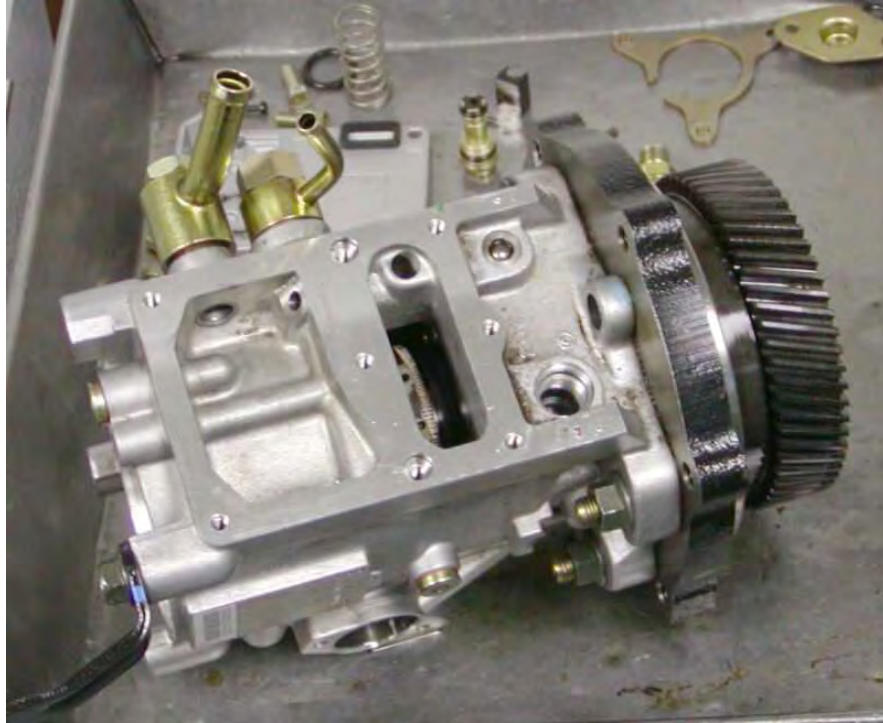


Figure 2-2: Photograph of a typical distributor type fuel-injection pump with electronic flow control. (Courtesy AJ von Wielligh & Associates)

The following stage of injection comprises the fuel injectors. A disassembled multi-orifice diesel injector is shown in Figure 2-3.



Figure 2-3: Photograph of a disassembled multi-orifice diesel injector. On the left is the injector body or holder. On the lower right the nozzle needle can be seen and above it, the nozzle tip. (Courtesy AJ von Wielligh & Associates)

On receiving the pressurized fuel from the pump, the liquid is “injected at high velocity as one or more jets through small orifices or nozzles in the injector tip, atomizes into small drops and penetrates into the combustion chamber. The fuel vaporises and mixes with the high-temperature high-pressure cylinder air. Since the air temperature and pressure are above the fuel’s ignition point, spontaneous ignition of portions of the already-mixed fuel and air occurs after a delay period of a few crank angle degrees. Injection continues until the desired amount of fuel has entered the cylinder. Atomization, vaporization, fuel-air mixing, and combustion continue until essentially all the fuel has passed through each process. In addition mixing of the air remaining in the cylinder with burning and already burned gases continues throughout the combustion and expansion process.” (Heywood 1988:491)

2.1.1 Fuel injection pumps

The pump’s function is to draw fuel from the fuel reservoir through a filter and deliver liquid fuel at high pressure via nozzle pipes to the following stage of injection. Figure 2-4 depicts a mechanical in-line diesel fuel injector pump.

2.1.1.1 In-line injection pumps

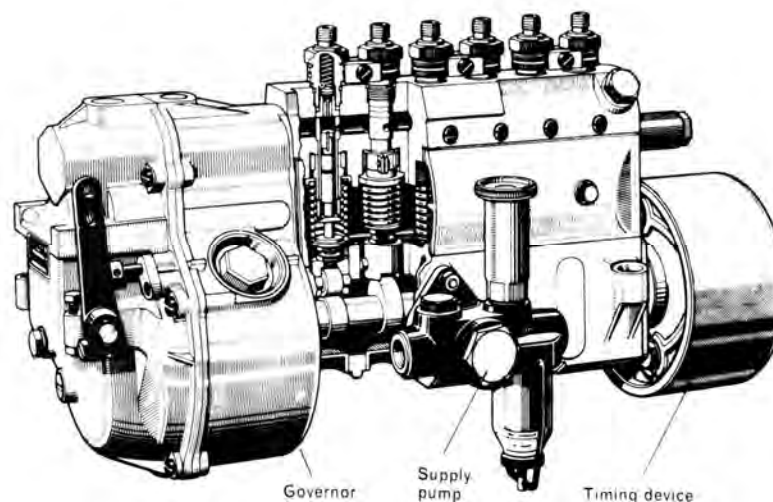


Figure 2-4: Typical mechanical in-line diesel fuel injector pump. (Heywood 1988:30)

“This type of pump is typically found in the 40 to 100 kW per cylinder maximum power range of engine. It contains a plunger and barrel assembly for each engine cylinder. Each plunger is raised by a cam on the pump camshaft (driven via gear or belt off the engine crankshaft) and is forced back by the plunger return spring. The plunger fits sufficiently accurately within the barrel to seal without additional sealing elements, even at high pressures and low speeds. Varying the effective plunger stroke alters the amount of fuel delivered. This is achieved by means of a control rod or rack, which moves in the pump housing and rotates the plunger via a ring gear or linkage lever. The plunger chamber above the plunger is always connected with the chamber below the plunger helix by a vertical groove or bore in the plunger. Delivery ceases when the plunger helix exposes the intake port (port opening), thus connecting the plunger chamber with the suction gallery. When this takes place depends on the rotational position of the plunger.” Figure 2-5 depicts the plunger movement during the metering of different quantities of diesel fuel.

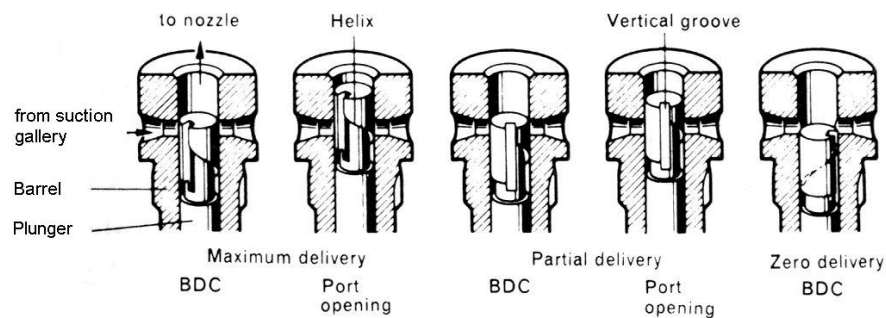


Figure 2-5: Helical control of fuel delivery by rotating plunger. (Heywood 1988:31)

In the case of a lower helix, delivery always starts (port closing) at the same time, but ends sooner or later depending on the rotational position of the plunger. With a plunger with an upper helix, port closing (start of delivery) not port opening is controlled by the helix and is varied by rotating the plunger.” (Heywood 1988:518)

2.1.1.2 Distributor or rotary-type fuel injection pumps

A diesel fuel system comprising of a distributor-type fuel-injection pump with mechanical governor is shown in Figure 2-6.

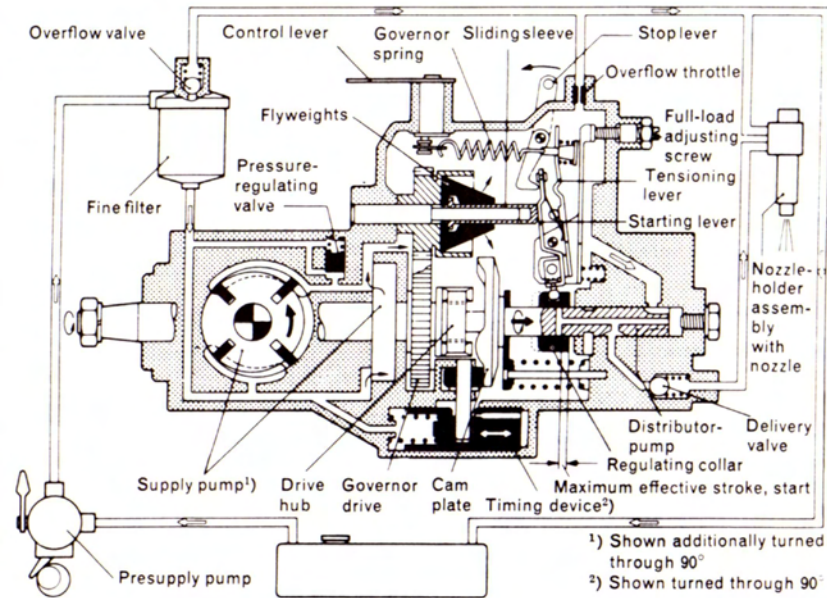


Figure 2-6: Distributor-type diesel fuel pump. (Heywood 1988:32)

“Normally used in multi-cylinder engines with less than 30 kW per cylinder maximum power with injection pressures up to 75 MPa. These pumps have only one plunger and barrel. The pump plunger is made to describe a combined rotary and stroke movement by the rotating cam plate. The fuel is accurately metered to each injection nozzle in turn by this plunger which simultaneously acts as the distributor. Such units are more compact and cheaper than in-line pumps but cannot achieve such high injection pressures. The distributor-type fuel injection pump is combined with an automatic timing device, governor, and supply pump to form a single unit.” (Heywood 1988:518) A large number of the latest generation passenger cars and light commercial vehicles are fitted with high-pressure rotary pumps with electronically controlled metering valves. Their compactness and flexibility make them well suited to modern emission and performance requirements.

2.1.1.3 Single-barrel injection pumps

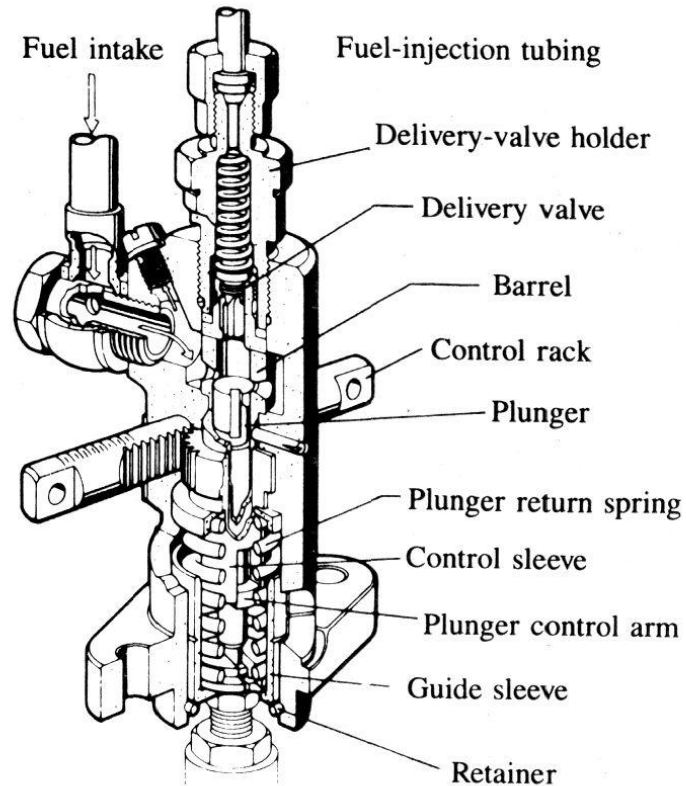


Figure 2-7: A single-barrel injection pump. (Heywood 1988:519)

Figure 2.7 shows a section view of a single-barrel fuel injection pump. The operation of the metering element of this type of injection pump has been discussed in section 2.1.1.1 and is depicted in Figure 2-7.

“Single-barrel injection pumps are used on small single and twin cylinder diesel engines as well as large engines with outputs of more than 100 kW per cylinder. Such pumps are driven by an auxiliary cam on the engine camshaft.” (Heywood 1988:519)

2.1.1.4 Unit fuel injectors

A fuel injector brings about the actual introduction of fuel into the combustion chamber of an engine. The cut-away view depicted in Figure 2-8 shows a unit fuel injector and its driving mechanism, as typically used in large diesel engines.

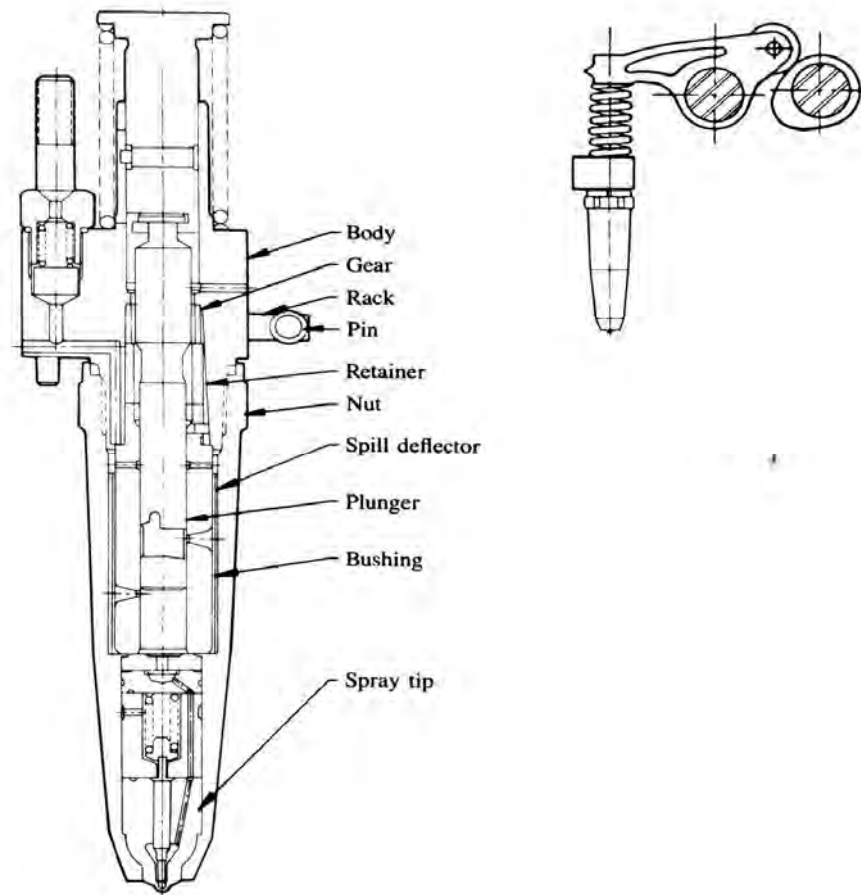


Figure 2-8: A cutaway view of a cam operated, pintle type fuel injector.
(Heywood 1988:520)

The injectors normally receive fuel from the pump via a fuel-distribution manifold of some type. This either comprises a set of separate fuel pipes from the injector pump to the individual injectors, or a single, high pressure fuel line (common rail) fed by the fuel pump, from which fuel is distributed to the injectors. Traditionally diesel injectors are actuated mechanically by means of

camshaft lobes depressing a plunger. Depressing the plunger blocks off the metering orifice that supplies fuel to the injector. This prevents more fuel from entering the injector body, ensuring that only an exactly metered out quantity of fuel is available for injection each time. Next the descending plunger compresses the fuel forcing it through check valves into the injector spray tip. The injector tip is the most critical part of the injection system. It consists of a body containing a spring-loaded needle valve blocking off single or multiple orifices. Once the fuel has been pressurised to a sufficient degree by the plunger it forces the needle off its seat against the spring and fuel can issue through one or multiple orifices, depending on combustion chamber design, into the combustion chamber. “ It is important to keep the volume of fuel left between the needle and nozzle orifices as small as possible to prevent any fuel flowing into the cylinder after injection is over, to control hydrocarbon emissions” (Heywood 1988:519), (and possible engine damage). An in depth discussion on this subject follows in latter texts.

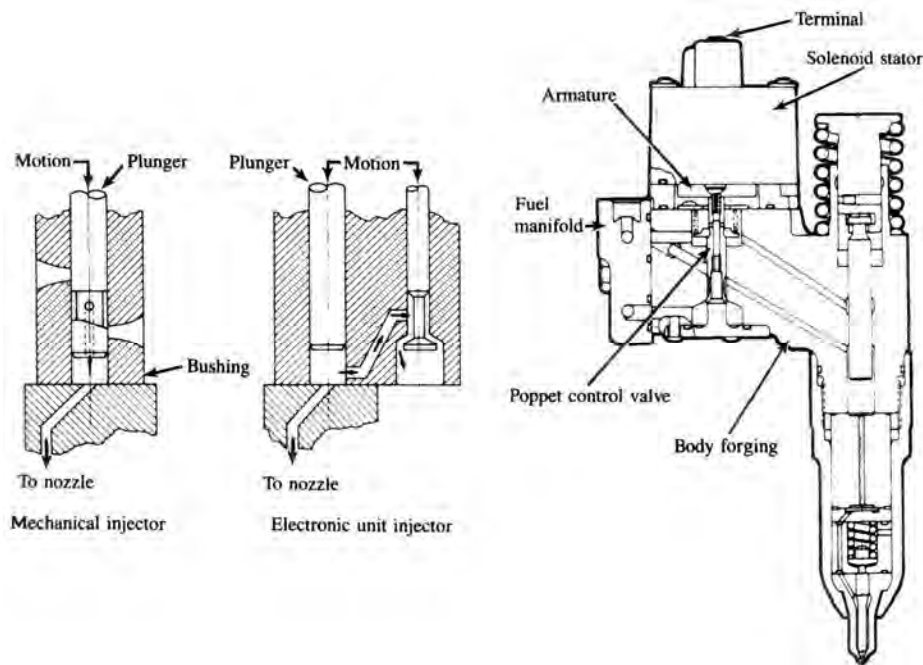


Figure 2-9: Electronically controlled unit fuel injector. (Heywood 1988:521)

More recently the technology for electronic control of injectors has become available. Figure 2-9 depicts the metering components of a mechanical injector compared to those of an electronically controlled unit. Instead of using a camshaft lobe to actuate the injector plunger, a solenoid operated control valve performs the injection timing and fuel metering functions. “Solenoid valve closure initiates pressurization and injection, and opening causes injection pressure decay and end of injection. Duration of valve closure determines the quantity of fuel injected. The unit,” [shown in figure 9 above] “still uses camshaft/rocker arm driven plungers to generate the injection pressure, and employs needle-valve nozzles of conventional design. Increased flexibility in fuel metering and timing and simpler injector mechanical designs are important advantages.” (Heywood 1988:520)

Naturally the evolution of diesel engines over the years has called for engines that are more powerful for their specific capacity while being more fuel efficient and forming less pollutants during the combustion process. All these factors have led to a steady rise in the injection pressures of modern engines. This development is taking place in order to facilitate reducing the droplet size of the ‘fuel mist’. The smaller the fuel droplets contained within the inlet charge are, the better the fuel will mix with the air within the combustion chamber and the more uniformly the combustion flame will propagate within the ‘squish’ volume above the piston releasing maximum energy in a controlled manner.

2.1.1.5 Common rail injection systems

With ever increasingly stringent emissions regulations being enforced world wide and the constant push to improve the performance and fuel economy of diesel engines, great emphasis has been placed in recent times on the development of common rail injection technology.

The common rail design gives engine developers much greater freedom to concentrate on the control of fuel injection using injectors with fewer moving components, as the generation of injection pressure is separated from the injectors themselves.

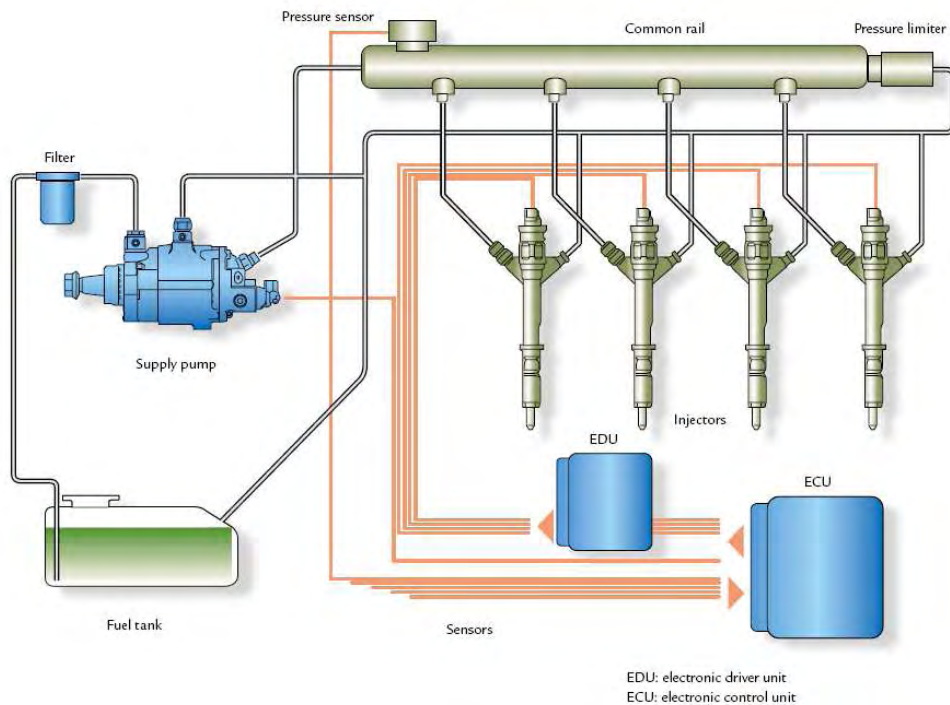


Figure 2-10: Common rail fuel injection system (GlobalDenso: 2001:13)

Figure 2-10 shows the components that constitute the ECP-U2P system manufactured by Nipon-Denso of Japan. A high-pressure supply pump generates a pressure of up to 160 MPa in an accumulator or “common rail” (determined by the injection pressure setting in the electronic control unit) independently of engine speed and the quantity of fuel injected. The fuel is fed through rigid pipes to the injectors, which inject the fuel in a fine spray into the combustion chamber. A dedicated electronic driver unit precisely controls injection parameters such as injection timing, number of injection pulses and the duration of these pulses relative to engine load and speed conditions.

The fact that the high injection pressures are no longer generated within the injector allows engine designers to use modern piezo-electric actuated injectors, similar in design to those used in modern petrol engines. This means that the injector needles are directly actuated by their piezo-electric actuators, instead of making use of the fuel pressure build up in the injector tip to actuate the injector needle as with traditional designs. These injectors have far fewer

moving components than tradition injector designs and much faster response times than the magnetic solenoids used in previous unit injectors. An example of this type of injector is shown below in Figure 2-11.

Injector -Charakteristics

- Basis: CRI3
- Systempressure 1600/1800 bar
- Space requirement as CRI3
- One row for part load
- Both rows for full load

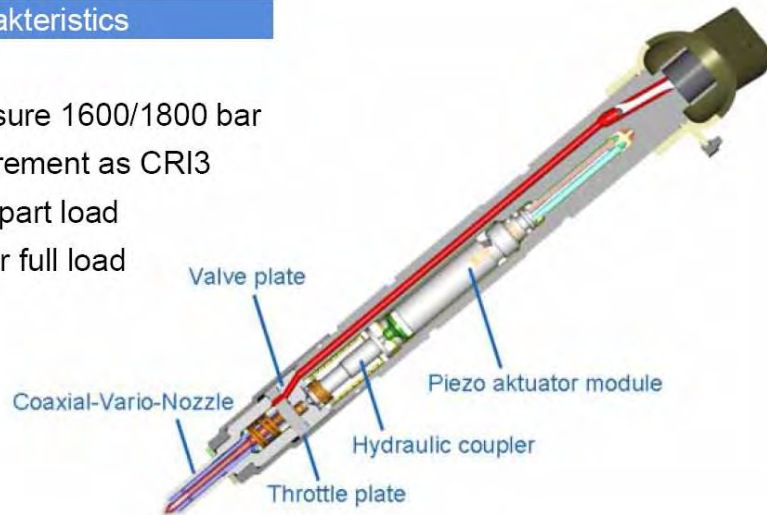


Figure 2-11: Piezo-injector with coaxial-vario-nozzle (Robert Bosch GmbH: 2004:14)

With companies such as Robert Bosch GmbH looking at concepts to push the pressure within the common rail to 200 MPa in the quest for more complete combustion, clearances between the moving components that comprise the system are becoming increasingly tighter to eliminate leakage. This places a greater emphasis than ever on clean fuels with adequate lubricity.

2.2 Combustion Systems in Diesel Engines

Many different configurations and designs of diesel engines are available. The following texts will concentrate on the more common types in general use around the world and specifically in South Africa, as background to this study.

The largest types of diesel engines are found in the marine and stationary power generating applications, and are slow moving two-stroke cycle engines of up to 25 000 litre capacity. Medium and small diesels found in commercial and passenger

vehicle applications are generally four-stroke cycle machines due to the superior emission and fuel consumption qualities of this cycle.

Diesel engines can be divided into two basic types according to the design of their combustion chambers. *Direct injection* and *indirect injection* engines.

2.2.1 Direct-injection engines

Figure 2-12 below shows three different combustion chamber designs for direct injection diesel engines.

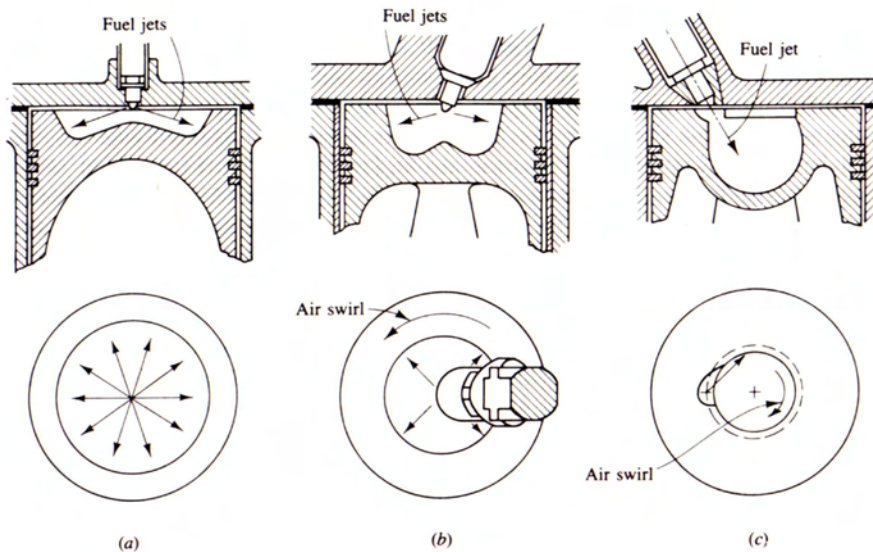


Figure 2-12: Common types of DI engine combustion systems. a) Quiescent chamber with multihole nozzle b) Bowl-in-piston chamber with swirl and multihole nozzle c) Bowl-in-piston chamber with swirl and single-hole nozzle. (Heywood 1988:494)

“These engines have a single open combustion chamber into which fuel is injected directly. The combustion chamber shape is usually a shallow bowl in the crown of the piston and a central multihole injector is used.” (Heywood 1988:493) In large, slow moving engines, the momentum and latent energy of the injected fuel spray is enough to cause proper mixing of the fuel vapour with the air. In smaller engines increasing amounts of air swirl, brought about by suitable inlet port design, are used to effect proper mixing.

2.2.2 Indirect-injection engines

“The combustion chamber is divided into two regions and the fuel is injected into a “pre-chamber” which is connected to the main chamber (situated above the piston crown) via a nozzle, or one or more orifices. IDI engine designs are only used in the smallest engine sizes.” (Heywood 1988:493)

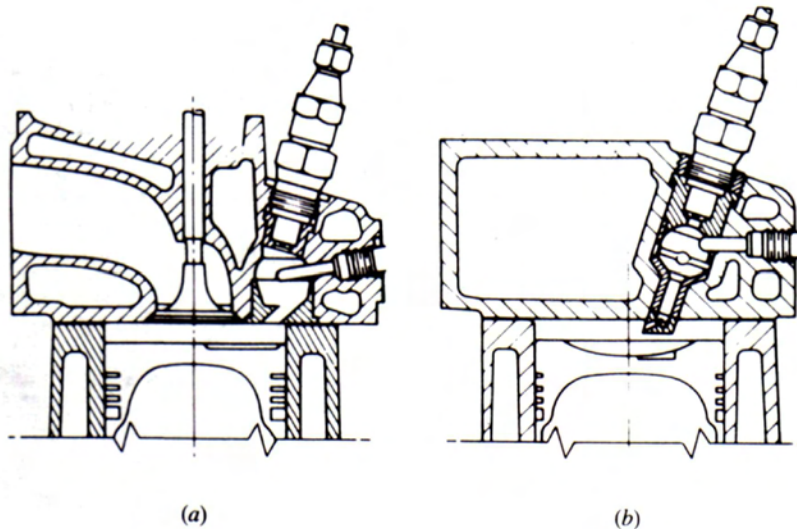


Figure 2-13: Two common types of small indirect-injection diesel engine combustion system: a) swirl pre-chamber b) turbulent pre-chamber. (Heywood 1988:495)

Figure 2-13 (a) shows a typical swirl chamber design while Figure 2-13 (b) portrays a turbulent pre-chamber design. The basic principle of operation is as follows: air is forced from the main chamber above the piston during the compression stroke through passages or nozzles into a pre-chamber. Depending on the chamber shape vigorous flow or rotation (swirl) of air can be set up to allow for adequate mixing of the air and fuel. The following excerpt from Heywood explains the pressure rise within the combustion chamber: “Fuel is usually injected into the auxiliary chamber at lower injection-system pressure than is typical of DI systems through a pintle nozzle as a single spray. Combustion starts in the auxiliary chamber. The pressure rise associated with

combustion forces fluid back into the main chamber where the jet issuing from the nozzle entrains and mixes with the main chamber air.” (Heywood 1988:495)

2.3 The Combustion Process in Diesel Engines

Photographic analysis has been used extensively to study the nature of combustion within the diesel engine. The following analysis of a commonly used combustion chamber design, serves to illustrate the process that occurs during normal operation.

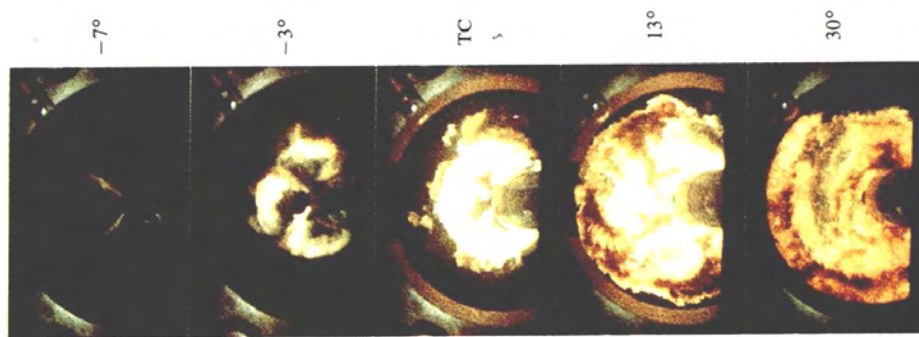


Figure 2-14: Sequence of photographs from high-speed cameras taken in a special direct injection engine. The sequence shows the combustion of a four-spray injector with counter clockwise swirl. (Heywood 1988:499)

The sequence depicted in Figure 2-14, takes place in the same bowl in piston combustion chamber design that is portrayed in Figure 2-12 (b). The photos have been taken through a quartz window inserted into the dome of the combustion chamber, directly above the piston crown. Negative degrees indicate that the piston is still moving upwards during the compression stroke. Top dead centre (TDC) is the point at which the piston reaches the top of its stroke and positive degrees indicate that the piston is moving down during the expansion stroke. The following points are taken from Heywood:

- “The fuel sprays (of which two are visible without obstruction from the injector) first appear at -13° before the piston reaches TDC.
- At -7° TDC they have reached the wall of the bowl; the tips of the sprays have been deflected slightly by the anticlockwise air swirl.

- The frame at -3° shows the first ignition. Bright, luminous flame zones are visible, one on each spray.
- Out by the piston bowl walls, where fuel vapour has been blown around by the swirl, larger greenish burning regions, indicating the presence of premixed flame, can be seen.
- The fuel downstream of each spray is next to ignite, burning yellow-white due to the soot formed by the richer mixture.
- Flame propagation back to the injector follows extremely rapidly and at TDC the bowl is filled with flame.
- At 5° after TDC the flame spreads out over the piston crown toward the cylinder wall, due to combustion-produced gas expansion and the reverse squish flow.
- The brown regions (13°) are a soot-laden fuel-rich mixture originating from the fuel that impinges on the wall.
- The last frame (30° after TDC) shows the gradual diminution of soot-particle-laden regions as they mix with the excess air and burn up.
- The final dull-red flame visible on the film is at about 75° after TDC, well into the expansion stroke.” (Heywood 1988:500-501)

It is important to note that in this scenario, where near complete combustion is occurring, the combustion of gasses takes place above the piston crown and not on the metal surfaces of the combustion chamber.

2.4 Spray Behaviour

2.4.1 Spray structure

“The fuel is introduced into the combustion chamber of a diesel engine through one or more nozzles or orifices with a large pressure differential between the fuel supply line and the cylinder. Different designs of nozzle are used (e.g. single-orifice, multi-orifice, throttle, or pintle) depending on the needs of the combustion system employed.” (Heywood 1988:522)

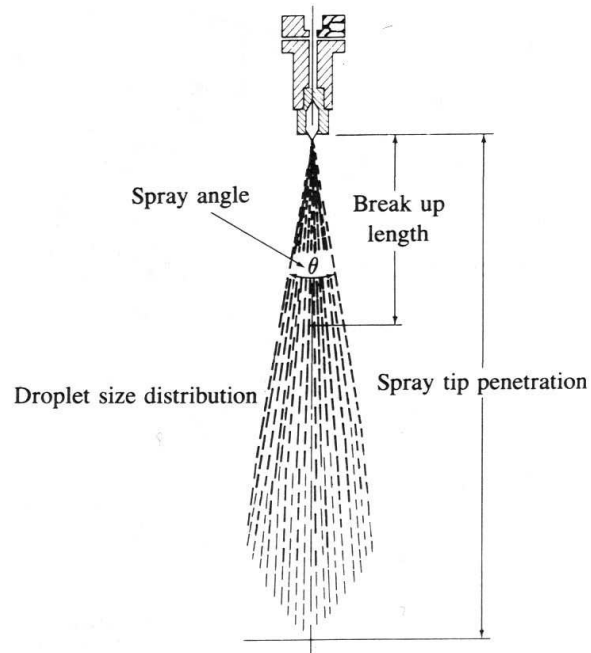


Figure 2-15: Schematic of diesel fuel spray defining its major parameters. (Heywood 1988:522)

Figure 2-15 illustrates the correct spray structure of a properly functioning typical direct injection (DI) pintle type injector nozzle. “As the liquid jet leaves the nozzle it becomes turbulent and spreads out as it entrains and mixes with the surrounding air. The initial jet velocity is greater than 10^2 m/s. The outer surface of the jet breaks up into drops of order $10\ \mu\text{m}$ diameter, close to the nozzle exit. The liquid leaving the nozzle disintegrates within the cylinder over a finite length called the *breakup length* into drops of different sizes. Moving away from the nozzle, the mass of air within the spray increases, the spray diverges, its width increases, and the velocity decreases. The fuel drops evaporate as this air entrainment process proceeds.” (Heywood 1988:523)

2.4.2 Atomisation, evaporation and mixing

“Both physical and chemical processes must take place before a significant fraction of the chemical energy of the injected liquid fuel is released. The physical processes are:

1. Atomisation of the liquid fuel jet
2. Vaporisation of the fuel droplets
3. Mixing of the fuel vapour with air.” (Heywood 1988:540)

The chemical processes involve the pre-combustion reactions of the fuel and reactions with residual gasses within the cylinder. However this dissertation focuses on the physical process and as such the following discussion concentrates on this subject.

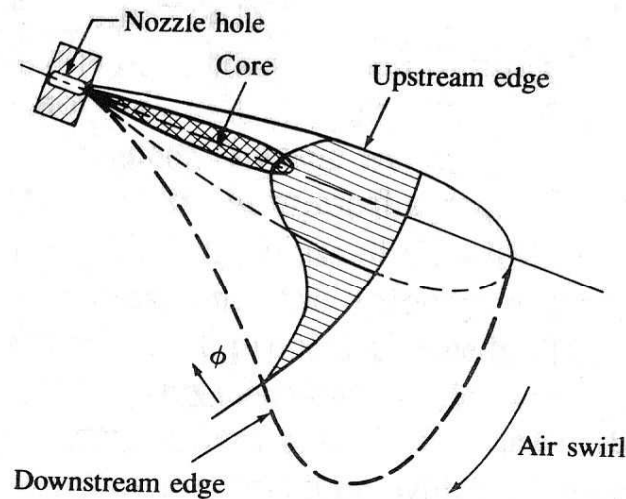


Figure 2-16: Schematic of fuel spray makeup as it is injected radially into swirling air flow. (Heywood 1988:524)

In Figure 2-16 the fuel spray composition is depicted under injection conditions. The physical makeup of the injected fuel spray is described in Heywood as follows:

- “Under diesel engine injection conditions, the fuel jet usually forms a cone-shaped spray at the nozzle exit.

- A liquid-containing jet forms in the region directly adjacent to the nozzle tip. This region contains liquid drops and ligaments and is referred to as the liquid ‘core’.
- Surrounding the liquid core the major region of the spray is made up of a substantial vapour cloud.
- The spray entrains air, spreads out, and slows down as the mass flow in the spray increases.
- The drops on the outer edge of the spray evaporate first, creating a fuel vapour-air mixture sheath around the liquid-containing core. This type of behaviour is classified as the atomisation break-up regime, and it produces droplets with sizes very much less than the nozzle exit diameter.
- The injected liquid fuel, atomized into small drops near the nozzle exit to form a spray, must evaporate before it can mix with air and burn.
- Good atomisation requires high fuel-injection pressure, small injector hole diameter, optimum fuel viscosity and high cylinder air pressure at the time of injection.
- The rate of vaporisation of the fuel droplets depends on the size of the droplets, their distribution and their velocity, the pressure and temperature inside the chamber, and the volatility of the fuel.” (Heywood 1988:526)

2.5 Improper Combustion

2.5.1 Causes of injection system malfunction

In the light of the afore mentioned facts, it becomes evident that in order to develop diesel engines that are both cleaner burning and more powerful than their forefathers, great advances have had to be made in decreasing droplet size and improving fuel atomisation and mixing within the combustion chamber of a modern diesel engine. One of the most significant methods of accomplishing this is to use extremely high injection pressures. With the aid of electronically

controlled common rail injection, a modern fuel-injector operates with pressures reaching 200 MPa. Engine developers envisage pressures of 280 MPa in the near future. Due to these extreme pressures, the clearances of moving components within a modern injector are extremely tight to enable the injector to generate such high pressures and prevent the leakage of fuel back up past the needle and plunger. An important consideration is that fuel itself serves as the only lubricant between the moving components of an injector. As such, any deficiency in the lubricating properties (lubricity) of the fuel or any ingress of contaminants into the fuel will have a detrimental effect on the injector components. Older generation diesel engines were much more tolerant of poorer quality fuels due to the larger clearances of components within the lower pressure injection systems. However the new generation of cleaner burning high performance diesel engines require clean fuels with good lubricity.

A typical properly functioning injector needle is shown in Figure 2-17.



Figure 2-17: 60X magnification of the unscarred surface of a properly operating injector needle. (Courtesy AJ von Wielligh & Associates)

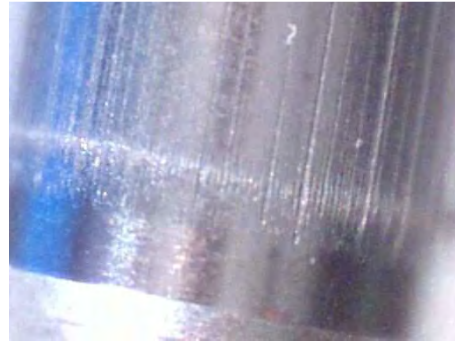


Figure 2-18: Score marks under 60X magnification of the needle in Figure 16a. (Courtesy AJ von Wielligh & Associates)

The abrasive scoring marks visible on the needle in Figure 2-18 have been caused by solid particle fuel contaminants being trapped between the needle and barrel during operation.

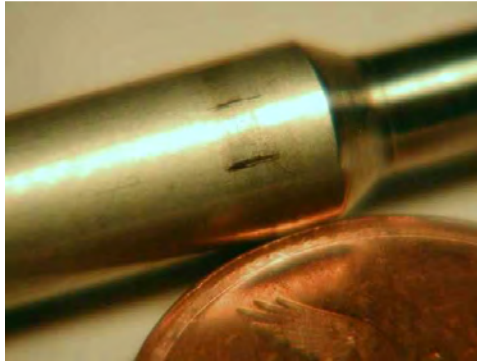


Figure 2-19: Example of injector needle damage. Note scoring marks on needle (Courtesy AJ von Wielligh & Associates)

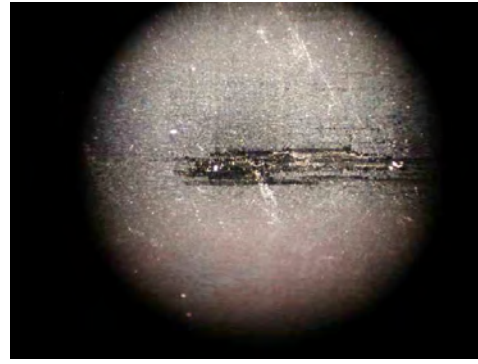


Figure 2-20: Score marks under 100X magnification of the needle in Figure 2-19. (Courtesy AJ von Wielligh & Associates)

Marks visible on the needle in Figure 2-19, are a result of poor lubricity fuel allowing metal to metal welding of the needle to the inside of the injector tip. Under 60X magnification the score marks are clearly visible in Figure 2-20.



Figure 2-21: Scorch mark damage on injector pump plunger. (Courtesy AJ von Wielligh & Associates)

Figure 2-21 shows blue scorch marks on an injector pump plunger that resulted from metal-to-metal contact within the pump. Fuel contaminated with paraffin,

and consequently with significantly reduced lubricity, has been identified as the cause of this damage. This type of scarring typically leads to the injector needle or plunger seizing within its barrel. The normally freely moving injector needles depicted in Figure 2-18 and Figure 2-19 seized so solidly within the injector tip barrel that they had to be pulled from their tips using a pair of pliers. This malfunctioning of the of the injection system elements logically has an adverse effect on their ability to generate the fuel injection pressures necessary to facilitate good atomisation and complete combustion. This can potentially cause serious damage to a diesel engine.

2.5.2 Resultant spray pattern due to malfunctioning injection system

The photographs below give a direct visual comparison between the spray patterns of a properly functioning multi-orifice type injector and that of a malfunctioning one.



Figure 2-22: Expected spray pattern from a properly functioning injector. (Courtesy AJ von Wielligh & Associates)

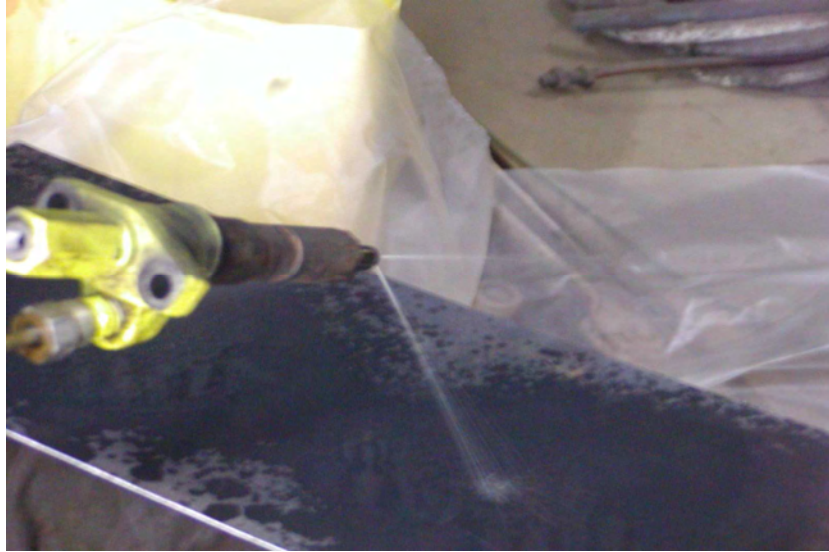


Figure 2-23: Poor spray pattern from a malfunctioning injector.
(Courtesy AJ von Wielligh & Associates)

The properly functioning injector is shown in Figure 2-22. The photograph illustrates the correct spray pattern discussed in section 2.4.1 and 2.4.2 required for good fuel atomisation and hence complete combustion. The liquid 'core' is visible directly adjacent to the nozzle tip while further upstream, the fuel is atomising into a fine fuel vapour mist. Figure 2-23 shows a malfunctioning injector, of the same type. Thick jets of fuel are squirting out of the nozzle and hardly any fuel atomisation is visible. This is typically the kind of spray pattern experienced when the injector needle is seizing within the injector tip barrel and/or fuel is leaking past the needle's sealing surfaces resulting in a significant decrease in injection pressure.



Figure 2-24: Poor spray pattern from a malfunctioning multi-hole injector.
(Courtesy AJ von Wielligh & Associates)

Figure 2-24 shows a malfunctioning four-hole injector. Once again, instead of a fine mist of tiny fuel droplets, jets of large fuel drops are issuing from the nozzle tip. This injector was removed from a failed light commercial vehicle engine, the piston damage of which is shown in Figure 1-1 in Section 1.3.

2.5.3 Damage caused by a malfunctioning injection system

Having discussed the process of combustion within the diesel engine and factors leading to a breakdown in this process, the focus of this text now turns to the detrimental effects of improper combustion on a diesel engine.

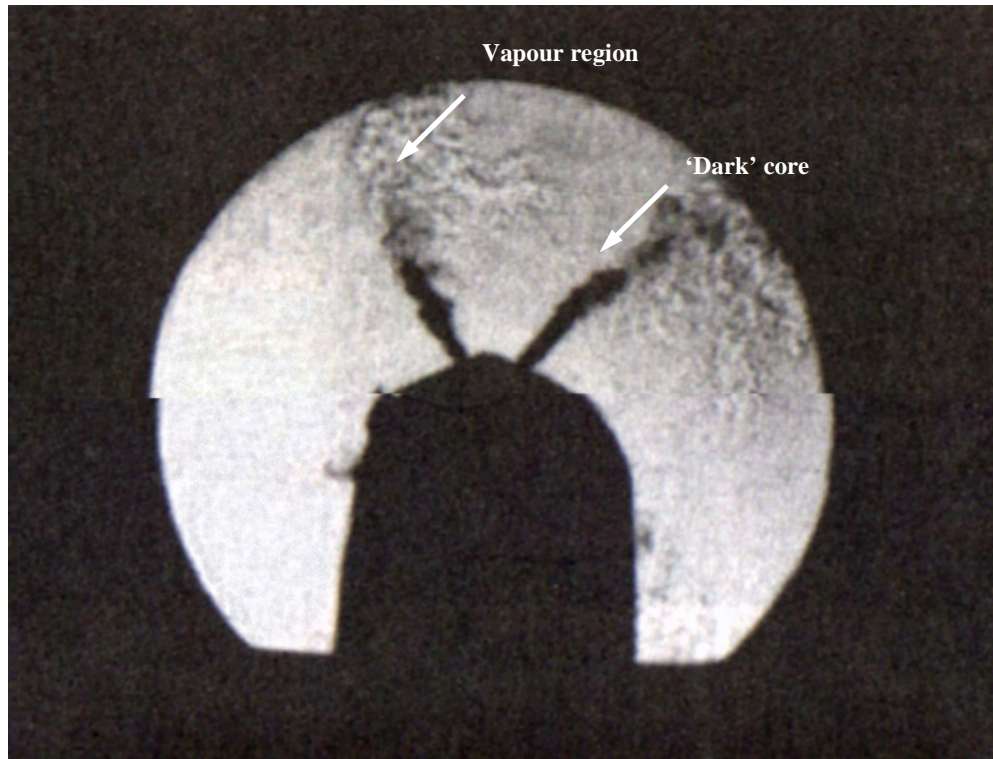


Figure 2-25: Schlieren photograph showing liquid-containing core (dark) in relation to vapour regions (Heywood 1988: 525)

During normal combustion conditions within a diesel engine's combustion chamber, the atomised fuel spray issuing from an injector propagates through the squish area above the piston. This occurs at such a rate that the majority of droplets evaporate before coming into contact with any of the relatively cool metal surfaces of the cylinder walls or piston crown. This can be seen in Figure 2-25 where the dark regions depict the liquid containing core and the lighter regions indicate the atomised vapour. At this point detonation of the premixed gas (air and evaporated fuel) occurs and it is the rapidly cooling, expanding gases that directly interact with the cylinder walls and force the piston downwards.

In the case of a malfunctioning injector, the liquid jet/s squirted from the injector over-penetrate into the combustion chamber and impinge on the cool metal surfaces of the cylinder walls and piston crown with very limited fuel atomisation and evaporation. This phenomenon is referred to as 'cold

combustion’. Initially this lowers mixing rates and increases emissions of unburned gases, but as the condition of the injector deteriorates so the impingement of liquid fuel worsens. The affected cylinder/s begin to misfire as the ideal mixing ratios are further deviated from and white exhaust smoke becomes visible. Eventually, excessive impingement of liquid fuel jets onto the cylinder walls has the effect of washing away the lubricating oil film from the cylinder walls. This results in piston to cylinder wall seizing as is evident from the damage depicted in Figure 2-26 and Figure 2-27 below.



Figure 2-26: With reference to Figure 1-2 Seizing marks indicating unlubricated metal-to-metal contact between cylinder wall and piston. (Courtesy AJ von Wielligh & Associates)



Figure 2-27: Corresponding seizing marks on cylinder wall. (Courtesy AJ von Wielligh & Associates)

Figure 2-26 is reproduced from Figure 1-2 of Section 1.3 depicted earlier in this document, and compares the seizure damage on the piston to the corresponding damage on the cylinder liner wall. The damage shown in Figure 2-26 and Figure 2-27 resulted from the spray pattern depicted in Figure 2-23 in Section 2.5.2.

Understanding the mechanisms involved in causing this type of damage requires a brief revision of the Stribeck/Hersey/Gumbel curve that relates friction coefficient to the dimensionless amalgamation of film thickness ($U\eta$) and surface roughness (λ) plotted on a logarithmic scale. The curve is depicted in Figure 2-28.

Furthermore, the Stribeck curve is broken up into four distinct lubrication regimes namely the:

1. Hydrodynamic lubrication regime
2. Elasto-hydrodynamic regime
3. Mixed film lubrication regime
4. Boundary lubrication regime

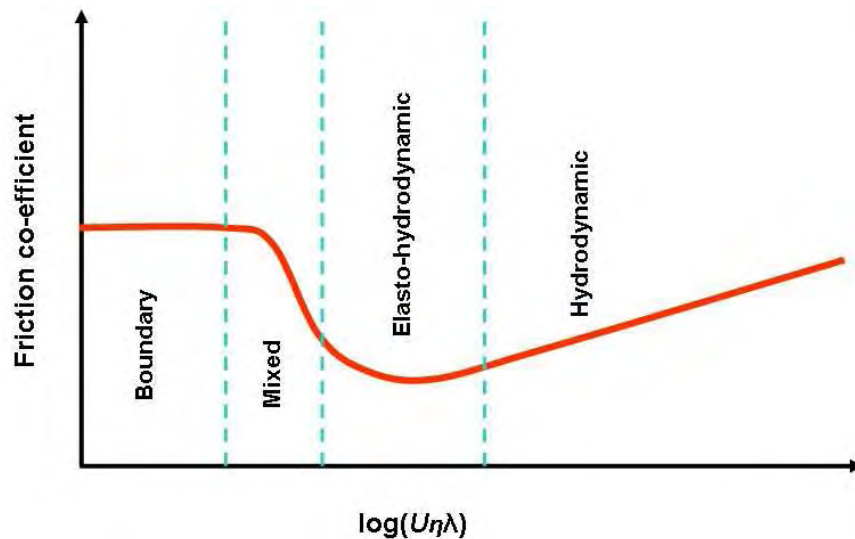


Figure 2-28: Stribeck/Hersey/Gumbel curve relating friction coefficient to film thickness and surface roughness (Spikes, Olver 2005: 6)

It is worth noting from Figure 2-28 that the friction co-efficient increases approximately 150 X from the lowest point in the elasto-hydrodynamic region to its maximum in the boundary lubrication regime. This brings about a proportional rise in heat generated due to friction greatly increasing the chances of seizure occurring.

The hydrodynamic lubrication regime relies on a pressurized lubricant film to separate relative surfaces and results in a constant controllable friction coefficient, provided the pressure distribution throughout the lubricant film is maintained. This type of lubrication regime is most commonly found in journal bearings and is depicted in Figure 2-29 below.

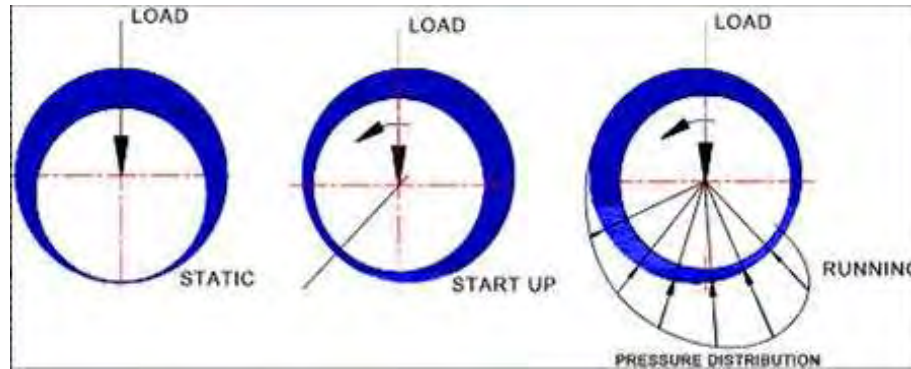


Figure 2-29: Boundary lubrication in a journal bearing (SKF International 2007: 28)

The elasto-hydrodynamic lubrication regime does not require a pressurised lubricant film. Instead this regime relies on line or point contact rolling surfaces which deform elastically, generating extremely high local pressures within the lubricant that becomes trapped between the two surfaces. This forces the lubricant to form a thin solid film. For this regime to exist it is paramount that there is no break down in the film thickness of the lubricant. The formation of this solid film is illustrated for a rolling element bearing in Figure 2-30.

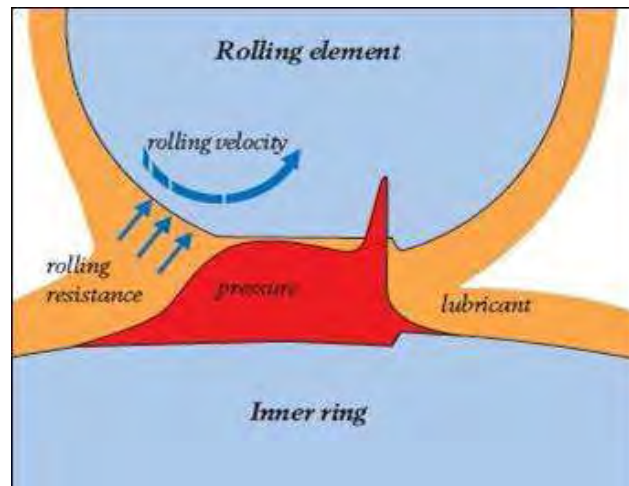


Figure 2-30: Elasto-hydrodynamic lubrication for a rolling element bearing (SKF International 2007: 29)

Mixed film lubrication is a transient regime that exists briefly as the conditions for stable elasto-hydrodynamic lubrication, namely high local pressures between relative surfaces, collapse and the regime deteriorates into the boundary

lubrication regime. This regime is in essence a mixture of elasto-hydrodynamic and boundary lubrication.

Boundary lubrication is the least desirable lubrication regime of the four demonstrated by the Stribeck curve and results in the types of damage illustrated in Figure 2-31 when two metal surfaces being moved relative to one another by a force (F_R) are simultaneously exposed to a normal force (F_N). If the lubricant is not equipped to deal with boundary lubrication conditions in the form of a strong anti-wear additive that forms a protective layer by chemically reacting with the metal surfaces, adhesive and abrasive wear will occur. Even with the protective layer, subsurface fatigue may still occur within the two surfaces.

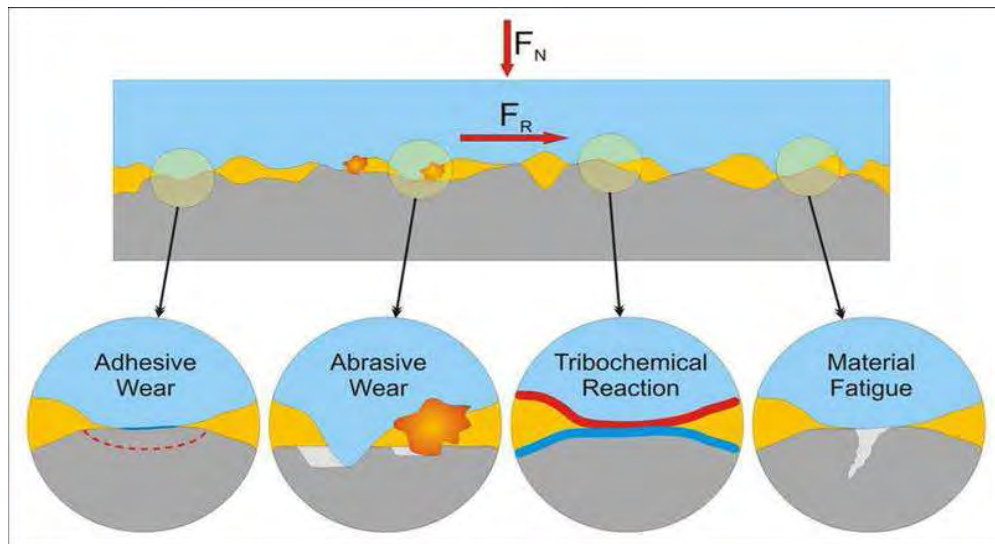


Figure 2-31: Damage resulting from a deterioration of the lubrication film into the boundary lubrication regime between two surfaces forced together under normal load F_N (SKF International 2007: 30)

Figure 2-32 shows the lubrication regimes that have been established to exist on the piston of an internal combustion engine during normal operation.



- Top sealing ring = Elastohydrodynamic
- Lower sealing ring = Mixed lubrication
- Oil scraper ring = Boundary lubrication
- Piston skirt = mixed film and boundary lubrication

Figure 2-32: Lubrication regimes existing at the various piston components that interface with the cylinder bore of an internal combustion engine during normal operation. (Esfahanian, Mohsen 1994)

Due to the extreme pressures generated during combustion the top sealing ring is forced outward against the cylinder wall. This not only prevents combustion gas blow-by past the piston but also sets up an elasto-hydrodynamic lubrication regime between the cylinder wall and top sealing ring. As previously stated any breakdown in the film thickness of the lubricant, such as dilution by liquid fuel, will result in deterioration into the boundary regime. Due to the extremely harsh conditions of pressure and temperature generated within the engine's combustion chamber the lubricant is then unable to separate the top-ring and cylinder wall under boundary conditions and the type of seizure pictured in Figure 2-26 and Figure 2-27 results.

2.5.4 Piston damage due to overheating versus injector malfunction

It is important to distinguish the difference between piston damage caused by overheating due to a malfunction in the cooling system and piston damage caused by improper combustion due to a malfunctioning injection system. The piston damage resulting from malfunctioning injectors is often attributed to overheating when there is a distinct difference between the two.



Fig. 1

Figure 2-33: Piston skirt damage due to overheating (Waldhauer, Schilling, Schnaibol, Szopa: 2004: 26)

Figure 2-33 depicts a piston displaying the typical flank and piston skirt damage associated with overheating of the engine due to a fault in the cooling system of the engine. The piston skirt is marked by darkly discoloured seizure marks, primarily concentrated on the piston flanks perpendicular to the gudgeon pin where the piston material is at its thinnest. The ring zone has only suffered minimal damage due to worn piston material that has been rubbed upwards.

Typical causes of this might be: loss of coolant, faulty water pump or pump drive, malfunctioning thermostat or clogged or damaged radiator in the case of water-cooled engines. Air cooled engines might overheat due to broken or dirt clogged cooling fins on the exterior of the cylinders or a break-down in ventilation air flow over the engine.

Figure 2-34 illustrates where the primary piston damage occurs due to an engine overheating.



Figure 2-34: Illustration depicting damage zone on piston skirt due to overheating
(Waldhauer, Schilling, Schnaibol, Szopa: 2004: 26)

Severe engine overheating results in a break-down in the lubricating properties of the oil on the cylinder wall as it loses its viscosity due to extreme heat. This is accompanied by excessive expansion of the piston material, particularly in the skirt area where the piston is at its least stiff. Consequently, seizure occurs between the piston and cylinder wall material. It is important to note that this type of failure originates at the base of the piston skirt and works its way up along the piston flank.

Figure 2-35 shows a piston, displaying the type of damage associated with washing away of the lubricant film off the cylinder walls due to a malfunctioning injector.



Figure 2-35: Piston skirt damage due to an injector malfunction (Waldhauer, Schilling, Schnaibol, Szopa: 2004: 21)

The piston crown has localised seizure marks that are primarily concentrated around the top ring land. The surface of the seizure area is rough and worn and it is evident that larger pieces of material have been torn out of the piston.

Typical causes of this type of seizure are leaking, clogged or damaged injectors. Incorrect installation of the injectors as a result of incorrect torque settings may result in bending of the injector body and leakage. Another cause may be incorrect injection timing resulting in fuel being injected at the wrong time into the combustion chamber

Figure 2-36 highlights the seizure zone on the piston due to the washing away of the lubricant film.

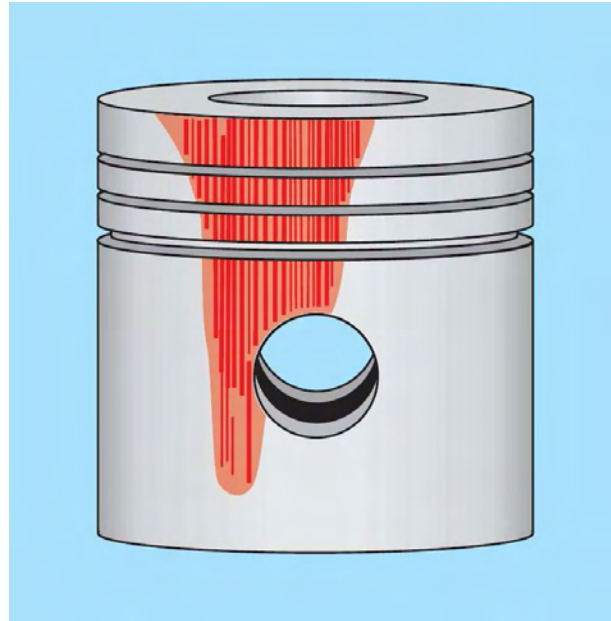


Figure 2-36: Illustration depicting damage zone on piston skirt due to a malfunctioning injector (Waldhauer, Schilling, Schnaibol, Szopa: 2004: 21)

It is worth noting that the washing away of the lubricant film initiates at the top land of the piston where it initially starts running “dry” due to non-atomised fuel dripping from the faulty injector. The damage then works its way down the side of the piston, towards the skirt.

In addition to the piston cylinder wall seizure, malfunctioning injectors may also result in ‘torching’ of the piston crown. When fuel burns in the space above the piston in the combustion chamber, some of the products of combustion form a stagnant layer of gas that protects the piston material from overheating. ‘Torching’ occurs when a dribbling injector causes pools of fuel to collect on the piston crown. These pools of fuel ignite instead of the premixed gases that should be ignited above the piston. This raises the surface temperatures on the crown above the melting point of the metal and a hole begins to form. If a fuel jet is squirted continually onto this ‘hot spot’ a hole can be burnt right through the piston. A case such as this is depicted in Figure 2-37 below, where a hole has been ‘torched’ through the piston crown material and out the piston flank.



Figure 2-37: Picture of piston damage due to malfunctioning injector. The picture shows the exit point of a hole burnt through from the piston crown, out the side of the piston skirt. (Courtesy AJ von Wielligh & Associates)

From the preceding texts it is evident that, although both engine overheating and injection system malfunction potentially result in piston seizure, the nature and progression of the damage are fundamentally different. As such, an engine overheating due to a cooling system break-down results in piston seizure that initiates at the base of the piston skirt and progresses upwards towards the rings. The seizure due to a malfunctioning injector initiates at the top of the piston ring lands and progresses downward toward the base of the piston.

2.5.5 The difference between cold combustion and over-fuelling

The destructive processes explained in the above text have been ascribed to the phenomenon of ‘cold combustion’ resulting from a malfunctioning injector, squirting streams of fuel into the combustion chamber instead of the fine atomized mist necessary for complete combustion. Simulation of this phenomenon by the author revealed that the process is accompanied by white exhaust smoke and a decrease in exhaust gas temperature from the norm. White smoke results from the ignition of raw fuel impinging on the relatively cool

metal surfaces within the combustion chamber hence the name ‘cold-combustion’. The drop in exhaust gas temperature (EGT) is ascribed to the significantly lower release of thermal energy from the fuel and the cooling effect that unburned raw fuel ligaments have on the exhaust gases exiting the combustion chamber.

Very often the cause of such catastrophic engine failures as have been presented in the above text is incorrectly ascribed to ‘over-fuelling’. Over-fuelling results from the injection of too large a quantity of fuel into the combustion chamber for the amount of air available. It may result from such causes as a blocked air filter or incorrect adjustment of the diesel pump pressure. This means that the mixture is over-rich and results in the charge mixture burning at a much slower rate than is necessary to facilitate complete combustion. Very often the combustion rate is so slow that the charge mixture is still burning while the exhaust valves are opening. Burnt valves result from this and excessively high exhaust temperatures are experienced. Excessive dark black smoke accompanied by extreme soot formation is often observed when over-fuelling is prevalent. Both cold-combustion and over-fuelling may result in an infiltration of fuel, past the piston rings into the engine’s oil sump. This is referred to as fuel dilution.

Little data is available on the cold combustion phenomenon, while over-fuelling is a commonly observed and documented process. The average diesel technician seems unaware that there is a difference between these two processes.

3.0 CHAPTER III – CURRENT INJECTION EQUIPMENT PREVENTATIVE MAINTENANCE AND MONITORING TECHNIQUES

3.1 Traditional Condition Based Maintenance Techniques

3.1.1 Fuel cleanliness monitoring

A major portion of injection equipment failure can be attributed to contaminated fuel. Essentially, eight types of materials can be found as particles in diesel fuel. These types are shown in Table 3-1 below, together with some examples.

Table 3-1: Material found as particulates in diesel fuel (Abraham 2001:1)	
<i>Type of Particulate</i>	<i>Examples</i>
Inorganic compounds	Dust, dirt, sand
Metals	Fuel pump wear particles, corrosion debris from bulk fuel tanks, filler caps, pipework.
Fuel container surfaces	Resins, fibreglass, high-density polypropylene, polymers/elastomers and polyurethane foams
Fuel filter media	Paper, cotton
Fungus	Cladosporium resinae
Yeast	Candida humicola
Bacteria	Pseudmonae
Organic compounds	Fuel-derived sediment and/or gum

South Africa has a particularly bad dust problem and injection equipment failure is rife under diesel machine operators and owners. “Ten years ago, maximum diesel fuel system pressures seldom exceeded 3 000 psi (20.6 MPa). Today’s state-of-the-art fuel system pressures can be as high as 30 000 psi (206 MPa). Therein lies the problem. The issue became apparent some 20 years ago -not in

fuel systems- but in the newly developed high-pressure hydraulic systems that utilized servo valves. It was noted that hydraulic system component life was drastically reduced in the new high-pressure systems. And for no readily apparent reason, pumps and valves that had previously lasted tens of thousands of hours in low-pressure systems were failing in only hundreds of hours in the new high-pressure systems.

The modern diesel fuel system is essentially an ultra high-pressure hydraulic system. So the same issues and parts failures apply there. In the case of the high-pressure hydraulic systems, it was determined that ultra fine particles that had not been a problem in lower pressure (1 000 psi, 7 MPa, or less) hydraulic systems were the cause of reduced pump, valve and component life. Particles in the 5 to 10 micro-millimetre (μm) size were determined to be the most abrasive particle size group and were the cause of severely reduced component life. In particular, the 7 μm particle was the perfect fit between the micro-machined clearances and would grind away on metal surfaces, causing accelerated wear.” (Sturgess 2003:78)

“Investigation has shown that the larger percentage of vehicles on our roads today use standard filters ranging from about 15 to 25 μm . More recently, high efficiency fuel filters- about 2 to 5 μm , have been introduced which are designed to cope with the higher pressures and smaller orifices (< 0.005 mm) of injector nozzles in modern engines. This places more demand on the need for a cleaner fuel to prevent premature blockage of filters which, in turn, will lead to filter replacement at frequencies shorter than the scheduled maintenance.” (Abraham 2001:1-4)

Thus, relying on filtration only to ensure clean fuel is not necessarily adequate in the prevention of injector damage and the potentially catastrophic engine failures associated with this. As such many large diesel consumers make use of test procedures to measure diesel cleanliness.

3.1.2 Gravimetric methods

“Gravimetric methods are specified to measure sediment (particulates) in diesel. A known volume of fuel is filtered through a pre-weighed test membrane filter (0.8 μm) and the increase in the membrane filter mass is determined after washing and drying. The change in the mass of the control membrane filter, located immediately below the test filter, is also determined. The particulate content is determined from the increase in mass of the test membrane filter relative to the control membrane filter. The result is reported in mg/L, which can be converted to mg/kg or ppm (parts per million) by dividing by the density. Table 3-2 shows the different gravimetric methods used for monitoring contamination in diesel. Note the wide range that exists in the maximum specifications, for example, SANS 342 through to the US federal specification.” (Abraham 2001:1-4)

Source	Test name	Number	Max. Specification m/m
SANS 342 - 2006	Sediment content	ASTM D473 /IP 53	50 ppm
European CEN (EN590)	Particulate	DIN 51419	27 ppm (24mg/L)
MTU/CAT	Total contamination	DIN 51419	24 ppm
US Federal (VV-F-800C)	Particulate contamination	ASTM D2276/IP 415	12 ppm (10mg/L)

It is notable that the standard set for South Africa (SANS 342:2006) has been amended to fall in line with the European EN 590 specification. However the total contamination limit for SANS 342, specified from the pump nozzle, remains the most relaxed. Although gravimetric testing goes a long way to preventing fuel induced injector failure it requires a laboratory for the testing to be conducted (either on site or independently). The success of this type of maintenance strategy relies heavily on regular testing and good house keeping by the user.

3.1.3 Particle Counters

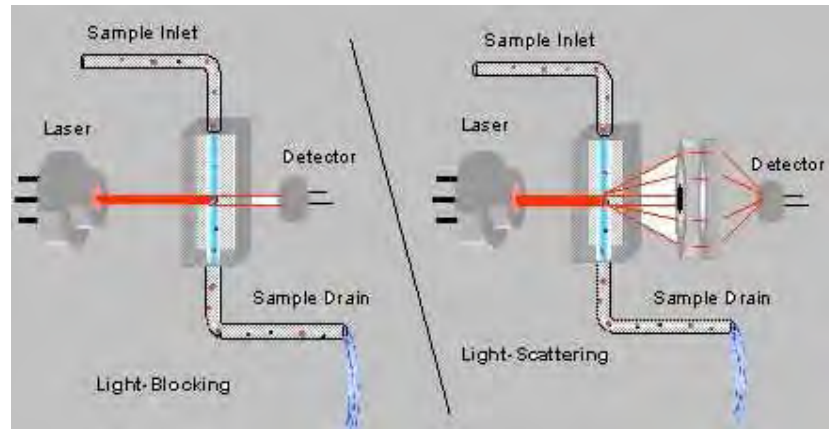


Figure 3-1: Chemtrac Systems portable fuel/oil particle counter.
(Courtesy Chemtrac Systems online catalogue 2004)

Figure 3-1 above depicts a Chemtrac PC 2400 PS particle counter (Chemtrac Systems online catalogue 2004). Several similar portable optical particle counters are available to measure the level of fuel contamination in the field and facilitate corrective actions to prevent injector failures due to solid particle ingress. Most counters used for fuel and oil contamination measurement, are claimed to be able to pick up particles in the order of 1 μm size.

The counters can also be used to determine the quantity of wear debris present in oil samples taken from an engine, thus serving to indicate the level of wear in the engine. “Most particle counters utilize light or infrared energy to illuminate individual particles one by one and are referred to as optical particle counters. They are most often used for detecting contamination and are sensitive to the parts per million range. Other particle detectors, like the electrical conductivity particle counter and most particle sizers, are not useful for contamination applications because they require special fluids or observe particle clouds and infer particle size distribution by settling time or complex optical diffraction patterns.” (Hunt 2004 1:3)

Typically counters that measure particles up to 1 μm detect the light blocked by particles as illustrated on the left of Figure 3-2 below. For fuel monitoring applications this type of counter works best since it more accurately sizes larger dark and rough particles.



• **Figure 3-2: Light blocking sensor (left) compared to a light scattering sensor (right) (Hunt 2004: pg 1)**

For particles smaller than 1 μm in size the counters use the more sensitive light-scatter sensors as depicted on the right of Figure 3-2 above.

“Portable particle counting systems are often self-powered, either by battery alone or in combination with pressurized gas cartridges. When the fluid is thin, a self-priming internal pump is used to aspirate the fluid from the sample source and draw it through the sensor. However, when the fluid is viscous the sample is driven through the sensor using gas pressure derived from an on-board pump, or high-pressure gas cartridge.” (Hunt 2004 1:3).

Although these counters are not 100% accurate due to deviations in liquid opaqueness and particulate shape, they do serve as a good tool for injector failure prevention due to fuel contamination. They can however, not give any indication of the lubricity levels of the fuel.

Affordable on-line particle counters have recently become available for real-time monitoring of fluid cleanliness. However these counters are not currently readily employed by machine manufacturers in their equipment, to alert the operator or

maintenance staff while the vehicle is being operated. As such, regular monitoring by maintenance staff is still required for this injector failure prevention tool to be effective.

3.2 Current Condition Based Maintenance Techniques

3.2.1 Engine signature analysis

3.2.1.1 Combustion pressure analysis

By inserting pressure sensors into the cylinder heads of diesel engines, pressure versus crank angle (P- θ) signatures may be recorded that form the basis for combustion analysis. This type of installation is typically accomplished by drilling a hole in the engine cylinder head and inserting a quartz piezoelectric pressure transducer. Such an installation (all be it in a petrol engine) is depicted below in Figure 3-3.

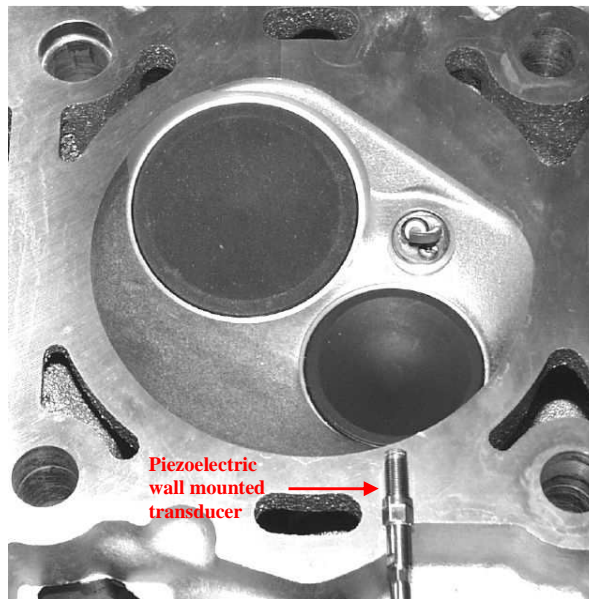


Figure 3-3: Wall mounted pressure transducer shown removed from its mounting location in the cylinder head, but directly positioned directly above it for clarity (mounting hole not visible in this picture) (Roth, Sobiesiak, Robertson & Yates 2002: pg2)

Figure 3-4 below depicts just such a P- θ signature for one cylinder of a Ford transit 2.5 litre diesel engine that has been recorded using a pressure transducer that measures cylinder pressures through a hole that was drilled in the engine cylinder head.

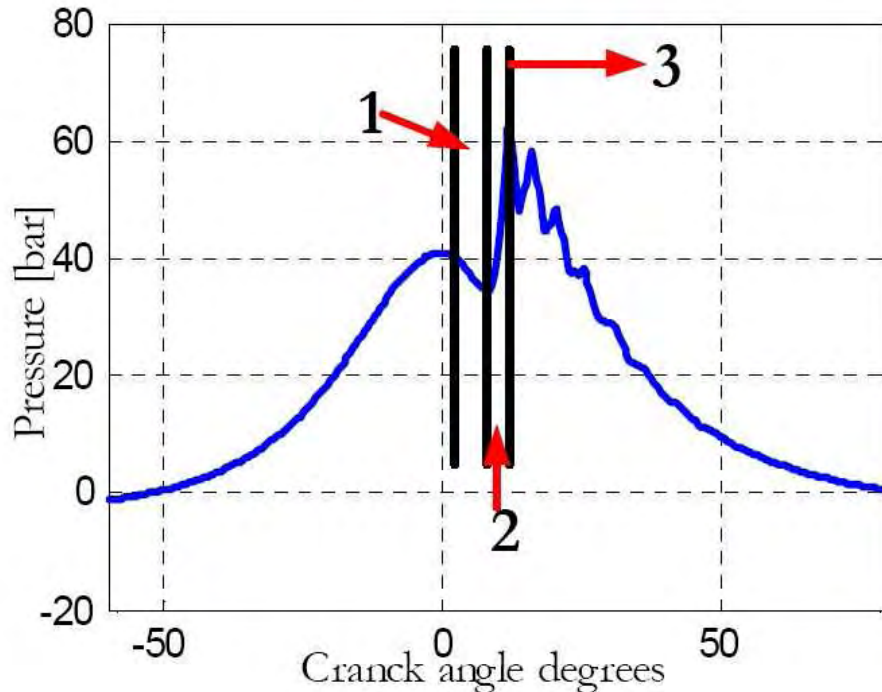


Figure 3-4: Pressure vs. crank angle signature (P- θ) diagram
(Goldwine, deBotton, Rivin & Sher 2004: pg 3)

A number of combustion parameters may be derived from this P- θ curve. With reference to Figure 3-4, the most critical combustion phases for a diesel engine are:

- Zone1: Ignition delay phase – the period between the start of fuel injection into the combustion chamber and the start of combustion, determined from the change in slope of the P- θ curve ($dP/d\theta$). Characterised by a slight drop in cylinder pressure as the injected fuel droplets partially evaporate to form premixed regions above the piston that are ready to ignite.
- Zone2: Rapid combustion phase – conditions within the cylinder become such that the fuel/air mixture autoignites resulting in rapid heat release.

Characterised by a sharp rise in pressure to a peak value over a few crank angle degrees.

- Zone3: Controlled and late combustion phase – a period of controlled heat release governed by the rate at which fuel vapour and air mix. Characterised by a tapering off in pressure as the piston is forced downwards before the hot gasses are exhausted.

Using combustion pressure signature analysis, a profile of these parameters may be recorded for each cylinder and stored for comparison with future readings. Should there be a significant deviation in the critical values from the norm, it may serve as an indication that a combustion irregularity is occurring. A lengthening in the ignition delay period may for instance amongst other factors flag a drop in the Cetane value of the fuel being used. Drop offs in peak cylinder pressure could be attributed to a number of factors; compression loss, change in fuel density and hence indicated power as well as injection equipment malfunction to name but a few.

From the preceding discussion it seems evident that combustion pressure analysis reveals a detailed picture of what is taking place within the combustion chamber and can with a high degree of confidence be used to identify a breakdown in the combustion process. As such the technique has been extensively applied by researchers and manufacturers to laboratory test engines to better understand the combustion process. Application of the technique does however require invasive machining that involves removal of the cylinder head to accurately drill the holes that the quartz piezoelectric pressure transducers will be mounted in.

Research has also been conducted on the feasibility of using far more compact optical fibre type pressure transducers that require less intrusive methods of mounting within an engine. Such research was conducted by Roth, Sobiesiak, Robertson and Yates (SAE paper 2002-01-0745). The research achieved fairly good correlation between the tradition piezoelectric type transducers and the optical fibre transducers which were compact enough (1.7mm diameter) to be mounted in a specially modified spark plug assembly that could be fitted to an

unmodified engine. It is envisioned that the same technology could be applied to diesel engines using specially modified injector tips that could house both the needle and the fibre optic pressure transducer. This would however require dedicated engine specific test injectors which would make it impractical and costly to transfer a system based on this technology between engines outside of the laboratory environment.

3.2.1.2 Vibration and ultrasonic data

Vibration analysis is used extensively in industry to detect faults in both stationary and mobile rotating machinery. Quartz piezoelectric crystal transducers called accelerometers measure tiny displacements over time from which velocity and acceleration time waveforms may be calculated using differentiation of the displacement signals. Application of Fast Fourier Transform mathematics to these time based waveforms transforms them into frequency based waveforms that allow a diagnostician to correlate peak amplitudes with specific frequencies. As such impacts from defects on components such as bearings and gears can be detected using accelerometer transducers mounted on or adjacent to components of interest. The transducers may be mounted using such non intrusive methods as magnets or simply bonding them to bare metal surfaces. Depending on the component of interest, experience shows that machines have one or more ‘sweet spots’ for transducer mounting that gives maximum signal with minimum background noise. The interpretation of vibration and ultrasonic signatures involves pattern recognition depicting:

- Increase or decrease in amplitude or change in shape
- Appearances of new or disappearance of previously seen vibrations
- Changes in timing of events

It seems plausible that this measurement technique could also be applied to engines, specifically the combustion process, as this is a cyclic process that

produces distinct pressure pulses as laid out in Section 3.2.1.1. Such a study has been conducted by Goldwine, deBotton, Rivin and Sher (SAE paper 2004-01-1786) to investigate the relationship between the vibration signatures measured on a diesel engine and the combustion process. The experimental procedure involved comparison of the pressure pulses measured within the combustion chamber of the engine using a pressure transducer (refer to Section 3.2.1.1 and Figure 3-4) with the vibration signatures measured using an accelerometer magnetically attached to one of the head bolts. This allowed the tensile displacement of the head bolt to be measured as pressure pulses within the combustion chamber lift and lower the cylinder head off the block deck during the combustion process. The vibration measurement produced acceleration/time waveforms as depicted in Figure 3-5.

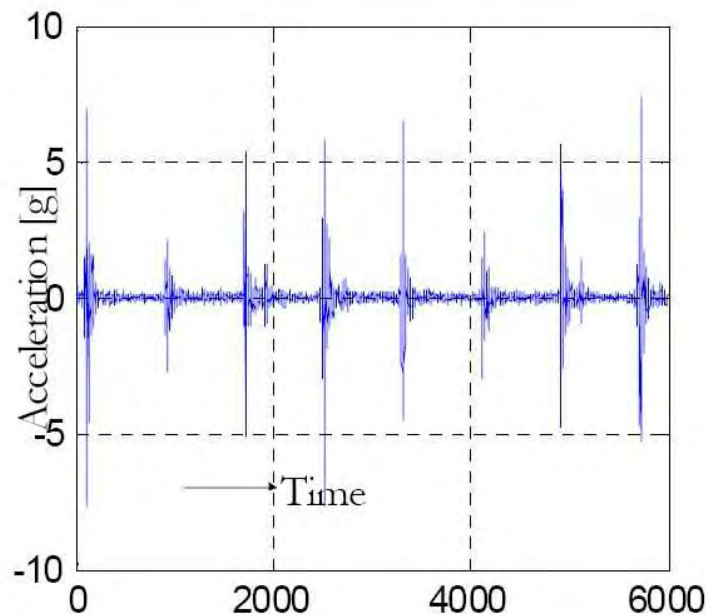


Figure 3-5: Acceleration/time waveform (Goldwine, deBotton, Rivin & Sher 2004: pg 4)

By overlaying a single power stroke pressure versus crank angle plot of Figure 3-4 with the associated vibration signature of Figure 3-5, correlated back to crank angle degrees, Figure 3-6 was obtained

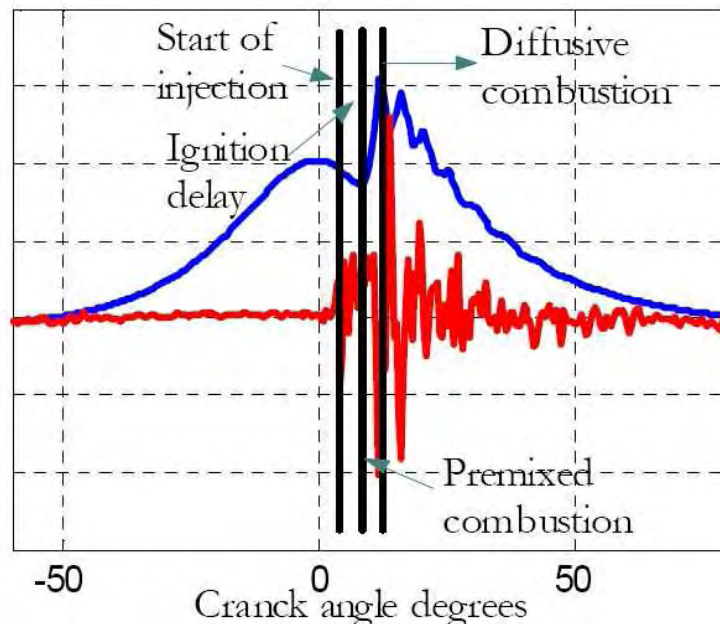


Figure 3-6: Pressure trace overlaid with vibration trace (Goldwine, deBotton, Rivin & Sher 2004: pg 4)

The researchers in this paper drew a correlation between the peak cylinder pressure brought on during the rapid combustion phase by autoignition of the fuel mixture and the peak vibration pulses measured. Thus parallels were drawn between the amplitudes of the pressure and vibration signatures as well as the timing of these events. Using this measurement technique would enable the contribution of each cylinder to the total engine power to be analyzed. Combustion malfunctions such as compression loss and a breakdown in fuel delivery were simulated on the instrumented cylinder of the test engine and changes in the amplitude and timing of the peak vibration were observed. The results from this study indicated that peak vibration measurement could be used as a diagnostic tool to ascertain the combustion strength within individual cylinders of an engine.

Vibration and ultrasonic engine signatures can also be used to indicate the mechanical condition of an engine's injection equipment. The data is analysed for event timing and magnitude to verify that events such as injection valve opening and closing occur at the anticipated time. For monitoring the injection

system, accelerometers could be situated on components such as the injector pump body or common fuel delivery rail.

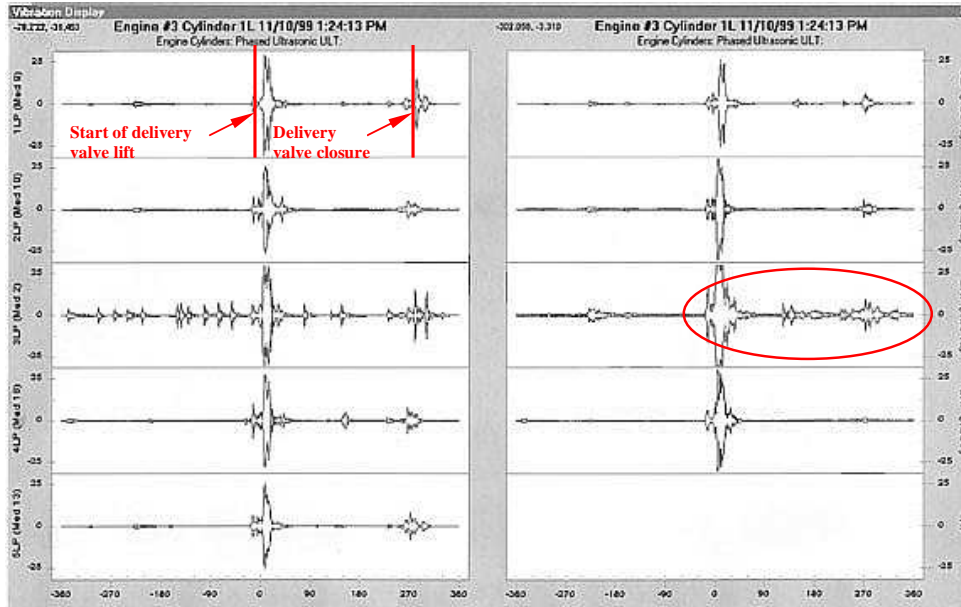


Figure 3-7: Vibration signatures for the 9 pump elements of a medium speed 9 cylinder diesel engine. (O’Connel & Haller 2002: pg 11)

Figure 3-7 illustrates the ultrasonic signatures of the pump elements of a medium-speed nine-cylinder diesel engine. Since the injectors were of the unit type, individual vibration transducers were placed on the base of each of the high-pressure fuel injection pumps. With reference to Figure 3-7, the delivery valve lift and fuel flow signals are readily apparent for each fuel pump. However there are extraneous events on the signature for cylinder no. 3 and the beginnings there of on cylinder no. 8 (encircled in Figure 3-7).

A repeating pattern of small mechanical impact spikes on the signature of cylinder no. 3 suggests degradation of a component operating at some multiple of the crankshaft speed. The fault could possibly be associated with a surface defect on the cylindrical cam follower roller that drives the rocker depressing the pump plunger. Inspection of the miscellaneous signal on the signature of cylinder no. 8 may also suggest that the pump plunger is sticking within or

rubbing against the inside of the pump body during the lift and return duration of the drive cam lobe.

The preceding texts indicate that vibration analysis can be used to indicate a breakdown in the combustion process as well as mechanical malfunction within the actual injection equipment. The technique is also relatively non invasive as vibration transducers can be fixed to the surfaces of components of interest without requiring any major material removal. However the cost of the accelerometers, data acquisition equipment and software necessary to analyse the data is substantial. Analysis of the waveforms such as those portrayed in Figure 3-7 is not trivial and discernment of the causes for the signal irregularities relies heavily on the skill and experience of the analyst as well as an intimate knowledge of the type of injection system being used on a specific engine. Afore mentioned factors would add to the cost and complexity of a system based on this measuring technique and detracts from its ability to be readily transferred between different engines.

3.2.1.3 Exhaust gas temperature measurement

Exhaust gas temperature measurement has been used extensively throughout the development of the internal combustion engine to better understand the heat transfer and hence thermal energy release to atmosphere process that takes place across the exhaust port during combustion. Traditionally thermocouple temperature transducers have been used to measure the average exhaust gas temperature per cycle during the operation of an internal combustion engine. Thermocouples do not measure the instantaneous exhaust gas temperature as their dynamic response to temperature changes is limited to approximately 5 Hertz depending on the type of thermocouple. This is far too slow to measure instantaneous temperatures in a four stroke diesel engine running at 4000 revolutions per minute which would be exhausting at 33 Hertz. However compensation techniques such as those developed by Kar, Roberts, Stone, Oldfield and French (SAE Paper 2004-01-1418) have helped these relatively simple thermometers recover temperature variations of up to 80 Hertz.

The relationship between engine load, engine speed and exhaust gas temperature has been well documented. Increasing load and speed in a diesel engine by injecting more fuel into the combustion chamber raises exhaust gas temperatures as the mass flow rate of combustion gasses is increased during the exhaust stroke and the time available for heat transfer to the cylinder walls, combustion chamber, exhaust valve and port is diminished.

Engine load and speed is expressed as power for a four-stroke cycle engine by the following equation:

Equation 3-1

$$P_i = 0.5\eta_f\eta_vNV_dQ_{HV}\rho_{a,i}(F/A)$$

Where:

- Fuel conversion efficiency (η_f)
- Volumetric efficiency (η_v)
- Engine speed (N)
- Displacement volume (V_d)
- Fuel heating value or energy content (Q_{HV})
- Inlet air density ($\rho_{a,i}$)
- Fuel/air equivalence ratio (F/A)

all contribute. These factors thus have a direct and measurable influence on the exhaust gas temperature.

The relatively low cost of thermocouples, their robust construction and the fact that a number of the larger diesel engines already come fitted with individual exhaust port mounted thermocouples lends itself to developing a technique around this particular measurement technology that can detect combustion irregularities due to injection equipment malfunction.

4.0 CHAPTER IV - INVESTIGATION INTO THE EFFECTS THAT DAMAGED INJECTORS HAVE ON EXHAUST GAS TEMPERATURE

4.1 Test Setup on University of Pretoria Dynamometer

4.1.1 Test Equipment

Laboratory testing was conducted, using a Ford R2, 2200 cm³ four cylinder normally aspirated diesel engine that was acquired and mounted on the University's SF-901 engine dynamometer. A photograph of the engine, mounted on the dynamometer, is shown below in figure 4.1.

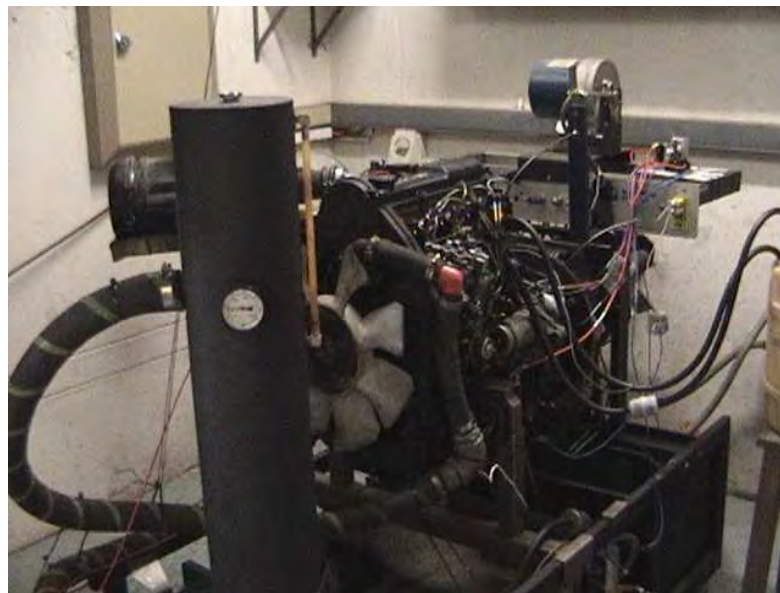


Figure 4-1: Photograph of engine mounted on SuperFlow dynamometer

“The SF-901 is an engine dynamometer test system manufactured by the American SuperFlow Corporation. It measures or calculates 43 engine performance characteristics. The basic system includes all parts necessary to provide accurate and reliable tests without adding additional equipment.” (SuperFlow Corporation 1992: 1-1). The dynamometer system is illustrated in Figure 4-2.

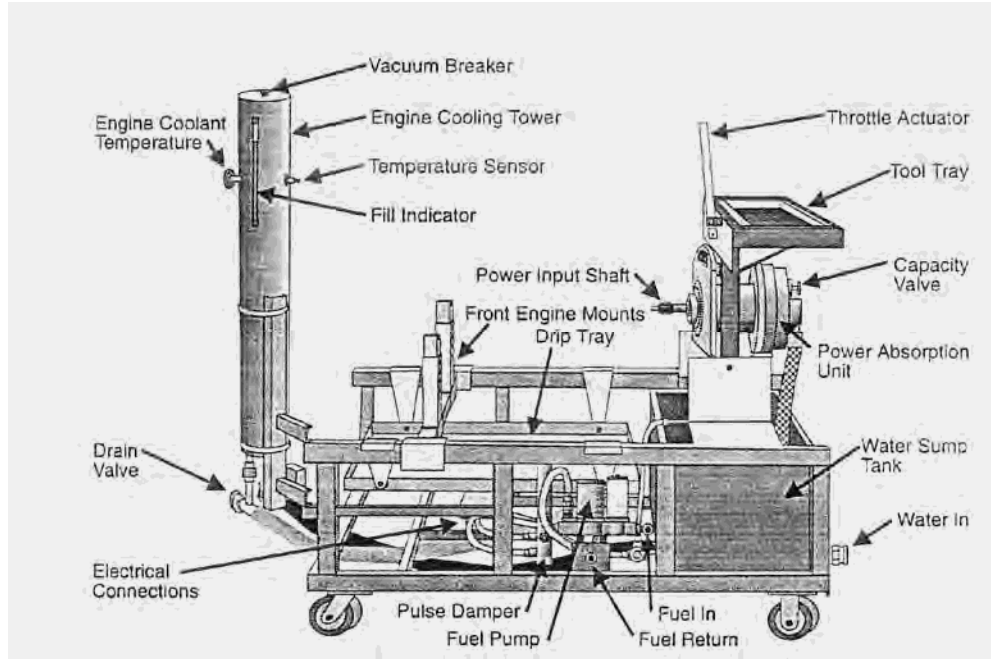


Figure 4-2: SF-901 dynamometer engine stand (SuperFlow Corporation 1992: 1-5)

The basic system components comprise:

- **Engine Stand-** “The SF901 engine stand provides all of the connections from sensors to the SF-901 Console. The stand also provides the mount for the engine and Power absorber. The fuel system and the Cooling Tower are part of the stand and a removable drip pan and dual battery mounting rack are attached to the stand base.” (SuperFlow Corporation 1992: 1-1)
- **Power Absorber-** “The standard engine power absorption unit provides all of the ability to handle torque of up to 1 350 Newton metre (Nm) and can operate up 10 000 RPM. This unit provides the ability to measure power up to 750 kilo watt (kW).” (SuperFlow Corporation 1992: 1-1)
- **Fuel System-** “The fuel system consists of a filter, pump, accumulator, flow sensors, pressure gauges and regulators to provide two measured fuel outlets. The fuel supply and return lines are connected to the SF-901 stand using 12 mm inner diameter fuel resistant hoses.” (SuperFlow Corporation 1992: 1-1)

- **Cooling Tower-** “The engine cooling tower replaces the radiator for water cooled engines. The thermostat on the cooling tower can be set to control the engine water temperature between 65°C and 90°C of a non-pressurized system. The cooling tower is mounted on the engine test stand and swings away for easy engine mounting.” (SuperFlow Corporation 1992: 1-1)
- **Control Console-** “The console displays and records data from the sensors on the engine test stand. The console has four large, mirror scale analogue metres for monitoring temperatures , voltages, power, torque, engine RPM and fuel. Two digital displays show the same information with greater accuracy. Control switches on the console allow for numerous pre-defined standard engine test cycles to be run.” (SuperFlow Corporation 1992: 1-2)
- **Desk Top Computer-** An IBM Pentium II desk top computer is attached via serial cable to the control console. A Microsoft Windows compatible version of the SuperFlow SF901 data storage programme called “Windyno” (SuperFlow Corporation 1996) has been loaded onto the computer. This not only allows the data downloaded from each dynamometer run to be imported and stored onto the computer using Microsoft Excel. It also allows all of the analogue gauges and displays on the Control Console to be integrated into a single display on the computer screen.

4.1.2 Experimental Setup

The test engine was mounted onto the dynamometer using a trolley hoist jack to slide the engine flywheel inner splines over the mating splines of the dynamometer power input shaft. Solid engine mountings were then manufactured out of 5 mm thick, 70 x 50 mm channel iron and bolted to the adjustable mounting posts of the dynamometer, using M8 x 90 mm grade 8.8 bolts and nylock nuts, to secure the engine in place.

The engine was operated in as close to standard setup as possible in an attempt simulate the state of tune and condition it would be in as fitted to a road going vehicle. This meant that the standard intake air filter was retained and that an

OEM equivalent specification 4 Micron (nominal) fuel filter was employed on the fuel supply line to the injector pump. Two small 20 Micron (nominal) inline strainers were also added to the tank and fuel supply line in an attempt to simulate the tank mounted and inline strainers fitted to the donor vehicle of the engine.

The SF-901 dynamometer caters for the measurement of exhaust gas temperatures of up to eight cylinders of a test engine. The SF-901 is supplied with a set of calibrated K-type thermocouples that plug directly into the sensor input panel at the rear of the dynamometer as indicated by the arrows in Figure 4-3.

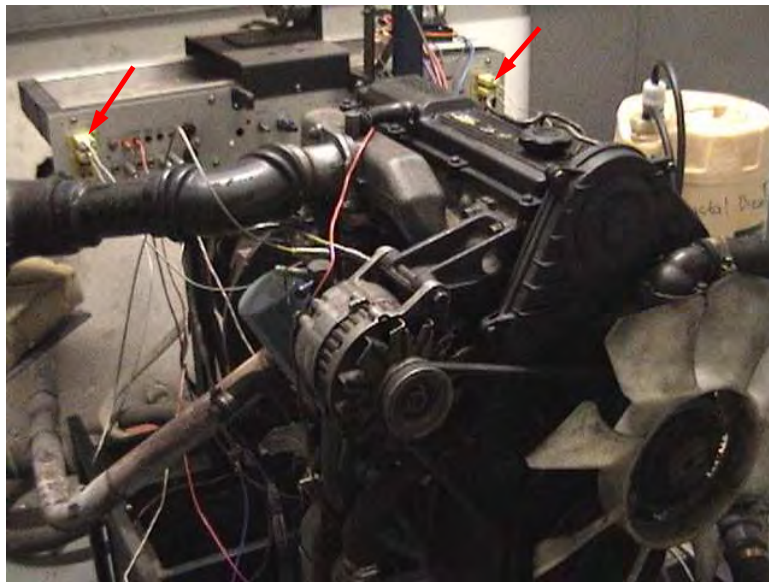


Figure 4-3: Photograph of thermocouples plugged directly into dynamometer sensor input panel

These thermocouples allow for temperature readings between 0 °C and 1000 °C and the dynamometer gives a temperature reading rounded off to the nearest 10°C. While it is granted that a relatively small, normally aspirated, four cylinder engine such as the afore mentioned will not generate exhaust gas temperature (EGT) readings that can directly be compared to the large turbo charged diesels used in mine applications, the Ford R2 is a simple engine that is cheap to operate.

The results discussed in the following text simply serve to illustrate that EGT monitoring can pick up faulty fuel injection and that this principle can be successfully applied to the larger diesel engines. These variances in EGT readings could be due to injectors malfunctioning as a result of damage resulting from diesel fuel laced with illuminating paraffin. Alternatively, the ingress of dirt particles and water into the injection equipment from contaminated fuel could also have a similar effect.

Holes were drilled in the engine's exhaust manifold and K-type thermocouples were inserted in the positions indicated in Figure 4-4.



Figure 4-4: Photograph of thermocouple mounting points in exhaust manifold

Due to space constrictions from engine components such as the alternator and oil cooler the thermocouples could not be placed identically with respect to one another on the manifold, as is evident from Figure 4-5. With this in mind an attempt was made to place the thermocouples in as similar a position as possible, relative to the exhaust ports and one another, along the bends of the manifold.

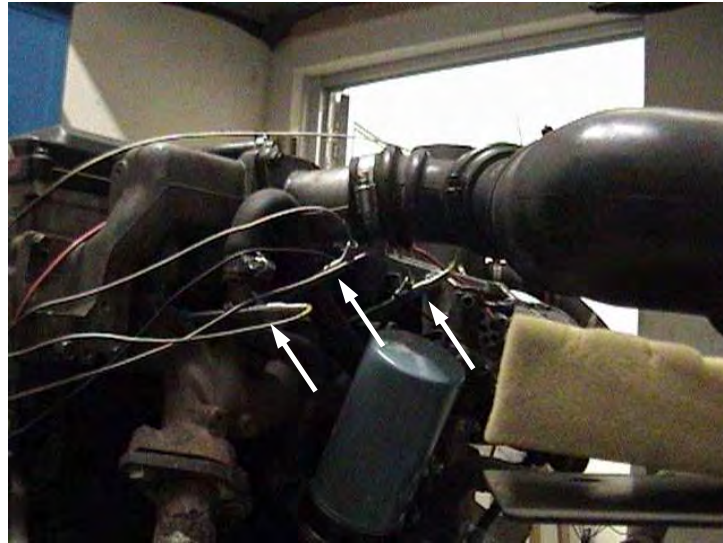


Figure 4-5: Arrows in photograph indicate thermocouple positions on engine exhaust manifold

The points of placement were estimated to be where the exhaust gasses would be at their hottest and most rapid on leaving the exhaust ports. Care was taken to insert each thermocouple to a uniform depth, with the tip protruding approx. 3mm into the inside of the manifold. Figure 4-6 and Figure 4-7 show the thermocouples protruding into the exhaust manifold on cylinders one and four.



Figure 4-6: Photograph of thermocouple protruding into cylinder 4 outlet



Figure 4-7: Photograph of thermocouple protruding into cylinder 1 outlet

4.1.3 Experimental Procedure

Initial experimentation led to the discovery that EGT deviation from the norm due to incorrect combustion, is most prominent under wide open throttle (maximum fuel delivery) conditions where the engine is working at its hardest. As such, the decision was taken to concentrate on maximum fuel delivery, full load conditions where the most severe engine damage takes place and where the temperature deviations are at their most extreme. These conditions are also typical of a great portion of the operating conditions experienced by mining and heavy earth moving equipment.

In order to investigate the combustion irregularities produced by a malfunctioning injection system, needles that had been adversely worn or purposely damaged were used. The test engine was operated on the dynamometer with the defective injectors consecutively inserted into different cylinders and the effect on exhaust gas temperature was recorded. This was then compared with the results obtained for the test engine operated with properly functioning, new injectors. The dynamometer runs for the properly functioning injector/cylinder combinations were repeated on five consecutive days to incorporate the effects of differing ambient temperatures on EGT. These

differences formed the ‘envelope’ for acceptable EGT readings under correct injection system operation.

4.1.3.1 Injector damage

Two types of damaged injector needles were used for the investigation:

A needle with excessive wear marks on the sealing face on its tip, evident under the microscope in Figure 4-8. This wear is typical of the long-term wear experienced on pintle type injectors during normal use.

A second needle with severe scratches on its flanks, applied to induce seizing within the injector tip body, is visible in Figure 4-9 and Figure 4-10. These scratches were purposely made on the needle to represent the type of damage caused by solid particle ingress into the injectors and/or poor lubricity fuel.

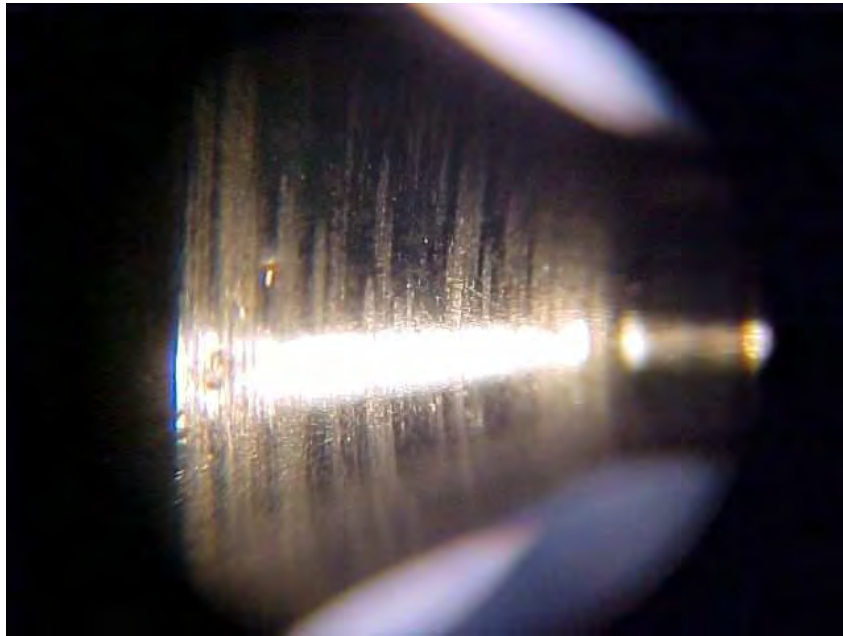


Figure 4-8: Photograph of wear damage induced on sealing face of injector needle to facilitate leakage at 20X magnification



Figure 4-9: The arrow on this photograph indicates a large vertical scratch purposely affected to facilitate seizing of the needle within the injector tip



Figure 4-10: A view of the needle damage captured under 100X magnification as indicated by the arrow. Note that small pieces of material were ripped out of the needle surface as it was forced to reciprocate within the needle

4.1.3.2 Fuel blending

Finally, illuminating paraffin was blended in with the diesel fuel to give a 2/3 IP to 1/3 diesel ratio. The engine was run at constant speed and maximum torque to study the effects on EGT of the degrading injectors.

4.1.4 Results

4.1.4.1 Properly functioning injectors

Working on the assumption that there would be a variance in exhaust gas temperatures from cylinder to cylinder in any internal combustion engine, initial testing consisted of establishing the degree of this variance in the test engine. After the engine had been put through a warm up cycle and had reached a normal operating condition of 74°C coolant temperature, multiple consecutive runs at maximum fuel delivery and load were completed. Figure 4-11 depicts a typical spread of the exhaust gas temperatures measured in each of the four cylinders across the engine operating speed range of 1 500 RPM to 4 000 RPM for a set of properly functioning injectors.

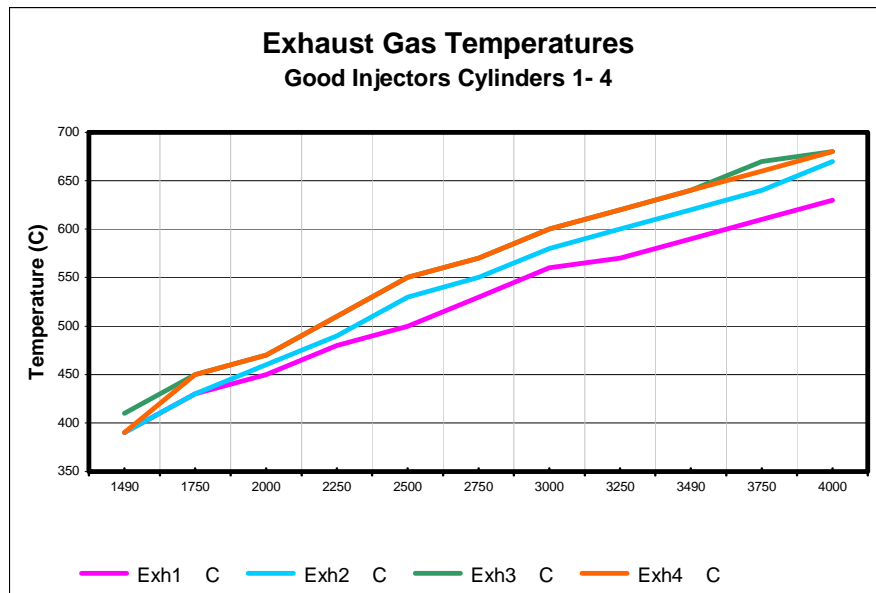


Figure 4-11: Exhaust gas temperature envelope for properly functioning injectors

The engine speed range of 1 500 RPM to 4 000 RPM was used as the standard for all laboratory testing as this is the range in which the engine delivers sufficient usable torque for the dynamometer to measure accurately. Figure 4-11 indicates that there is a variance in temperature between the different cylinders of the test engine for the operating engine speed range. This may be ascribed to the following factors:

- The thermocouples could not all be mounted in the exhaust manifold with identical orientation with respect to the respective exhaust ports in the cylinder head. (Section 4.1.2: 59)
- Figure 4-11 indicates that cylinder number one and to a slightly lesser degree, cylinder number two, produces EGT readings that are markedly lower than those measured for cylinders three and four. The reason for the front two cylinders running cooler may be explained by their immediate proximity to the water pump outlet. It seems reasonable to conclude that cylinder number one would receive the coolest charge of cooling fluid and that its cylinder walls would benefit most from the convection of heat by the coolant, followed by cylinder number two. This would certainly also contribute to lower combustion chamber temperatures in the front cylinders than the rear ones.
- Atmospheric and ambient temperature conditions vary from day to day resulting in slightly different readings from one day to the next on the same cylinder.

The above results led to the need to establish the degree of variance between the four cylinder EGT readings across the usable engine speed range for properly functioning injectors. Statistical analysis was applied to multiple dynamometer runs conducted on different days to account for differences in atmospheric conditions and temperatures. 24 data points per engine speed range were analysed in an attempt to assess how great the temperature spread between cylinders is at a given engine speed and load. The standard deviations

for both full load and half load conditions were calculated, (refer to Annexure: A) and are listed in Table 4-1.

Table 4-1: Table of engine speed vs. EGT standard deviations for half and full load conditions over multiple dynamometer runs

Engine Speed (RPM)	EGT Standard Deviations Under Full Load Conditions		EGT Standard Deviation Under Half Load Conditions	
	σ (°C)	1.6449 σ (°C)	σ (°C)	1.6449 σ (°C)
1 500	11	18	9	15
1 750	11	19	15	24
2 000	13	22	15	25
2 250	16	26	18	29
2 500	21	35	22	35
2 750	20	33	21	35
3 000	20	33	22	36
3 250	22	36	24	39
3 500	22	36	23	38
3 750	26	42	25	41
4 000	23	38	25	40

Table 4-1 contains both one standard deviation (σ) and the “90%” error deviation (1.6449 σ) across the usable engine speed range. The “90%” error values represent a tolerance band, within which, there is a 90% probability that the engine EGT readings will fall. (Beckwith, Marangoni, Lienhard 1995: 61) It is evident from Table 4-1 that the largest deviation between cylinder to cylinder EGT readings across the four cylinders occurs at an engine speed of 3 750 RPM for both full load and half load conditions.

The normal distribution of EGTs, under full load conditions for all four cylinders, with properly functioning injectors at an engine speed of 3 750 RPM has been plotted in Figure 4-12 for an engine speed of 3 750 RPM.

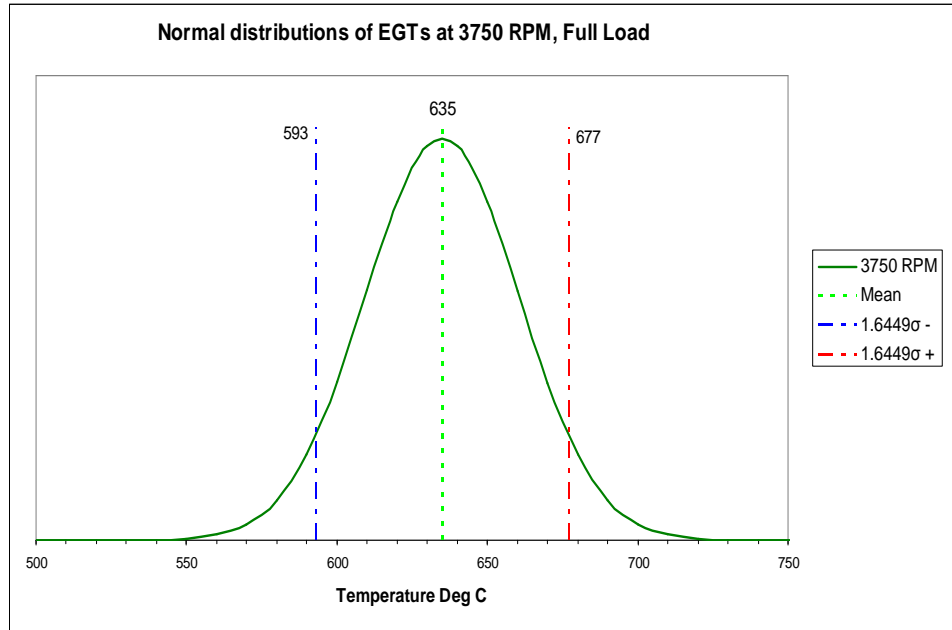


Figure 4-12: Normal distribution across all four cylinders of EGTs for properly functioning injectors at 3 750 RPM

Its associated histogram is plotted in Figure 4-13. The histogram serves to indicate in which 10°C incremented temperature bands the majority of readings from all four cylinders occur. Figure 4-13 shows that the majority of readings taken at this particular engine speed and load (21 of the 24 data points) occur within an 80°C envelope.

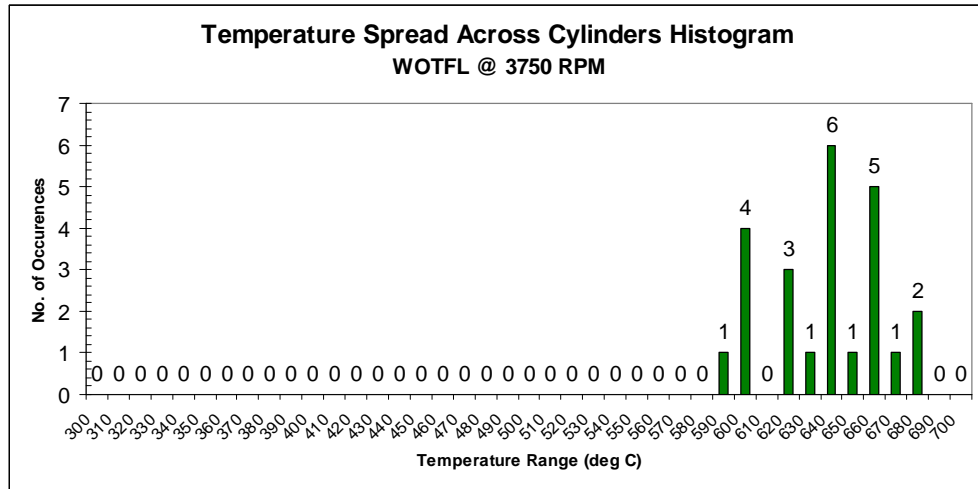


Figure 4-13: Histogram of measured temperature range distribution across all four cylinders for properly functioning injectors at 3 750 RPM

The mean of the EGT readings from which the normal distribution was calculated, together with the “90%” probability or 1.6449σ standard deviation points ($\pm 42^\circ$ Celsius) are overlaid on the normal distribution plotted in Figure 4-12. This means that for a set of properly functioning injectors, under normal operating conditions at 3 750 RPM, there is a 90% probability that the EGT temperature from each of the four cylinders will fall within the tolerance band of 593° Celsius to 677° Celsius.

Taking the afore mentioned data into account a decision was taken to adopt a $\pm 40^\circ$ Celsius envelope about the mean or average of the EGT readings recorded throughout the engine speed range. Figure 4-14 shows the $\pm 40^\circ$ Celsius envelope, overlaid onto a typical spread of the exhaust gas temperatures, measured in each of the four cylinders across the engine operating speed range of 1 500 RPM to 4 000 RPM for a set of properly functioning injectors.

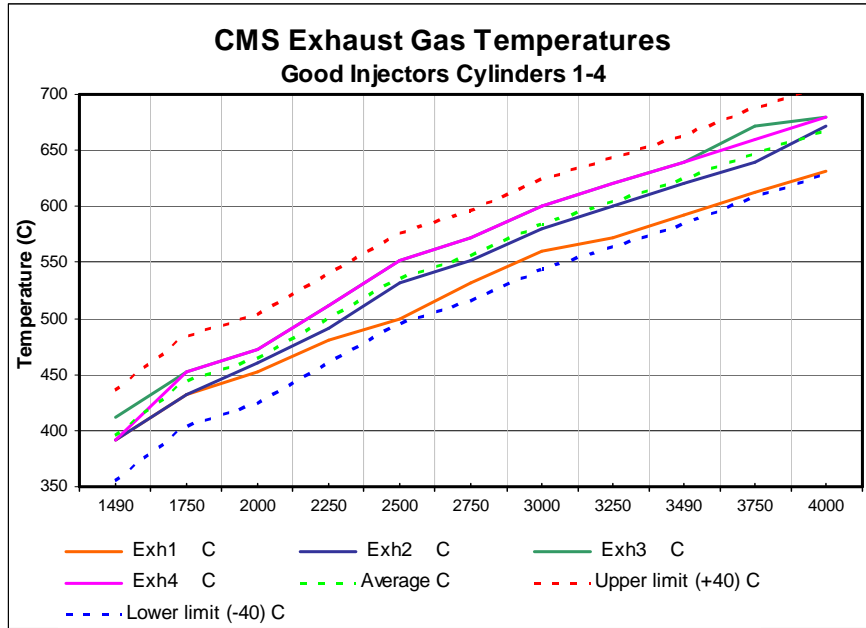


Figure 4-14: Exhaust gas temperature envelope for properly functioning injectors

Figure 4-14 confirms the statistical prediction of the normal distributions that the range of temperature variance between cylinders falls within a $\pm 40^\circ$ Celsius envelope about the average of the four cylinder's EGT readings.

4.1.4.2 Injector damage

Figure 4-15 shows the EGT readings from cylinder number one of the Ford R2 test engine. The data compares the EGT readings recorded for a properly functioning injector to that of the purposely damaged injector, previously shown in Figure 4-9 and discussed in section 4.1.3.1.

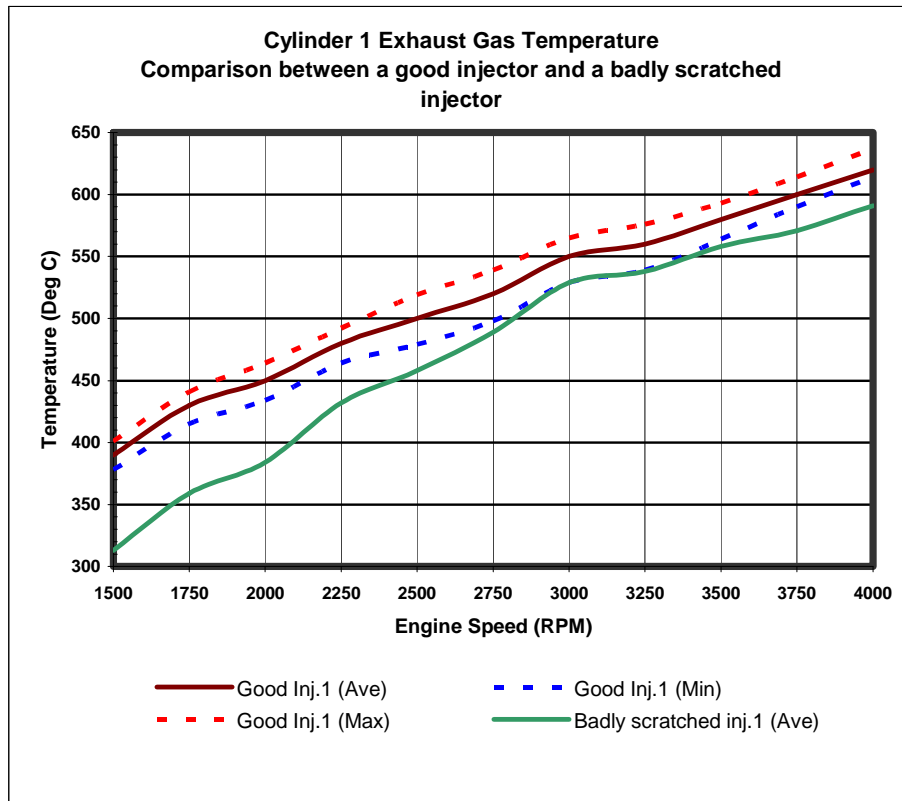


Figure 4-15: Good and badly scratched injector comparison graph of EGT readings taken from the thermocouple mounted in cylinder 1 exhaust

Four data plots have been constructed on this graph. The brown solid line represents the mean value of consecutive runs with a good injector in cylinder number one. The red and blue dashed lines represent the maximum and minimum values recorded during the five test runs respectively. They fall well within the $\pm 40^\circ$ Celcius tolerance band discussed in section 4.1.3.1, considered to be the acceptable EGT temperature variation per cylinder, during normal operation.

Figure 4-16 compares the EGT readings of the injector with damage to its sealing face (shown in Figure 4-8 and discussed in section 4.1.3.1), to that of a properly functioning injector.

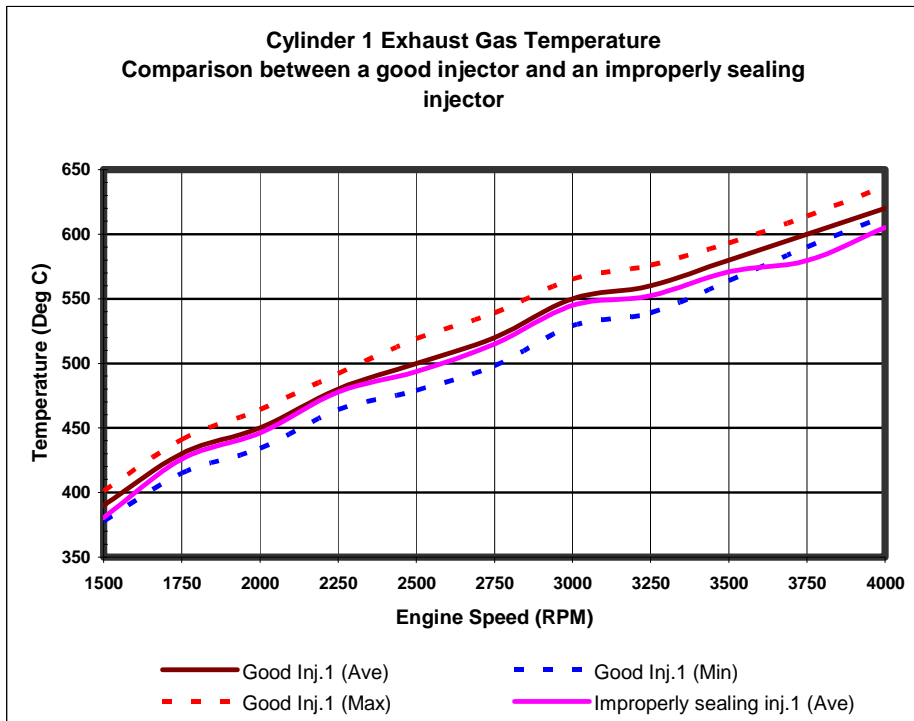


Figure 4-16: Good and improperly sealing injector comparison graph of EGT readings taken from the thermocouple mounted in cylinder 1 exhaust

The pink solid line in Figure 4-16, represents an injector with damage to its sealing face. It falls within the $\pm 40^{\circ}\text{C}$ tolerance band, regarded as “normal” for the greatest part of the engine speed range, only deviating below the bottom limit past 3 500 RPM. As such, the EGT variation is considered insufficient to raise alarm and thus cannot with be used to indicate this type of damage from the EGT readings with any certainty.

Figure 4-17 to Figure 4-22 hereafter plot the EGT readings for the scratched and improperly sealing injector tips vs the good injectors for the remaining cylinders on the test engine. The results are similar to those measured for cylinder number one.

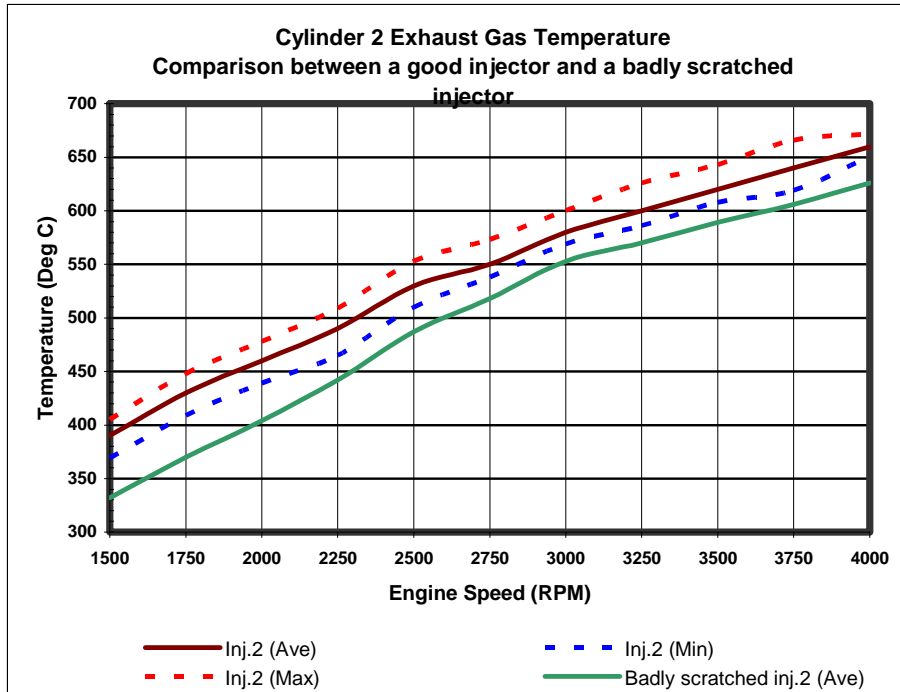


Figure 4-17: Good and badly scratched injector comparison graph of EGT readings taken from the thermocouple mounted in cylinder 2 exhaust

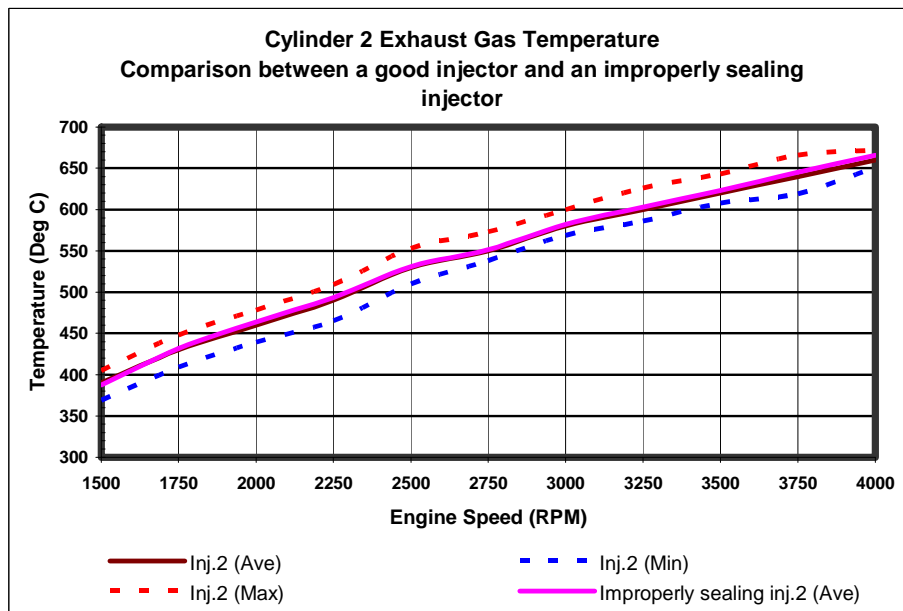


Figure 4-18: Good and improperly sealing injector comparison graph of EGT readings taken from the thermocouple mounted in cylinder 2 exhaust

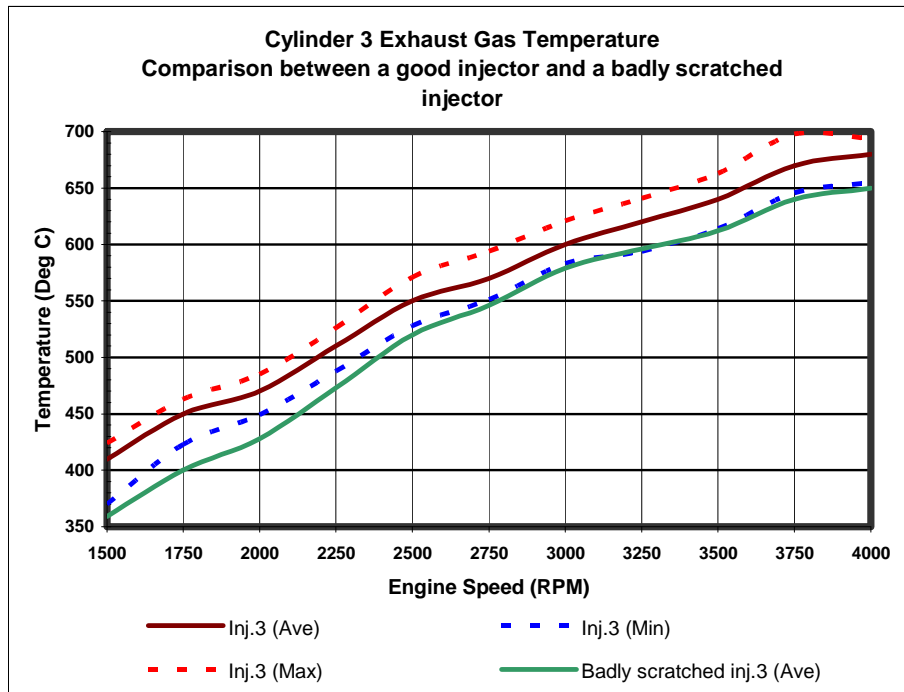


Figure 4-19: Good and badly scratched injector comparison graph of EGT readings taken from the thermocouple mounted in cylinder 3 exhaust

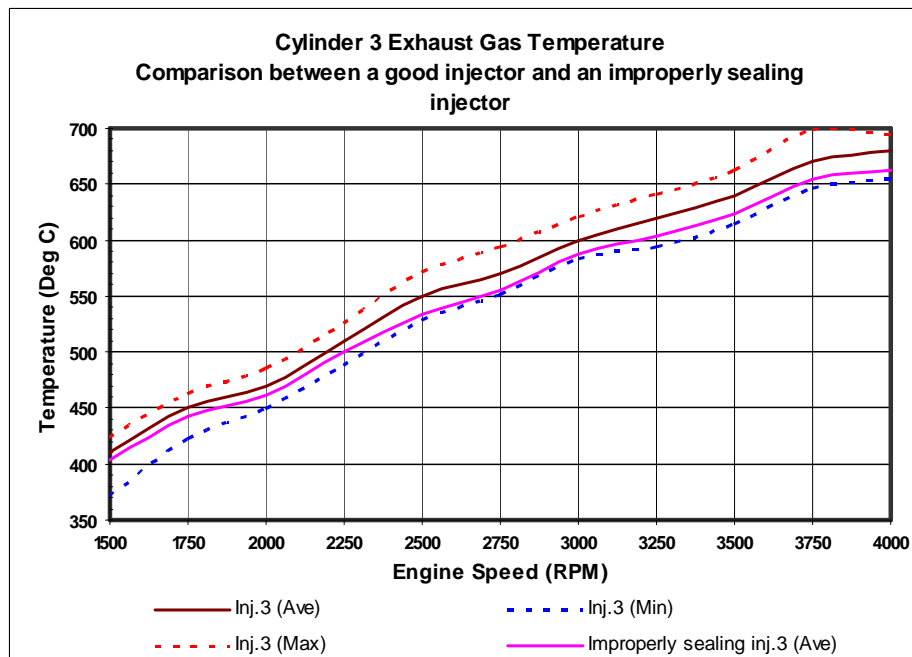


Figure 4-20: Good and improperly sealing injector comparison graph of EGT readings taken from the thermocouple mounted in cylinder 3 exhaust

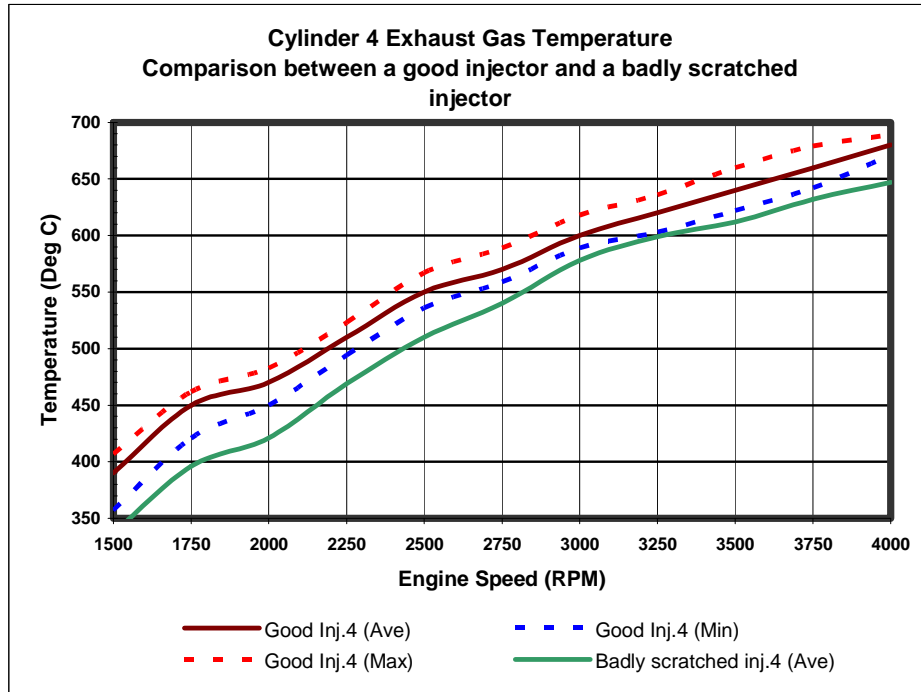


Figure 4-21: Good and badly scratched injector comparison graph of EGT readings taken from the thermocouple mounted in cylinder 4 exhaust

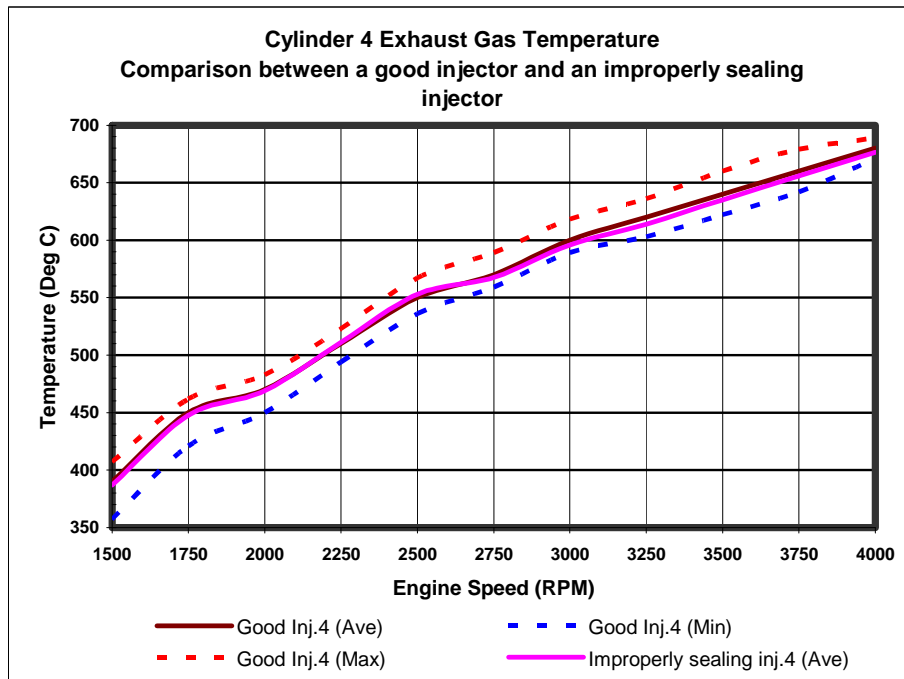


Figure 4-22: Good and improperly sealing injector comparison graph of EGT readings taken from the thermocouple mounted in cylinder 4 exhaust

The above results indicate that the effect of an injector, with a tip that has been scratched to such an extent that it seizes within its barrel, is measurable. The associated cylinder EGTs fall below the ‘normal operation envelope’ thus providing an indication of incomplete combustion. This can be ascribed to the cooler unburnt fuel droplets lowering the temperature of the exhaust gasses that are blown out of the exhaust manifold. *It should be noted that puffs of white smoke were visible from the external exhaust at this point during testing and that the engine experienced a marked loss in power.*

4.1.4.3 Fuel blending

The graphs depicted in Figure 4-23 to Figure 4-26 for cylinders 1 to 4 show the detrimental effects of blending in paraffin with a competent diesel fuel. Full load conditions were maintained at a constant engine speed of 2450 RPM for a period of 70 minutes for each test. Each test was carried out with a brand new injector tip.

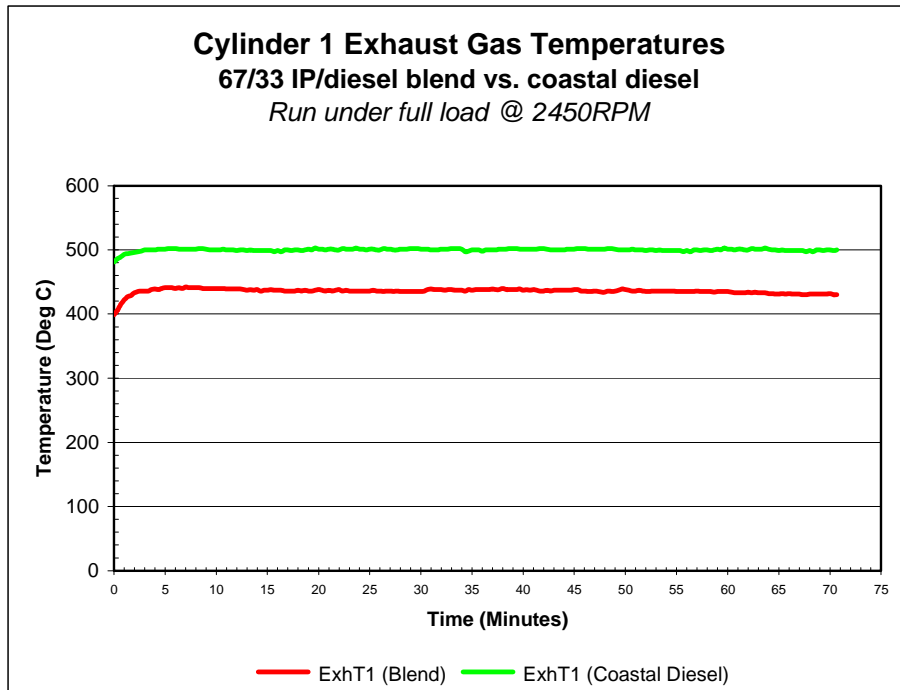


Figure 4-23: Injector degradation graph of EGT readings taken from the thermocouple mounted in cylinder 1 exhaust

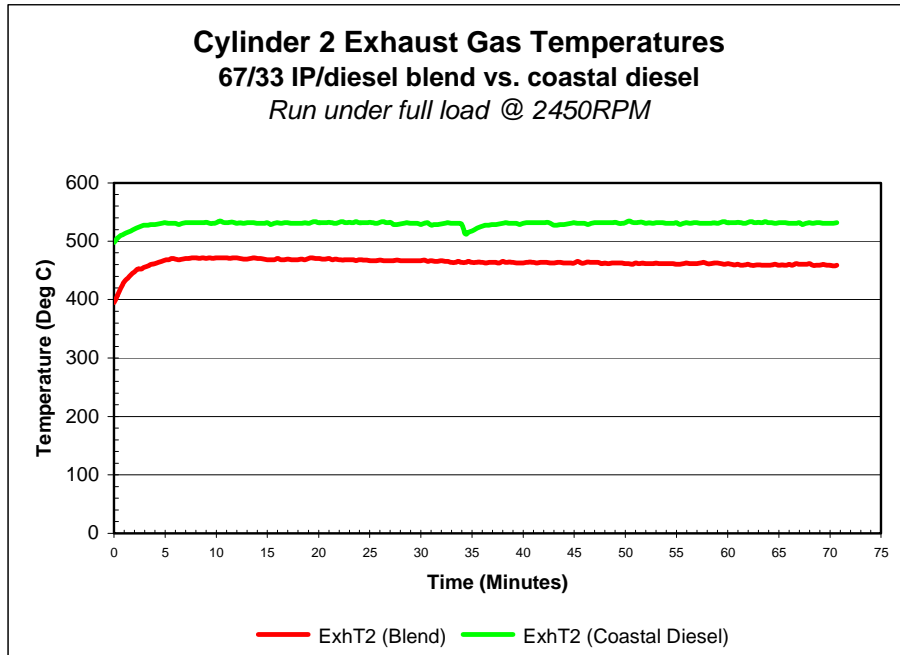


Figure 4-24: Injector degradation graph of EGT readings taken from the thermocouple mounted in cylinder 2 exhaust

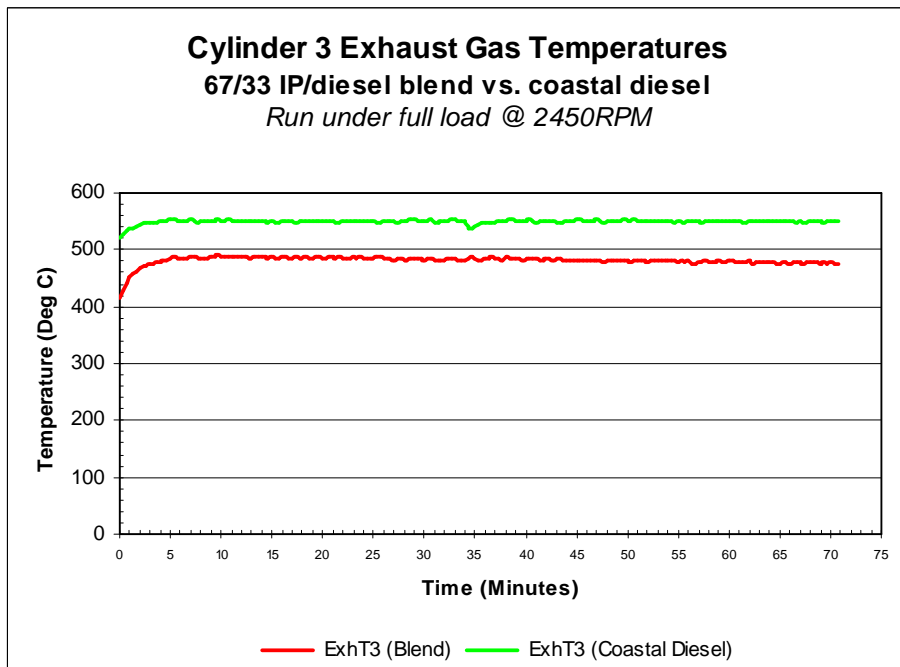


Figure 4-25: Injector degradation graph of EGT readings taken from the thermocouple mounted in cylinder 3 exhaust

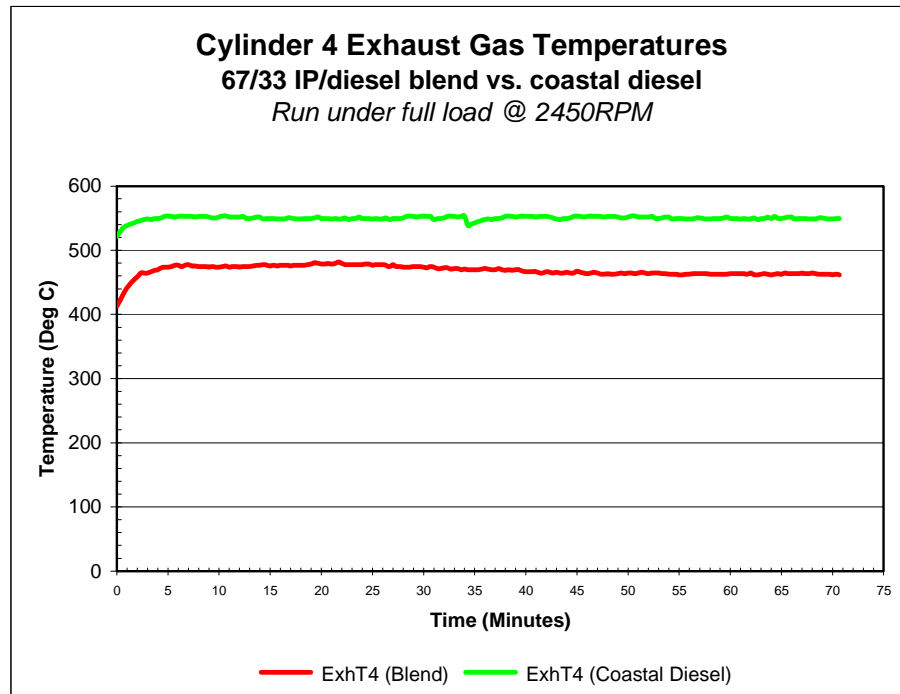


Figure 4-26: Injector degradation graph of EGT readings taken from the thermocouple mounted in cylinder 4 exhaust

For each cylinder, the green line represents the EGTs recorded using clean coastal diesel from a large fuel supplier. The red line represents the EGTs recorded using a blend of clean illuminating paraffin (IP) and afore mentioned coastal diesel, mixed in a $\frac{2}{3}$ illuminating paraffin to $\frac{1}{3}$ coastal diesel ratio. The graphs show that using the fuel blend produces EGTs that are more than 100° Celsius lower from the onset of each test, for the individual cylinders, than the coastal diesel. Further more the graphs also show how the EGTs slowly start to drop away, using the blend, as the test continues.

Engine torque was also recorded during these runs and the torque plot for the test conducted in Figure 4-26 is displayed for reference purposes in Figure 4-27.

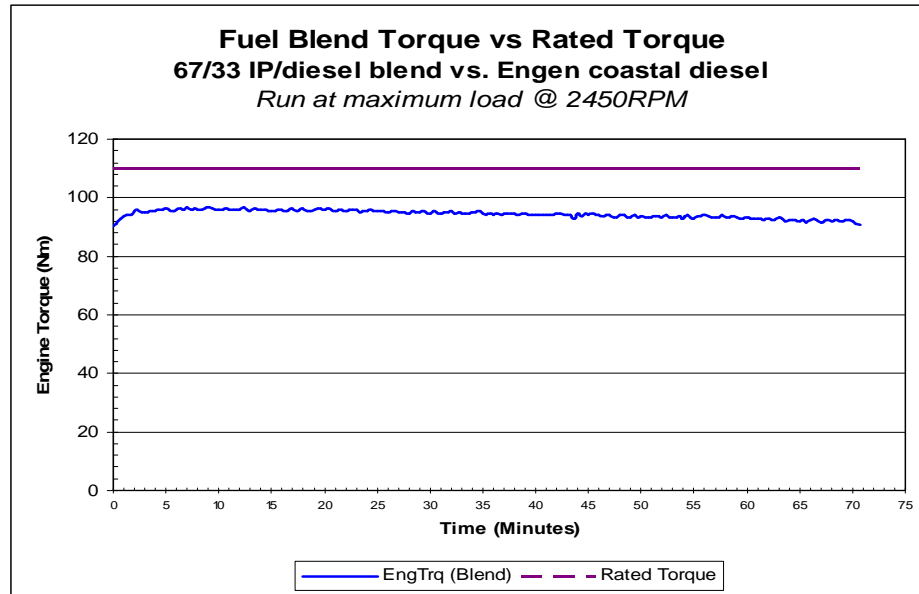


Figure 4-27: Comparison of engine torque measured during run with fuel blend and average value measured during previous runs using good fuel and new injectors

The lower initial EGTs, using the blend, may be explained by studying Equation 3-1 of Section 3.2.1.3. If 100% volumetric efficiency is assumed, the equation may be simplified to:

Equation 4-1

$$P_i = \eta_f \dot{V}_f Q_{HV} \rho_f$$

Two components account for the initial drop in EGTs recorded.

- The blended fuel will have a lower density (ρ_f) than that of pure coastal diesel due to the lower density of the paraffin. Inserting a lower value for fuel density into Equation 4-1 produces a lower indicated power value and hence lower EGTs.
- The combustion efficiency or fuel conversion efficiency (η_f) will be affected due to lower pressures generated in the injection equipment as a result of leakage brought on by the lower viscosity and diminished lubricating properties of the blended fuel. Higher leakage rates past the

injector needle shank result in smaller quantities of fuel being properly atomised during injection which reduces the thermal energy released.

As is evident from both Equation 4-1 and Figure 4-27, both factors lead to lower engine power output and consequently lower EGTs. As the test continues EGT temperatures slowly drop as the condition of the injection equipment degrades. This is most evident in Figure 4-26 for injector number 4. Injector number 4 was removed from the engine and its spray pattern evaluated using a mechanical, hand operated test bench, pictured in Figure 4-28.

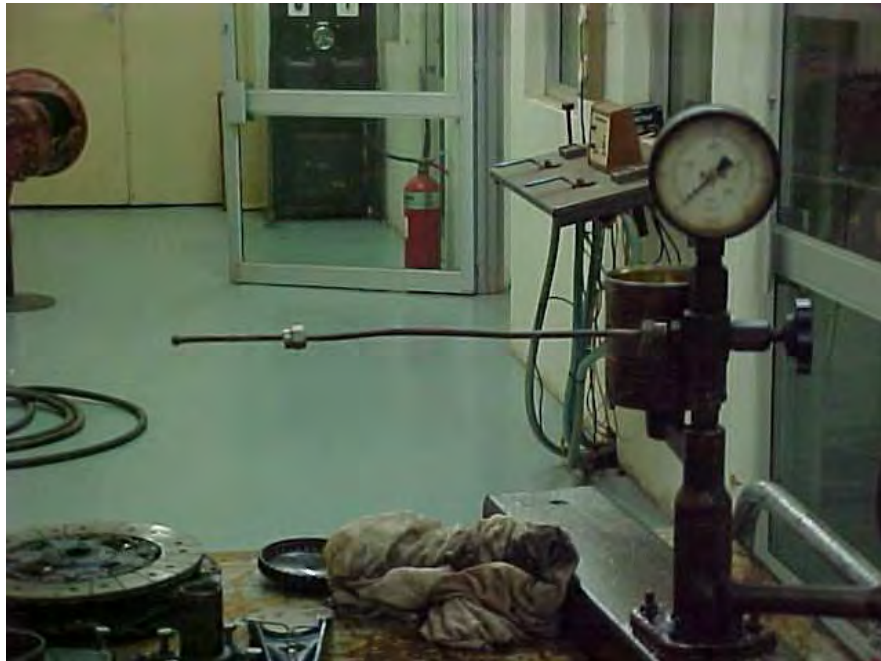


Figure 4-28: Photograph of hand operated injector test bench

When fitted to this test bench, the injection process can be simulated by pumping diesel through the injector when depressing the piston lever on the bench, allowing hydraulic pressure to build up in the injector tip until the needle is lifted off its seat. A pressure gauge mounted on the unit allows the “cracking” pressure to be indicated and the resultant spray pattern to be observed. The spray pattern for injector number 4 is shown in Figure 4-29 compared to that of a brand new injector in Figure 4-30.



Figure 4-29: Injector number 4 spray pattern



Figure 4-30: Spray pattern of a new injector

It is evident from the Figures that the injector from cylinder number 4 produces less of a plume of fine fuel droplets and more of a concentrated stream. When the injector tip was disassembled the needle was found to have visible surface damage along its flanks.



Figure 4-31: Close-up photograph of damage on needle surface



Figure 4-32: 100X magnification of score mark on needle surface

Closer examination of this surface damage revealed what appeared to be score marks or scratches as is indicated by the arrow in Figure 4-32. It is surmised that this degradation, if left longer to operate, will accelerate as the wear on the injector tips and pump elements becomes more and more pronounced leading to incomplete combustion.

This test highlights the severity of mixing paraffin with a good diesel fuel. The above data shows that the EGT drop that occurs, when the blended fuel is used, is significant and measurable.

4.2 Caterpillar 3412 and 3512 Tests

4.2.1 Test setup

Two of the Caterpillar range of large diesel engines, were made available to the student for monitoring EGTs by Barloworld Equipment. The purpose of these tests was to measure the temperature variation across cylinders on industrial type engines with no combustion malfunctions taking place. This would indicate how

broad a “tolerance band” around the average of the individual cylinder EGT readings would be, that encompasses normal injector operation. The tests would also indicate if the EGTs vary so wildly from cylinder to cylinder, under the most extreme conditions of load and engine speed where these variations would be the greatest, that a system based on EGT measurement would simply trigger endless false alarms. A smaller 3412 V12 engine fitted with Caterpillar’s Hydraulically operated Electronic Unit Injection (**HEUI**) system and a larger 3512 V12 fitted with the conventional Mechanically operated Electronic Unit Injection (**MEUI**) system, pictured in Figure 4-33.



Figure 4-33: Caterpillar 3512 V12 engine on which testing was conducted

The 3512 engine is factory fitted with thermocouples. On this engine the thermocouples are mounted in the engine head for each cylinder. These thermocouples protrude directly into the exhaust port and so provide an excellent facility for monitoring EGT. Figure 4-34 and Figure 4-35 below illustrate the positioning of the thermocouples both externally on the engine and relative to gas flow through the exhaust port.

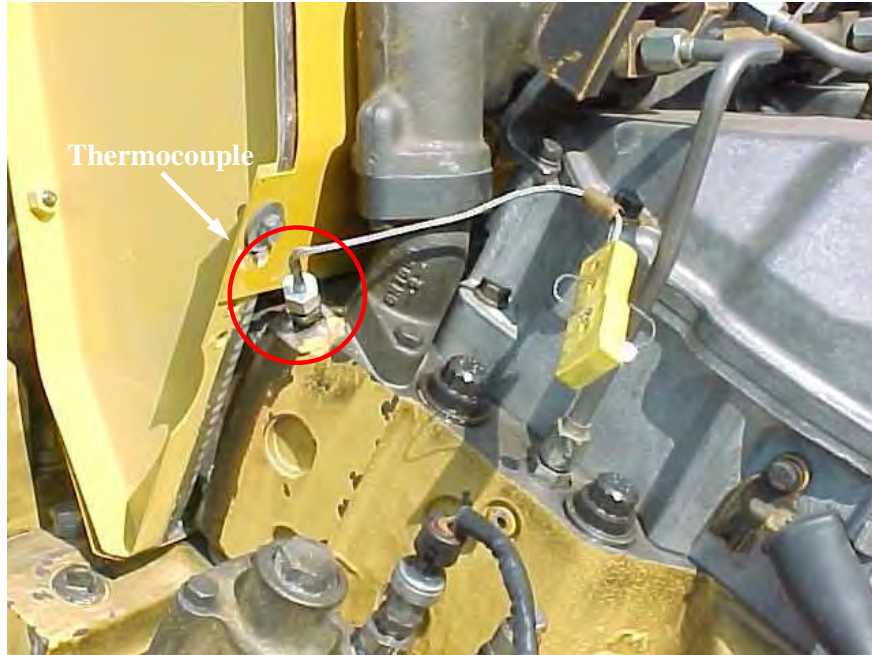


Figure 4-34: Photograph of thermocouple mounted in CAT 3512 head



Figure 4-35: Photograph of the thermocouple protruding into the exhaust port on a stripped 3512 head

The 3412 engine however, does not come fitted with thermocouples, so the exhaust manifold was modified to accommodate them. It is worth noting that the large size and shape of the exhaust manifold flanges allows for the thermocouples to be fitted directly adjacent to the exhaust ports. This will in all probability not be the case on all other manufacturer's engines, depending on the design and exhaust manifold configuration. The location of the thermocouples on the exhaust manifold is shown in Figure 4-36.

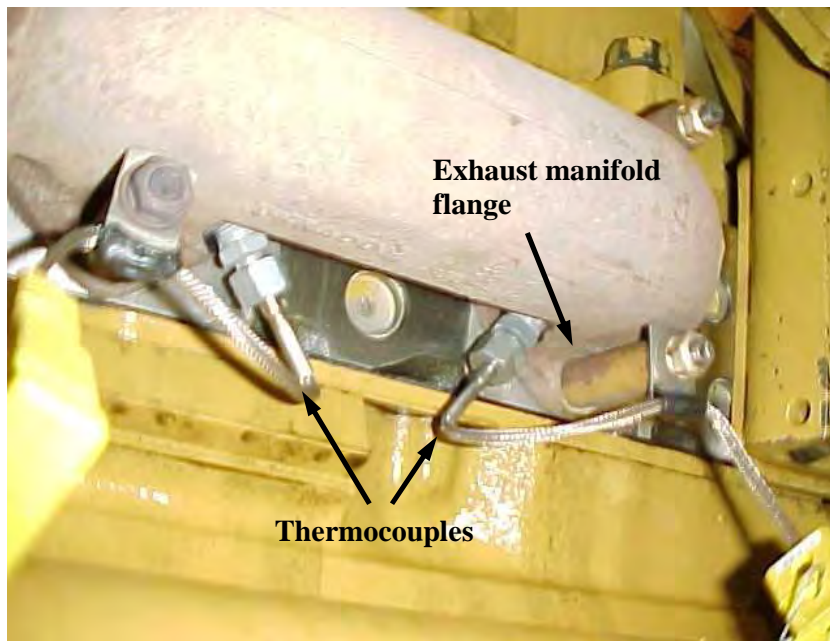


Figure 4-36: Photograph from below of thermocouples mounted adjacent to exhaust port in manifold of 3412

Locating the thermocouples in this manner means that the probe ends are positioned adjacent to the exhaust ports, but not protruding directly into the ports. Because of this, the thermocouples measure the temperature of the gases as they pass out of the exhaust ports and enter the manifold bends. As such, the flow of the combustion gases is not necessarily laminar as mismatching of the manifold to the ports and casting burs within the manifold, disturbs the flow. The result is a non-homogeneous gas temperature distribution at the point of measurement, which is not ideal.

4.2.2 Test results

4.2.2.1 Caterpillar 3512 MEUI

Temperature monitoring was carried out using a Caterpillar multi channel temperature selector with eight channel monitoring capability at the Barloworld facilities in Johannesburg. The harness was only sufficiently long enough to reach the thermocouples on one bank of the engine.

The decision was taken to only monitor the right hand bank of the engine due to time and practicality constraints. Temperature readings were only recorded after a sufficient time period had passed for the temperatures at the specific load and throttle settings to stabilize. As this was an engine that had been newly rebuilt by Barloworld for a client it was being run-in on the dynamometer so as to make it available to the client as soon as possible. Due to this, on the day of testing this specific engine was only run at quarter and half throttle. The results of these runs can be seen from the bar graphs depicted in Figure 4-37 and Figure 4-38 below.

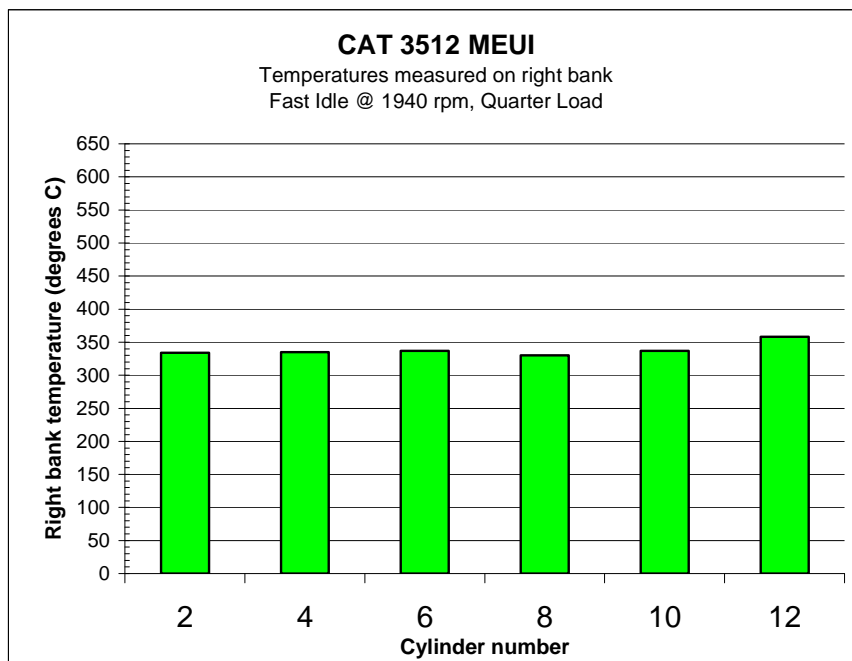


Figure 4-37: EGT readings taken from the head mounted thermocouples on the 3512 engine at quarter load

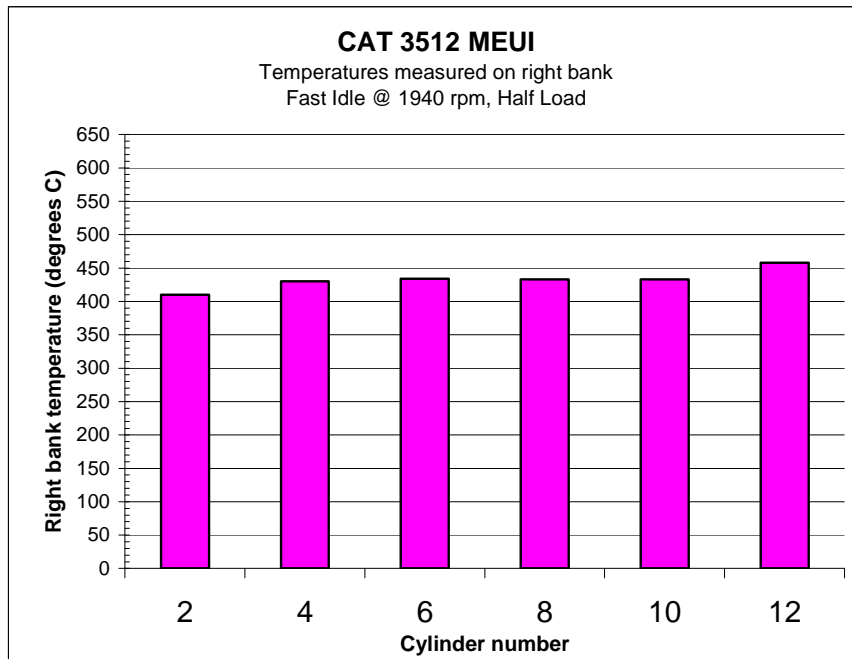


Figure 4-38: EGT readings taken from the head mounted thermocouples on the 3512 engine at full load

Note that the greatest variance between highest and lowest cylinder EGTs is approximately 50°C for both quarter and half load. Table 4-2 shows the standard deviation and “90%” probability deviation limits, calculated from the dynamometer runs.

Table 4-2: Table of EGT standard deviations for quarter and half load conditions on the Cat 3512 MEUI engine				
Engine Speed (RPM)	EGT Standard Deviations for Quarter Load Conditions		EGT Standard Deviation for Half Load Conditions	
	σ (°C)	1.6449 σ (°C)	σ (°C)	1.6449 σ (°C)
1 940	9	15	14	23

Note that the greatest deviation occurs under half load conditions and predicts a value of 23° Celsius.

4.2.2.2 Caterpillar 3412 HEUI

The 3412 engine was only made available to the student for a very limited period on the Barloworld dynamometer. This was due to the last minute fitment of a new electrical harness to the engine in an attempt to cure an intermittent misfire and that the client was in a hurry to receive the engine back from Barloworld. As a result of the time constraints and with permission from the client, the only data that could be captured on this engine was under full load conditions at a fast idle of 1940 RPM. This time it was possible to measure EGT s on both the left and right banks. The results are presented on the bar graphs depicted in Figure 4-39 and Figure 4-40 below.

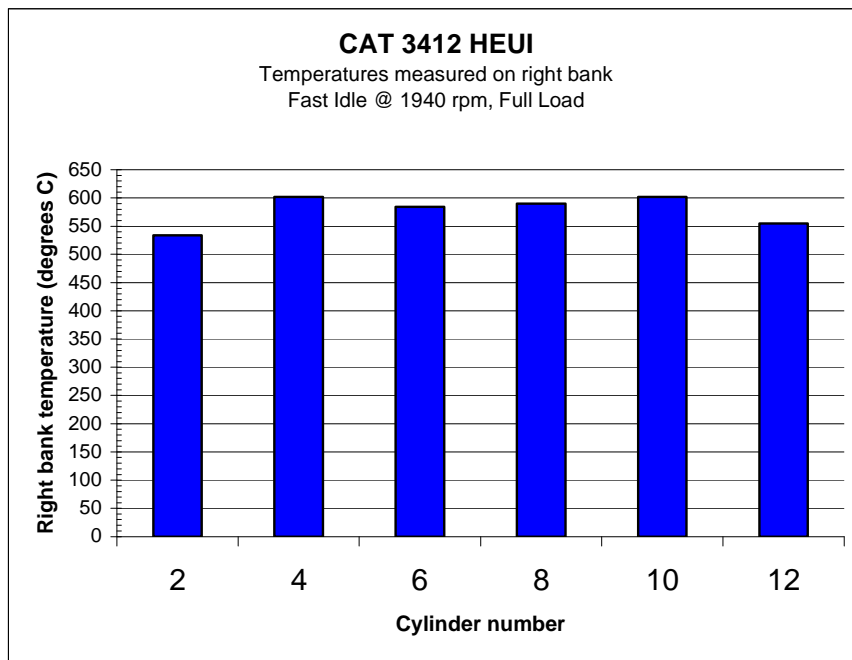


Figure 4-39: EGT readings taken from the manifold mounted thermocouples on the right hand bank of the 3412 engine

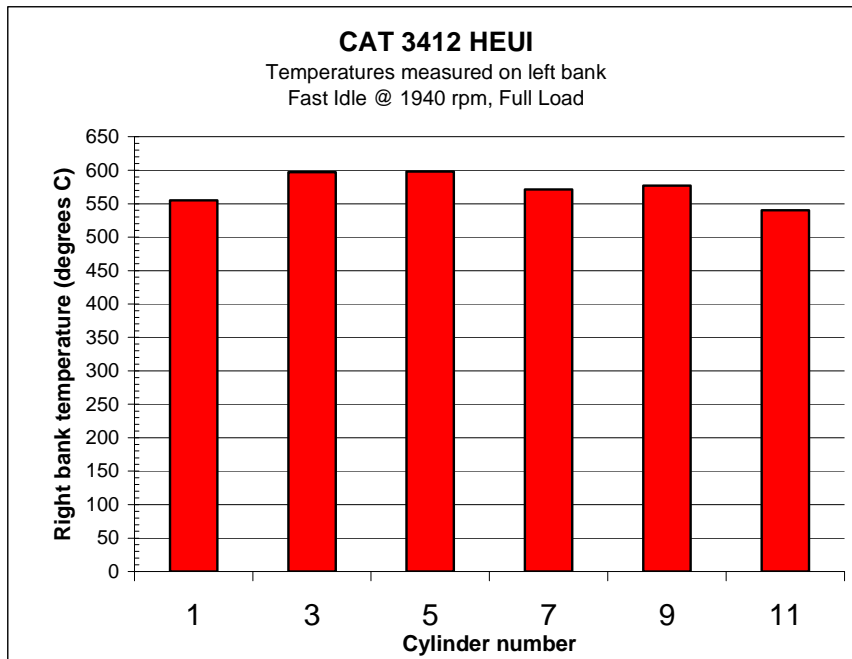


Figure 4-40: EGT readings taken from the manifold mounted thermocouples on the left hand bank of the 3412 engine

Note that the largest temperature difference between cylinders is greater than the 50°C band encountered on the MEUI 3512 engine with factory fitted thermocouples in the cylinder heads. The temperature difference band for the HEUI engine with thermocouples retro fitted to the exhaust manifold is approximately 70°C. Table 4-3 shows the standard deviation and “90%” probability deviation limits, calculated from the dynamometer runs.

Table 4-3: Table of EGT standard deviations for left and right hand banks on the Cat 3412 HEUI engine				
Engine Speed (RPM)	EGT Standard Deviations for Left Hand Bank		EGT Standard Deviation for Right Hand Bank	
	σ (°C)	1.6449 σ (°C)	σ (°C)	1.6449 σ (°C)
1 940	21	35	30	49

Note that the greatest deviation occurs on the right hand bank predicts a value of 49° Celsius.

4.2.3 Findings

The HEUI system, through individual hydraulic control, allows injectors to be individually adjusted by the vehicle's Electronic Control Unit (ECU) for optimum power delivery. The MEUI system is camshaft operated and does not allow for individual injector control.

From the above data it appears that the EGTs of the different cylinders, on diesels fitted with the more conventional MEUI systems, are very similar under different load conditions. It seems evident that temperatures vary by less than 50°C. The engine fitted with the HEUI system however exhibits a variation in temperatures of up to 70°C between cylinders. This large variation may be ascribed to the individual injector control metered out by the engine ECU. It is able to increase or decrease injector spray time (pulse duration) according to sensor readings such as power output, average exhaust gas temperature, manifold pressure and oxygen (O₂) readings from the exhaust.

Service bulletins from some of the large diesel manufacturers (Caterpillar SIS 2002: 3) support the theory that injector condition can be monitored by individual EGT measurement. Averaging out the EGT readings from the individual cylinders, and prescribing a set tolerance within which the EGTs may safely vary from this average value, provides an indication of injector condition.

A good starting value for large commercial diesels, from engine tests conducted, appears to be a value of 40°C above or below the calculated average value. This will give a tolerance band of 80°C. This value appears to hold for engines with conventional MEUI systems but cannot be applied with the same amount of certainty to engines with individual injector control such as the Caterpillar HEUI system.

5.0 CHAPTER V – ELECTRONIC MONITORING AND DETECTION SYSTEM

5.1 System Requirements

From the data gathered during experimental testing, discussed in Chapter IV, the following list of requirements was set out for a system that can successfully monitor and detect injector related combustion irregularities in a diesel engine:

- The system must be able to individually monitor the exhaust gas temperatures (EGT) of each of the cylinders of a 12 cylinder engine. Twelve thermocouple inputs were deemed to be sufficient for the majority of small and large industrial engines. (It may however be extended to 16 or more if needed).
- It must electronically calculate an average value from these readings every 1 second. Any deviations, of more than a fixed value (e.g. 40° C) above or below this average value, by any of the cylinders when compared to this average should be indicated.
- If the fault persists for more than 30 seconds a visual and audio alarm will sound.
- The system must be programmable so that the acceptable EGT deviations of the individual cylinders from the average EGT of an engine (an upper and lower temperature limit) can be programmed/ altered for different engines.
- The visual alarm for the system should consist of some type of flashing indicator for each individual cylinder. This will be labelled to indicate which cylinder(s) is/are experiencing combustion trouble. The visual alarm should be complemented by an audible alarm as well.
- A ‘normal’ indicator could also be incorporated to indicate which of the cylinders are linked to the system and that the system is operating properly
- A cancel button must also be included to reset the system after an alarm has sounded.
- System electronics must monitor the temperatures only when the ignition is switched on.

- The system must be able to operate off the vehicle's 24 Volt supply.
- The system would need an input for each temperature sensor (Thermocouple). As previously mentioned the system would need up to 12 inputs in order to accommodate a 12 cylinder engine.
- The system must be compact, so that it can easily be carried by one person and mounted in the vehicle control cabin in close proximity of the operator.
- A laptop connection port must be incorporated into the system so that a numerical reading of the recorded temperatures may be exported to a laptop.

5.1.1 Discussion of requirements

- The requirement of individual cylinder monitoring is a necessity for pinpointing the location of an injector or injectors that are malfunctioning within an engine. Several of the large mobile equipment engines are already equipped with a single sensor measuring EGT readings at the junction point of the exhaust manifold. This sensor is used as an input to the Engine Control Unit (ECU) to aid in calculating injection timing and injection duration. It also serves as an alarm should there be a significant increase in EGT (possibly caused by a blocked air filter) over and above the norm.
- The sensor cannot however detect a change in temperature in one of the cylinders of a multi-cylinder engine. The effect of the single cylinder's temperature deviation from the norm is cancelled out by the remaining properly functioning cylinder temperatures. Often with injector related engine failures, the failure begins with one of the injectors malfunctioning before any of the others. The idea with the monitoring system is that upon alarm, the vehicle can be stopped and the offending injector removed for investigation to try to pinpoint the source of injection system malfunction before piston or cylinder/liner damage starts to occur.
- Using the average temperature of all the cylinders at any one time as the basis or norm with which to compare the individual cylinder temperatures is a compromise in the interest of simplicity. A more comprehensive method would be to have a complete 'map' of all the possible temperatures of the

individual cylinders during all stages of normal engine operation and to use this map as the basis for comparison. However, the complexity of taking all the different operating conditions such as external temperature, throttle position, engine water temperature and a host of others into account, presents serious time and computing power obstacles.

- The best compromise is to make use of all the cylinder temperatures to form an average with which to compare. It has been demonstrated in Chapter-IV, Section 4.1.4.1, both statistically and experimentally, that the four cylinder temperatures of the Ford R2 diesel engine vary from hottest to coldest by no more than 40°C. This occurs under maximum load and maximum fuel delivery operating conditions, where these deviations are the greatest.
- Section 4.1.4.2 further demonstrates that a malfunctioning injector produces EGT readings that fall outside the normal distribution limit ‘envelope’ ($\pm 1.6449\sigma$) of EGT readings for properly functioning injectors. Imposing a temperature limit of $\pm 40^\circ\text{C}$ for this particular engine outside of which the injectors are deemed to be malfunctioning appears feasible in attempting to pinpoint a malfunctioning injector. Imposing a requirement of recording the temperatures every second is easily achievable electronically and is a more than an adequate sampling frequency when recording temperatures that change over a number of seconds.
- Due to the variance of the individual cylinder EGT readings at any one time in a diesel engine, there may be short periods where one of the cylinder’s EGT readings falls outside the ‘envelope’ around the calculated average produced by the cylinders during normal operation. Allowing for the fault to persist continuously for a short period of time before sounding the alarm seeks to eliminate the possibility of false alarms.
- Allowing for the deviation ‘envelope’ limits to be set for different engines is a necessity as different engines have different temperature limits within which the injectors are operating properly. A limit of $\pm 40^\circ\text{C}$ seems feasible for the Ford R2 engine. As demonstrated in Section 4.2 the greatest variance between injectors in the Caterpillar 3512 engine with MEUI injection is approximately 50°C from hottest cylinder to coolest, while that of the

Caterpillar 3412 fitted with HEUI injection is approximately 70°C. The “90%” probability deviation limits (1.6449σ) calculated in Table 4-2 and Table 4-3, predicts an “envelope” of $\pm 23^\circ\text{C}$ above the calculated average for the 3512 engine and $\pm 49^\circ\text{C}$ for the 3412 engine. From this it appears that each engine has a particular ‘tolerance band’ and this must be accounted for in the monitoring system.

- A clear visual and audible alarm to alert the vehicle/engine operator is critical in warning the operator to stop the vehicle. The alarms must be such that they cannot easily be missed or ignored by the vehicle operator. Pinpointing the offending injector/s is a crucial requirement for the system. Since injector failure seldom occurs in all the injectors at once, detecting which cylinder’s injector is malfunctioning before the others begin to degrade can result in great cost savings benefits. The idea being that the vehicle may be stopped for the malfunctioning injector to be replaced so that the vehicle can return to work.
- The incorporation of a ‘normal’ indicator is simply there to inform the vehicle operator or mechanic that all the thermocouples are connected and are reading properly. Should one of the thermocouples or connecting wires be damaged the operator/mechanic can easily identify the malfunctioning sensor before operating the vehicle.
- Having an alarm cancel button on the monitoring unit prototype is considered a necessity for continued repetitive testing. It is envisaged that the fully developed unit fitted to a machine in general operation would only have a cancel function accessible to the engineer or technician sent with a laptop computer to access the data on the device. This would prevent vehicle operators from simply cancelling a fault registering on the monitoring system and continuing to operate the machine.
- It was envisaged that the unit would only be operational when the ignition of the vehicle is switched on. Thus the unit would be hardwired to the key ignition system in the cab of the vehicle and only receive power once the operator has turned the start key and the engine has fired up.

- The requirement for the monitoring system to run off 24 volt (maximum) supply is simply to accommodate the majority of mobile equipment that run off 24 volt batteries. The inclusion of a transformer into the circuit would also allow the device to run off an AC mains (240 volt) power supply.
- Having twelve thermocouple inputs allows the monitoring system to accommodate a 12-cylinder engine. Although 16 cylinder engines are used in extremely heavy earth moving applications, they are less common. The decision was taken to limit the monitoring system to 12 thermocouple inputs, with the provision to expand it to 16 inputs should the need arise.
- The restriction imposed in the point above, would also allow for the prototype unit to be as compact as possible. This is an important consideration for the test unit as it should be as portable and easy to install in restricted spaces as possible.
- For the purposes of development and experimentation it has been decided that the actual milli-volt readings taken from the temperature sensors on the engine should be displayed on a separate laptop computer. This requires the inclusion of an output socket on the monitoring system for easy connection to the laptop by means of an inexpensive cable.

5.2 Development of the Combustion Monitoring System (CMS)

In order to practically demonstrate the feasibility of using EGT readings to detect injection equipment malfunction to the contributors to this research project, Kumba resources and Anglo Coal, a prototype Combustion Monitoring System (CMS) was constructed. This was done in conjunction with Mr Johnathan Smit, a post-graduate electronic engineering student in his final year of post-graduate study at the University of Pretoria. Mr Smit designed the electronic circuit board that allows the CMS prototype to carry out the design functions laid out in the aforementioned text. The printed circuit board designs were then sent to a circuit board manufacturer for production. The assembled prototype is depicted in Figure 5-1.

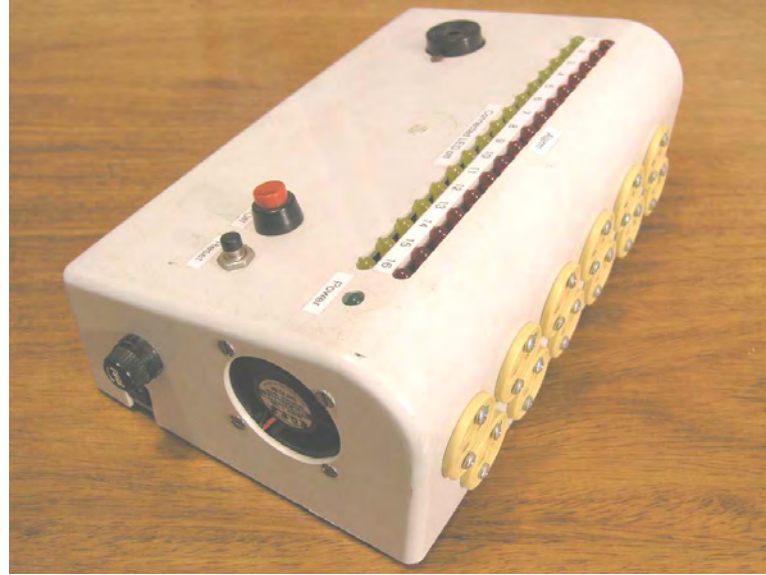


Figure 5-1: Photograph of the CMS prototype.

5.2.1 Functional layout

The CMS prototype unit is packaged in a compact and lightweight plastic housing weighing less than 300 grams. A solid model of the CMS prototype depicting the dimensions of the unit is shown in Figure 5-2.

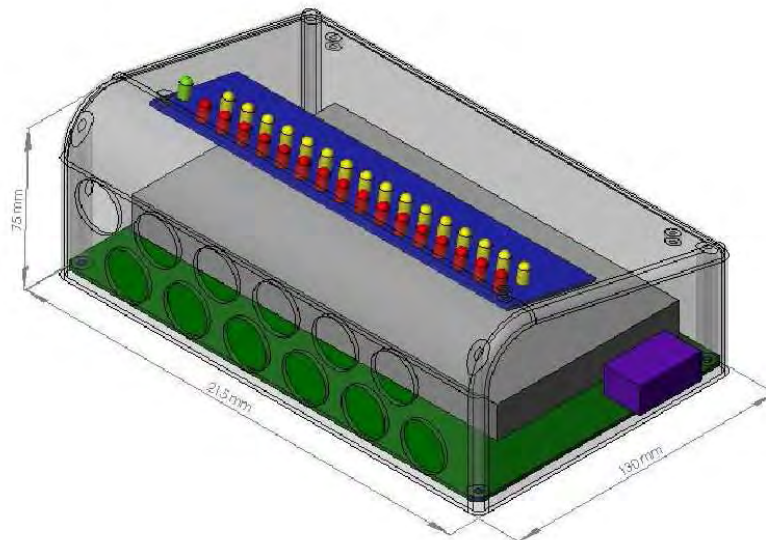


Figure 5-2: Solid model of CMS prototype unit.

The CMS unit houses two printed circuit boards. The bottom “functional” circuit board houses the power and processing circuitry as well as the inputs from the thermocouples. Its circuit diagram is shown in Figure 5-3. (See Annexure B for detailed diagram)

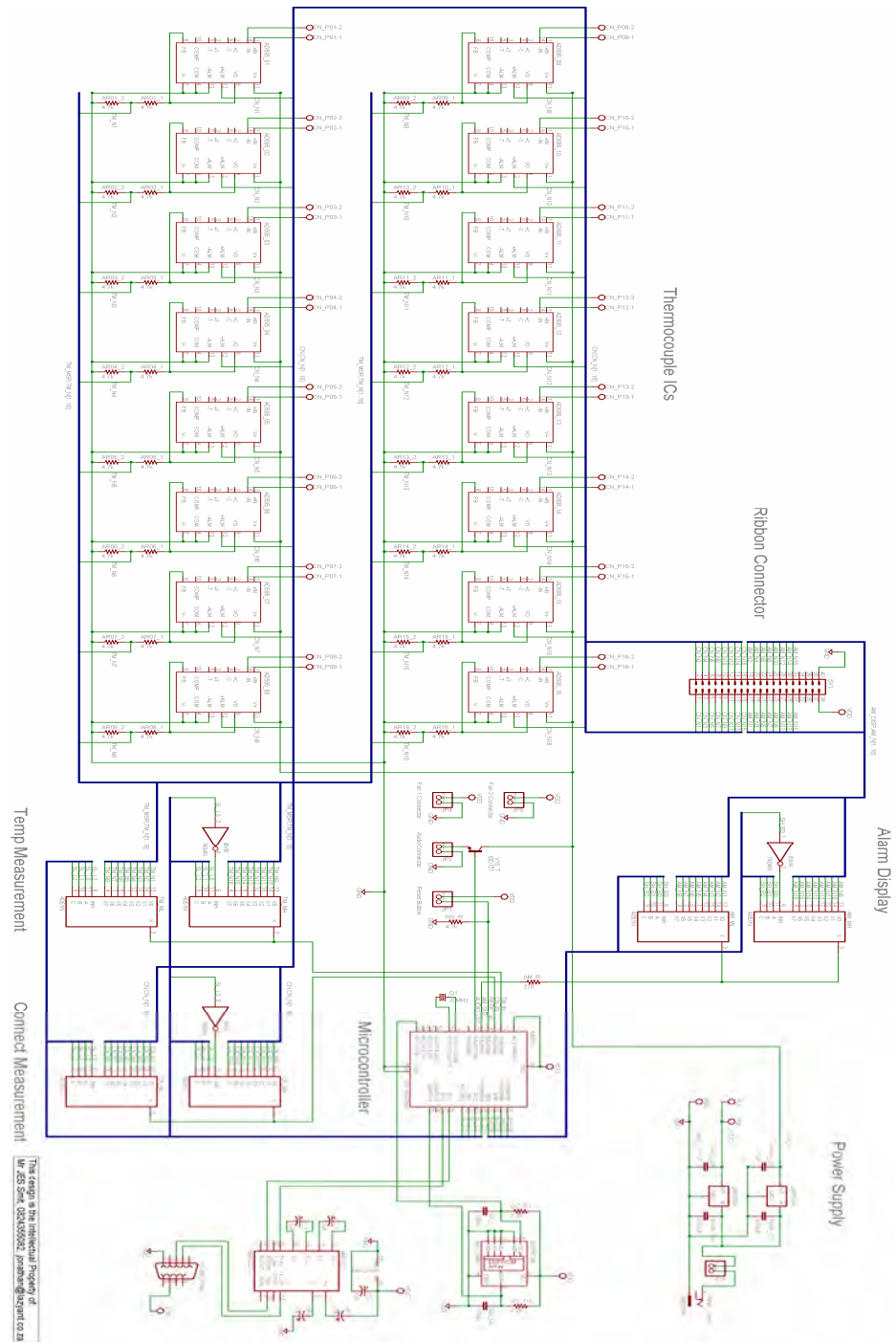


Figure 5-3: “Functional” printed circuit board diagram

This board is responsible for calculating the average values and comparing the individual temperatures to this calculated average.

The upper “display” printed circuit board houses the alarm circuitry, containing the LEDs and connections for the audible alarm. The display circuit diagram is depicted in Figure 5-4. (See Annexure B for detailed diagram)

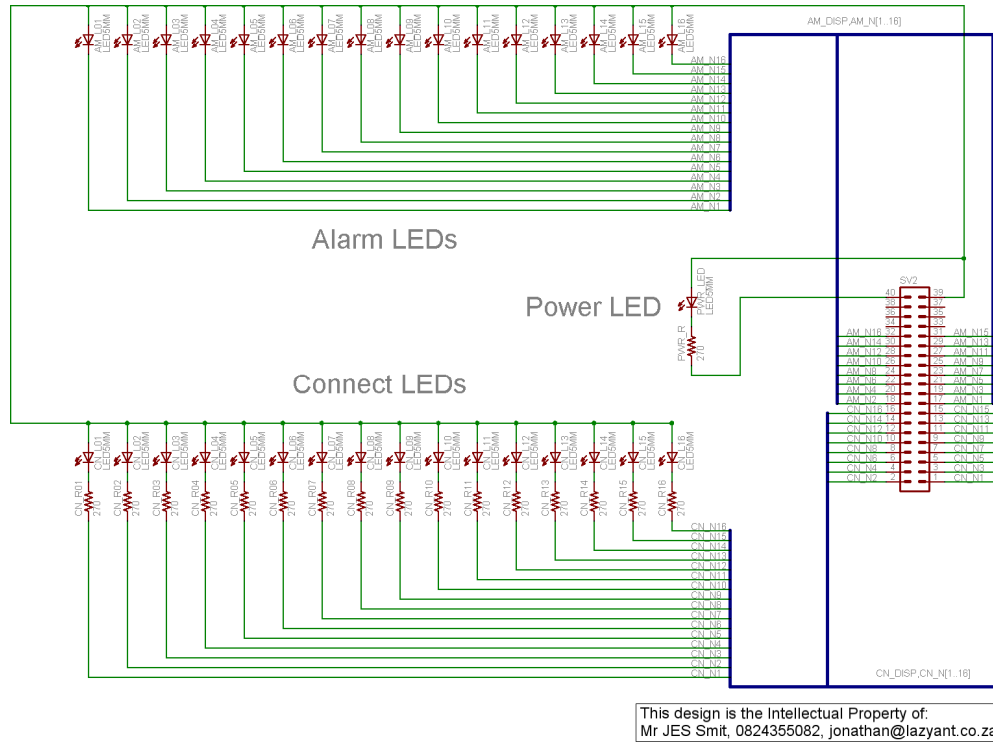


Figure 5-4: “Display” printed circuit board diagram

Figure 5-5 shows the layout of the CMS unit’s display and control panel

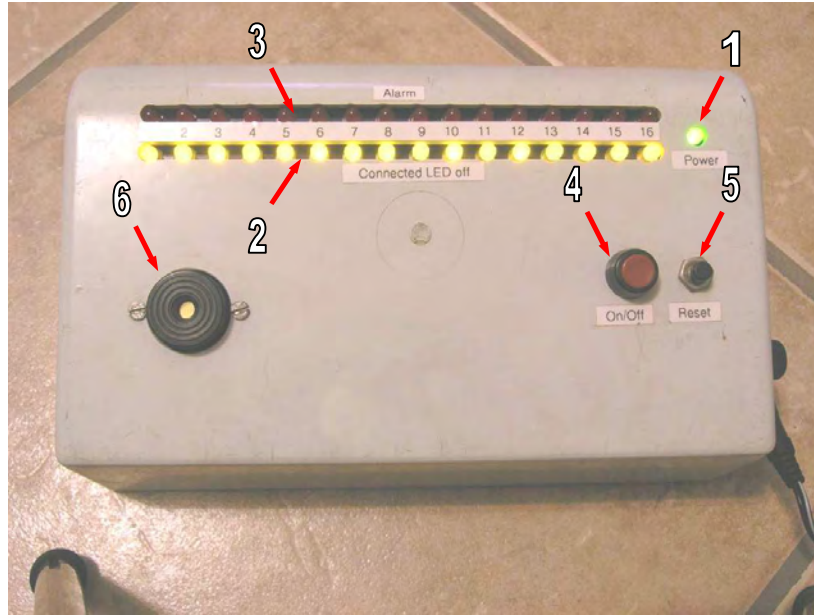


Figure 5-5: Photograph of the CMS unit. Green LED indicates unit has power and is switched on.

The display panel consists of the following components:

1. A green POWER LED indicator
 2. A row of amber CONNECTION LEDs
 3. A row of red ALARM LEDs
 4. An ON/OFF switch
 5. A RESET switch
 6. An audible alarm buzzer
- The green (power indicator) LED lights up when the CMS unit is connected to a power source and is switched on as can be seen in Figure 5-5.
 - Amber LEDs serve to indicate which of the temperature sensor inputs have been connected. The LEDs remain lit when not connected and are ungrounded when connected to a temperature sensor, thus going dead. The arrow in Figure 5-6 points to the display LEDs indicating that four thermocouples have been connected.

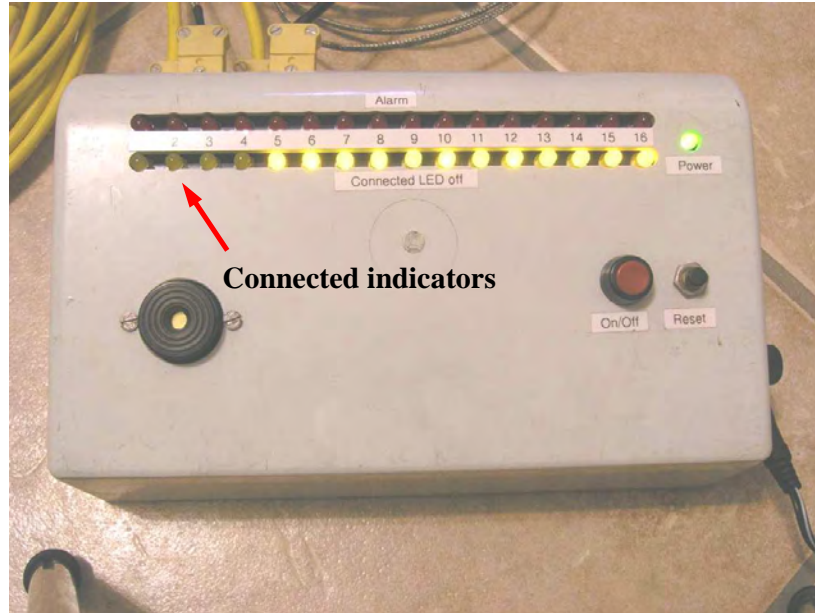


Figure 5-6: Photograph of CMS display indicating that thermocouples have been connected to slots 1 to 4.

The decision was taken to have the amber LEDs light up when not connected so as to give an active indication of whether the slots are working properly or not when nothing is connected to them. Should an LED remain dead when nothing is connected to it this will alert the operator to a possible fault with the sensor circuit.

- Red LEDs serve as visual warning alarms. As soon as one or more of the temperatures measured by the connected thermocouples starts to deviate by a predetermined amount from the calculated average of all the connected thermocouples, its corresponding LED will begin to light up. To demonstrate this, heat was applied to the thermocouple plugged into sensor input number four. The illuminated red alarm indicator LED can be seen, indicated by the arrow, in Figure 5-7.

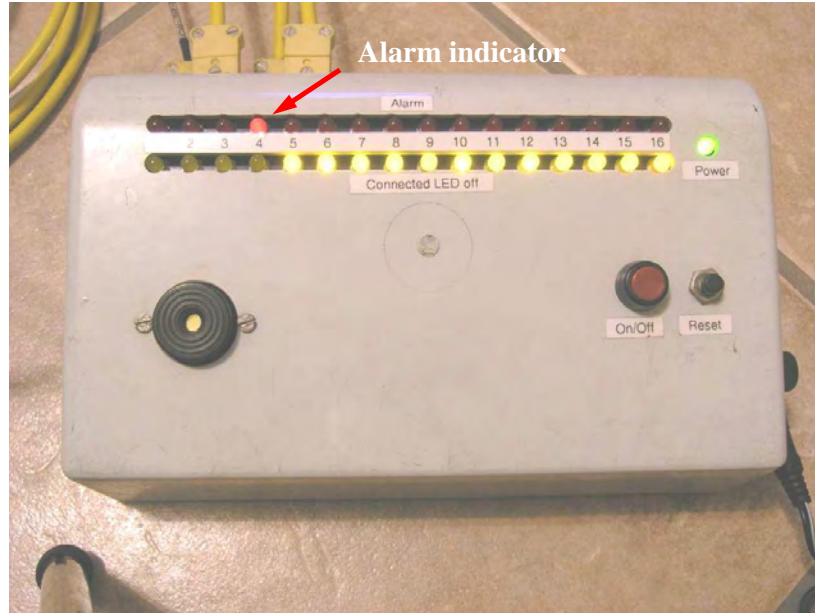


Figure 5-7: Photograph of CMS unit indicating a deviation in temperature on the no. 4 thermocouple from the average of the other three thermocouples.

- The unit is fitted with its own on/off switch so it can be isolated from its power source independently.
- A reset switch allows both the visual and audible alarms to be cancelled.
- An audible alarm buzzer emits a loud, high pitched sound when a fault persists. The buzzer sounds when one or more of the red alarm LEDs continues to flash for a predetermined period of time. It will continue to sound indefinitely until the reset switch is depressed or the unit is switched off.

The front face of the CMS unit is fitted with a bank of miniature female thermocouple connectors (Temperature Controls model H132 K-type) as shown in Figure 5-8. These connectors were chosen for their compactness as well as easy integration with the thermocouple extension looms used by engine manufacturers such as Caterpillar for the K-type thermocouples already installed in some of their engines. Although the CMS unit's circuit board is equipped to handle sixteen thermocouple inputs, the available space only allowed for twelve

of these connectors to be mounted to the CMS prototype unit. This was deemed as an acceptable number of sensor inputs as the majority of diesel engines in South Africa would fall in the twelve cylinders or less bracket.



Figure 5-8: Photograph of female miniature thermocouple input sockets.

Figure 5-9 depicts some of the components built into the CMS unit.

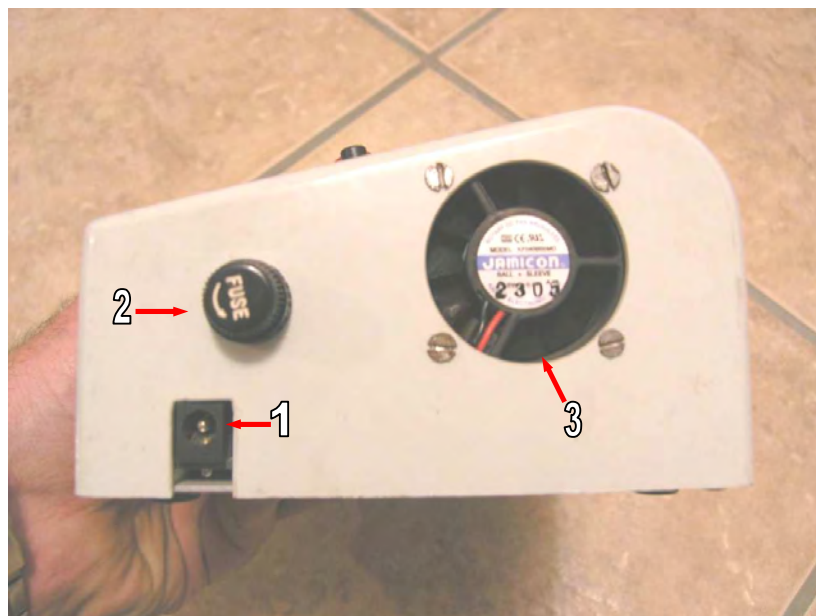


Figure 5-9: Photograph of CMS prototype right hand side panel.

With reference to Figure 5-9, the labels indicate the following components:

1. The direct current (DC) power jack allows the CMS unit to be connected to a power supply. The prototype is designed for the 24 Volt systems used in most mining and earthmoving equipment. It is ideally suited to taking off power from the ignition system in the operator cabin and requires a minimum of 20 Volts and between 0.8 and 1 Ampere to function properly.
2. A 1 Ampere fuse has been included to protect the integrated circuitry from over-current.
3. Cooling fans are a necessity to keep the circuitry cool under any high temperature operating conditions that may be encountered.

5.2.2 Data capture and interfacing

Figure 5-10 depicts the serial port connector on the left hand side panel of the CMS unit.

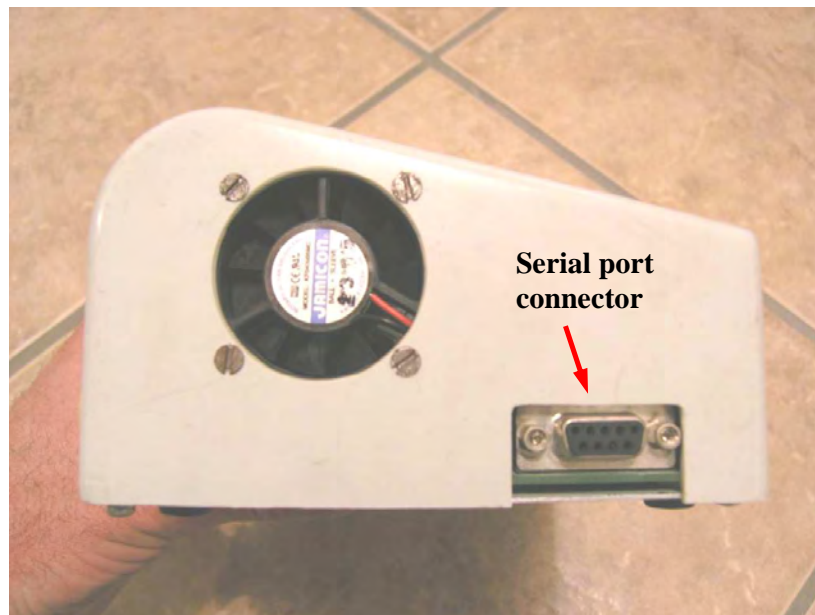


Figure 5-10: Photograph of CMS prototype left hand side panel.

The serial port connector allows the unit to interface with any laptop or desktop computer so that data may be downloaded or CMS setting changes may be made. The connection is made by means of a serial to serial or serial to USB (RS232) converter cable depending on the type of communications ports available on the laptop being used. In Figure 5-11 the connection is accomplished by means of a serial to USB cable



Figure 5-11: Photograph of CMS and laptop interfacing.

To make the CMS prototype accessible from any personal computer (PC) or laptop the decision was taken to use the Windows communications programme, 'Hyper Terminal'. The temperature readings from the CMS unit are displayed, real-time on the computer screen through Hyper Terminal as text.

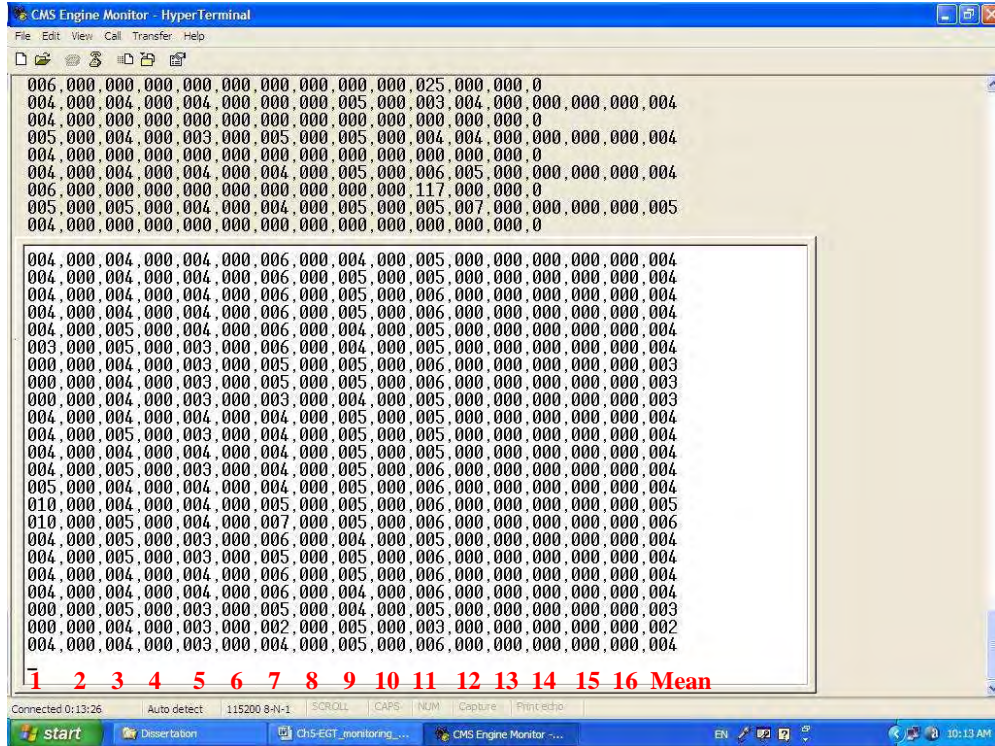


Figure 5-12: CMS text file output to Hyper Terminal

Figure 5-12 illustrates a screen capture of the temperature readings being dumped to screen while six thermocouples are connected to the CMS prototype. Seventeen columns of text are visible on the capture screen. Six thermocouples are connected to input jacks 1, 3, 5, 7, 9 and 11. The last (seventeenth) column represents the calculated average or mean of all the connected thermocouple readings. The CMS prototype uses this value to compare all the individual thermocouple readings to for alarm purposes. The left most column contains the outputs from thermocouple (potentially engine cylinder) number one with the following columns representing thermocouple (cylinder) number two, three and so on up to a maximum of sixteen. Since there are only twelve physical thermocouple input connections on the CMS box only the first twelve columns would yield temperature data values when connected. The actual values represented on the screen are the direct milli-volt reading outputs by the individual processing chips assigned to each thermocouple input. *To calculate*

*the actual temperatures that the thermocouples are reading, the values have to be multiplied by a factor of **four**.*

Thus a data output value of 003 represents 12°C that the thermocouple is measuring. The factor of four is simply a function of the type of processor chip used but it does mean that the temperature reading is only accurate to 4°C. This accuracy is considered acceptable as actual diesel engine exhaust gas temperature readings are in the hundreds of degrees Celsius with the tolerance band around the average being $\pm 40^\circ\text{C}$ or more.

5.2.3 Operation of the CMS prototype

Once the unit has been connected to a 24 Volt power supply and switched on, it is ready to operate. Monitoring the exhaust gas temperatures (EGT) of an engine requires either mounting thermocouples in the individual header pipes of an exhaust manifold or making use of the thermocouples already mounted in the head of certain manufacturer's engines. It is advisable to make use of K-type thermocouples with stainless steel shielding to protect the thermocouples from the fierce temperatures and corrosive products of combustion that they will be exposed to. These thermocouples have a useful operating range of 95°C to 1260°C which is well suited to the diesel engine EGT range. The slight delay in response time due to the shielding does not adversely affect the effective operation of the CMS unit as its sampling frequency is limited to one 1 Hertz and the effects on EGT of combustion related anomalies are not instantaneous.

Thermocouples that are factory fitted to diesel engines by original equipment manufacturers (OEMs) such as Caterpillar and MTU, may have the standard pin type male connectors fitted to the thermocouples or the miniature spade type connectors compatible with multi-meters such as those supplied by 'Fluke Instruments' that can be used as thermocouple temperature displays.

The CMS unit was designed to be mounted in the operator cab, close to the operator so extension cables would have to be used to take the signals from the thermocouple positions on the engine to the CMS unit location. It is advisable to

use cables with polyvinyl chloride (PVC) electrical shielding, covered by a stainless steel braid for added protection against heat and abrasive wear.

Communication with the CMS unit consists of entering the protocols described in Table 5-1 (See Annexure C for full operating instructions). All commands are executed by simply typing them in followed by the ‘enter’ key, in the Hyper Terminal window once connected to the CMS unit.

Table 5-1: CMS communications protocols

Command	Description
V	Displays the current settings of the engine monitor (values).
Sxx	Changes the sample time, where <i>xx</i> is the time between samples given in seconds.
Txx	Changes the tolerance of the Engine Monitor to <i>xx</i> , where <i>xx</i> is the new tolerance value given in degrees. (Note: The value is automatically converted to a multiple of 4 by the monitor)
Pxx	Changes the number of samples for which an alarm condition must persist before it is registered as an actual alarm. <i>xx</i> represents the number of samples.
Oxx	Changes the preference to have the temperature values output as they are read or not, where <i>xx</i> is either <i>00</i> (to disable to output) or <i>01</i> (to enable the output)
Bxxyy	Changes the calibration settings for a thermocouple where <i>xx</i> represents the number of the thermocouple (from 01 to 16) to change, and <i>yy</i> indicates the calibration value. The calibration value is the number to be added to the temperature as displayed by the monitor (ie. it is the degree value to compensate by, divided by 4) to ensure it displays the correct value. eg. to set Thermocouple 01 to read 16 degrees higher than it is, enter: <i>b0104</i>
C	Development: Display which thermocouples are currently connected and which are not (000 = disconnected, 001 = connected)
R	Development: Display the persistence values of all the thermocouples.
A	Development: Display the alarm status of all the thermocouples.
L	Not Yet Implemented: List values stored in external EEPROM

All commands are case insensitive and feedback is given to the user should the command be successful or not. Via a laptop or desktop computer, the CMS unit can be tailored according to the characteristics of the engine being monitored

and the alarm requirements of the user. Displaying the current settings of the CMS unit requires entering the letter ‘v’ in the Hyper Terminal window. This allows for quick simple evaluation and adjustment of the CMS alarm settings for the particular engine it is connected to. The resultant display is depicted in Figure 5-13 when the letter ‘v’ is entered.

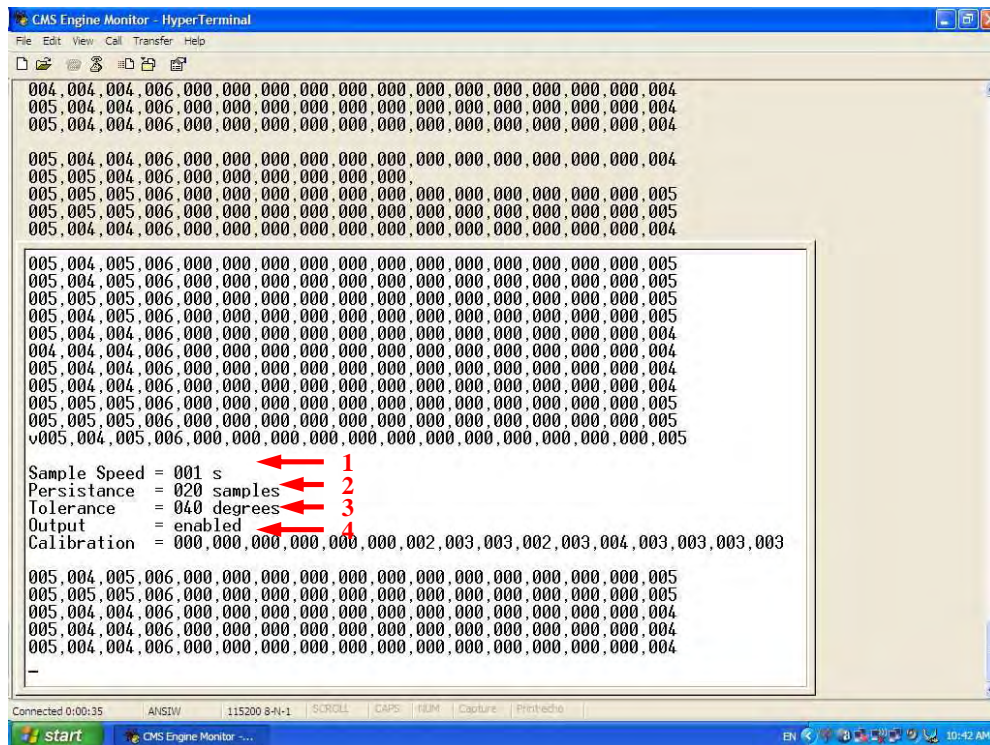


Figure 5-13: CMS current settings displayed in Hyper Terminal window

With reference to the numbering in Figure 5-13 the most important settings are:

1. Sampling frequency of the unit (Sample Speed)
2. Persistence of the fault before the alarm sounds (Persistence)
3. The alarm tolerance band for the engine (Tolerance)
4. The calibration values for the thermocouples (Calibration)

Provision has been made to adjust the sampling frequency of the unit. This is adjusted by changing the time in seconds between the CMS unit reading the

temperature outputs from the thermocouples. Ordinarily this would be set at the system minimum value of 1 second. However should the need arise for data to be recorded onto a laptop for an extended period of time, such as an entire ten hour vehicle operating shift on a mine, it may be necessary to decrease the number of data points collected in the interests of hard drive space restrictions. It is envisaged that this function would only be used in exceptional cases.

The persistence value refers to the number of consecutive repetitions of the CMS unit detecting a temperature deviation, outside the set tolerance band, before the alarms are activated. This feature has been incorporated into the CMS unit as a safeguard against false alarms. The reasoning behind this is that a genuine injector malfunction would result in a consistent temperature deviation from the norm in that injector and not just sudden random spikes. The tests conducted on the University of Pretoria's dynamometer, indicated that a genuine injector malfunction would cause the associated drop in that cylinder's EGT to persist for more than 30 seconds. As such a 'safe' persistence value setting of 30 seconds was chosen for the tests conducted using the Ford R2 engine. At a sampling frequency of 1 Hertz this means that the fault would have to persist for 30 seconds before the alarms would be raised. Again choosing a persistence value for a particular engine would require experimentation to yield effective protection without potentially costly false alarms.

In conjunction with the persistence value, the allowable temperature cylinder EGT band must be decided upon. The alarm tolerance band for the engine refers to the degrees Celsius value that any one of the thermocouples may deviate from the average value of all the connected thermocouples. If this is exceeded the CMS audio and visual alarms activate.

This value will be specific to a particular engine type and manufacturer since no engine's cylinder-to-cylinder exhaust gas temperatures will be identical at different loads and engine speeds. Deciding on the optimum value that will prevent any false alarms due to temperature deviations between cylinders, but

will still deliver early warning of an injector malfunction, will require some experimentation on the engine to which the CMS unit is coupled. A good 'rule of thumb' starting value from the data collected during experimentation and statistical calculation (discussed in the Chapter 4) is $\pm 40^{\circ}\text{C}$. Thus typing in the letter 't' followed by '40' in the Hyper Terminal window (see Figure 5-13) will set a tolerance band of 80°C about the average of all the connected thermocouples.

Calibration of the thermocouples is normally only conducted once when a set of new thermocouples is connected up to the CMS unit. In most cases this is accomplished by directing a stream of hot air from a hair-dryer over them and adjusting their calibration factors so that they all give the same reading that corresponds to a separate thermometer also placed in the hot air stream. Changing the calibration value by '1' for a particular thermocouple results in the thermocouple reading '4' degrees Celsius above or below its previous reading.

Table 5-1 also contains a number of secondary command protocols for development purposes to aid the user in tailoring the CMS unit for a particular engine.

- Entering the letter 'c' in the Hyper Terminal window (see Figure 5-13), displays which of the thermocouples are currently connected to the CMS inputs. This is intended to help identify malfunctioning thermocouples or bad connections between the thermocouple plugs and circuit board.
- Entering the letter 'r' in the Hyper Terminal window when an alarm condition arises displays the number of counts for which the thermocouple/s causing the alarm have fallen outside the alarm temperature tolerance band.
- Entering the letter 'a' in the Hyper Terminal window, during an alarm condition, identifies which of the thermocouples is responsible for the alarm condition. This is intended to confirm the number of the cylinder where a combustion abnormality is taking place.

5.3 Evaluation of the CMS prototype

Evaluation of the effectiveness of the CMS prototype again took place on the University of Pretoria's SuperFlow engine dynamometer using the Ford R2, four cylinder, normally aspirated diesel engine.

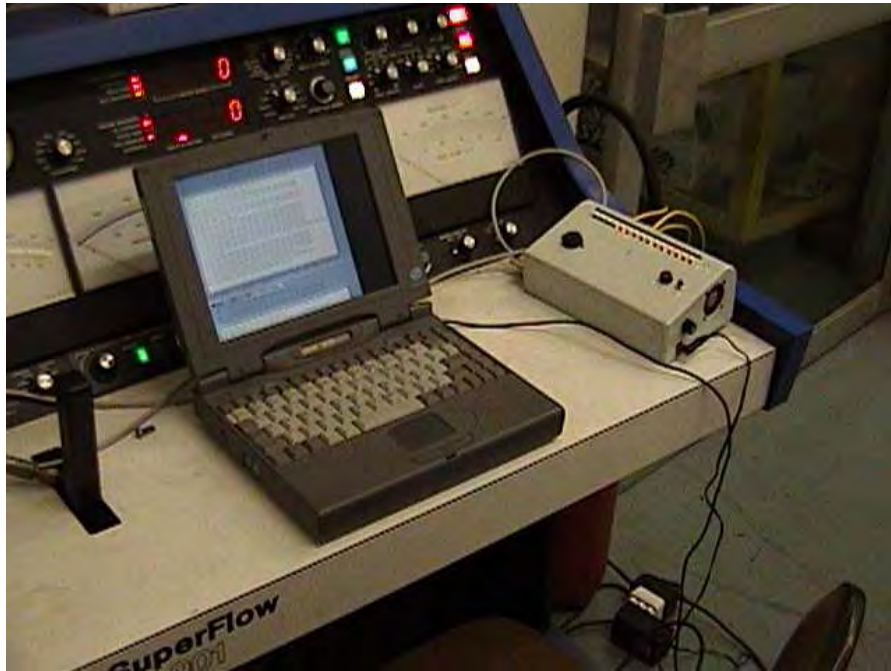


Figure 5-14: Photograph of CMS prototype with laptop interface on SuperFlow dynamometer control panel

Figure 5-14 shows the CMS unit and laptop computer interface during testing. This setup simulates the way it would be implemented on an actual vehicle. The CMS unit would be mounted in the operator cabin so that it could provide feedback to the operator and allow for easy access via a laptop computer. The thermocouple output signals would be carried to the CMS unit by means of thermocouple extension cables as pictured in Figure 5-15.

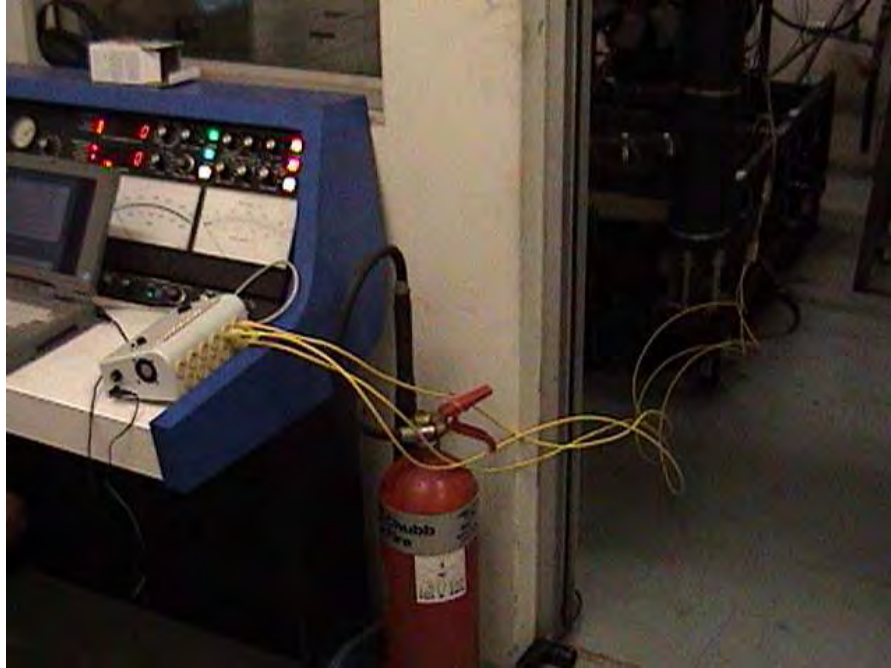


Figure 5-15: Photograph of engine thermocouple to CMS connections

The extension cables used under laboratory conditions consisted of single pair, PVC insulated and electronically shielded, stranded conductors in a PVC sheath. The electronic shielding is considered a necessity on engines that have ancillary components that may produce strong magnetic fields or any type of radio frequency interference. When being used on any type of mobile equipment it is envisaged that thermocouple extension cables with a braided stainless steel sheath will have to be used to make the cables more resistant to mechanical damage due to chafing, vibration and high temperatures. However, these cables are significantly more expensive than the PVC sheathed ones and were considered excessive for laboratory test conditions.

The identical engine/thermocouple setup was used, to that described in Chapter 4, for base data collection. In Figure 5-16 the unlit LEDs on the CMS display indicate connection to the thermocouples mounted on cylinders 2, 3 and 4 while the engine is running at idle, with no load being applied to it by power absorption unit of the dynamometer.



Figure 5-16: CMS display upon thermocouple connection

The thermocouple for cylinder number 1 was not connected in this photograph as it was plugged into the SuperFlow dynamometer input for comparison purposes. Figure 5-17 shows a photograph of the actual milli-volt output values being displayed on the laptop screen in the Hyper Terminal window.

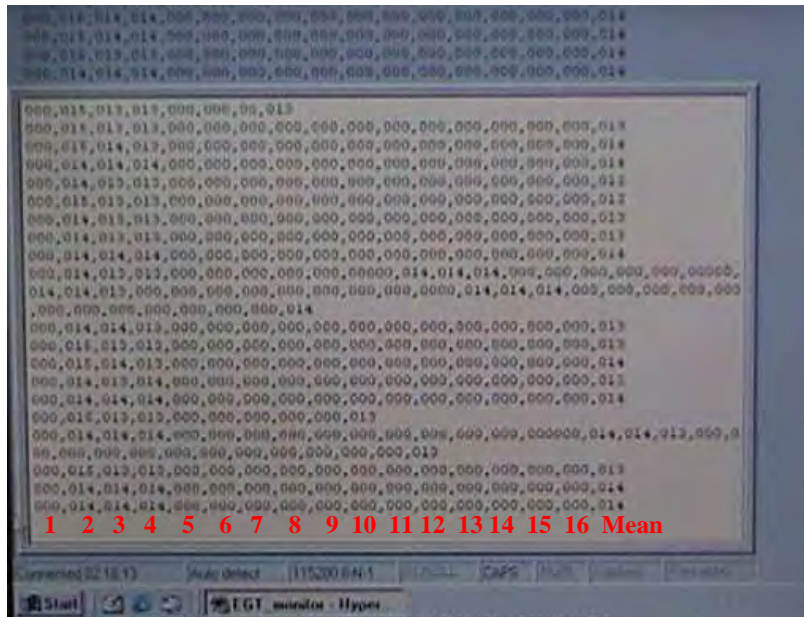


Figure 5-17: Hyper Terminal display screen of temperature values

The output voltage values for cylinders 2, 3 and 4, shown in Figure 5-17, are listed in Table 5-2 under the ‘Output’ column. As discussed in Section 5.2.2 these milli-volt outputs have to be multiplied by a factor of four (4) to convert them to the actual temperatures being measured in degrees Celsius. The results are displayed in Table 5-2 under the ‘Temperature’ column.

Table 5-2: Results with reference to Figure 5-17

	Output	Temperature (°C)
Cyl 2	014	56
Cyl 3	014	56
Cyl 4	014	56

Thus all three connected cylinders produced identical exhaust gas temperatures of 56°C that compared favourably with the 53°C measured on cylinder number 1 using the dynamometers onboard measuring equipment and software.

5.3.1 Results at full load maximum fuel delivery

In Figure 5-18 the data points collected from the CMS prototype are plotted for the properly functioning test engine at full load and maximum fuel delivery.

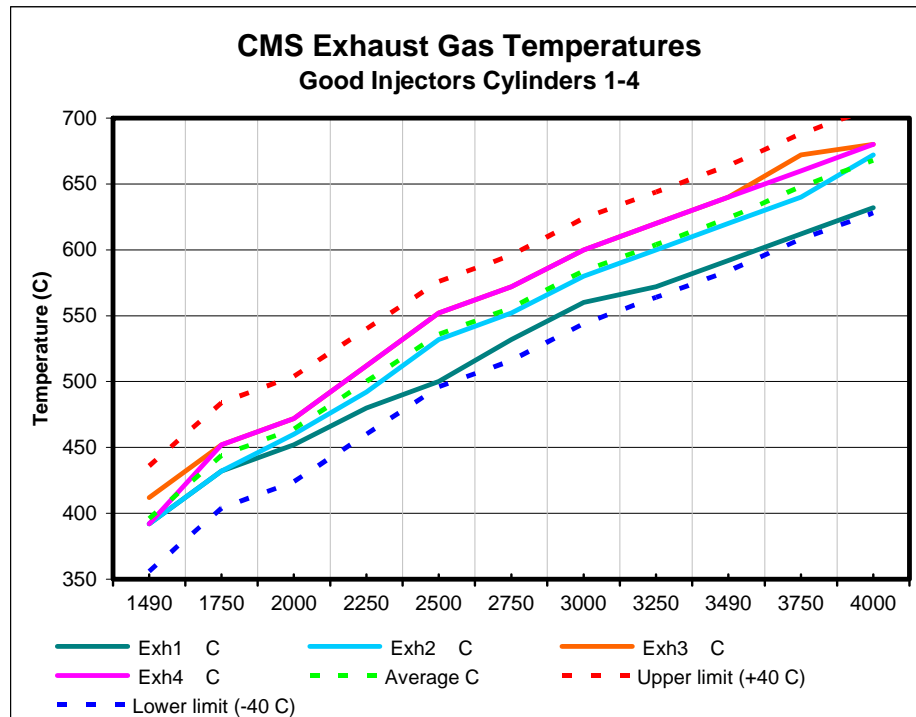


Figure 5-18: Graphic representation of CMS output values for properly functioning injectors at maximum fuel delivery, full load

Using the portable laptop computer and via Windows Hyper Terminal, the data could be stored and plotted against engine speed. This graph is similar to the plot of the data collected in Chapter 4 (refer to Figure 4-14, pg 69) for a properly functioning set of injectors on this particular engine.

The green dashed line represents the average temperature values calculated by the CMS unit for the four cylinders at each data point. The red and blue dashed lines represent the temperature tolerance band limits of + 40°C and - 40°C respectively, at which the CMS unit had been set to alarm during the test runs on this engine. As can be seen from Figure 5-18 the four EGT readings remain within this preset band throughout the entire engine speed range at full load. However EGT readings from cylinder number one can be seen to be significantly lower than the other three cylinders and only just falls within the lower tolerance band from 3250 RPM upwards to the maximum RPM. As discussed previously in Chapter 4, this is possibly due to the superior cooling effects of cylinder number one's close proximity to the water pump outlet. Thus,

the CMS prototype was able to monitor the individual cylinder exhaust gas temperatures throughout the most demanding engine operating condition that could be simulated without giving a false alarm.

To test whether the CMS prototype could pick up a combustion abnormality, the purposely-damaged injector tip (discussed in Section 4.1.3.1), used for previous tests, was inserted into cylinder number 3. The damage to the injector is visible in Figure 5-19.



Figure 5-19: Damaged injector test needle

The data collected through the CMS unit during the dynamometer run with the damaged injector inserted into cylinder number 3 is plotted in Figure 5-20.

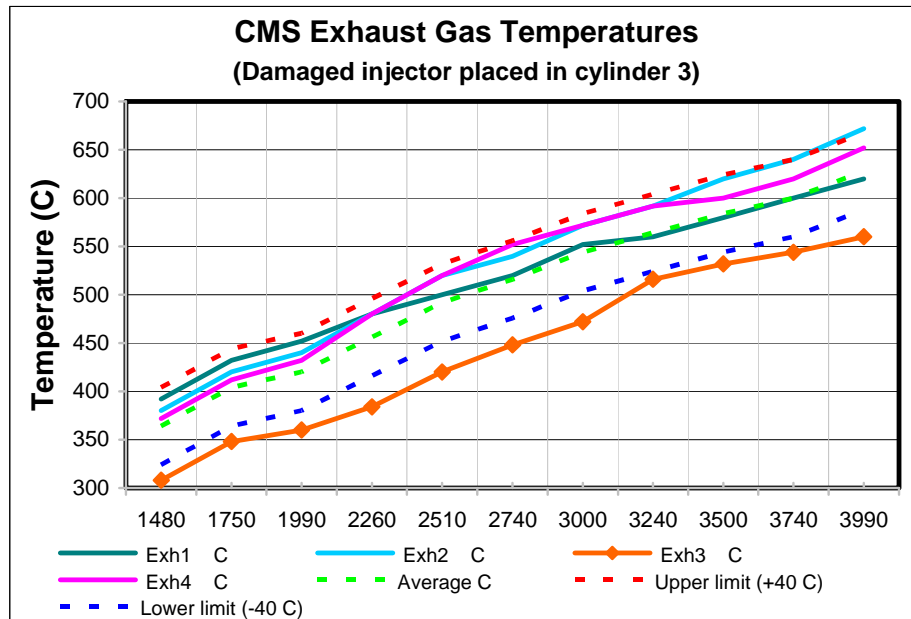


Figure 5-20: Graphic representation of CMS output values for damaged injector in cylinder number 3

The recorded temperature values for cylinder number 3 could be seen to fall well below the preset tolerance band. As such the CMS unit was observed to indicate an alarm condition for cylinder number 3 as indicated in Figure 5-21.

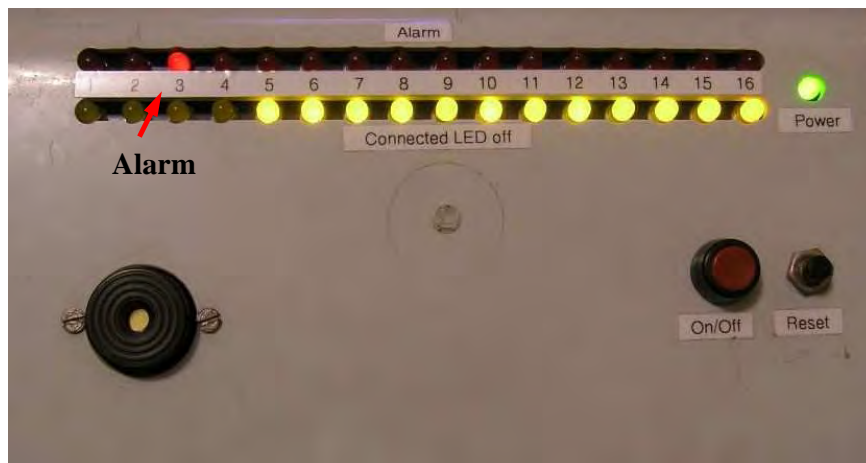


Figure 5-21: CMS visual alarm for EGT drop in cylinder number 3

The fault condition can be seen to have persisted throughout the entire engine speed range at maximum fuel delivery and full load.

To verify whether the CMS unit could genuinely detect improper combustion within any of the cylinders of the test engine, the above experiment was repeated by placing the defective injector in all three remaining cylinders and repeating the dynamometer runs at maximum fuel delivery and full load. The results for these runs are depicted in Figure 5-22, Figure 5-23 and Figure 5-24.

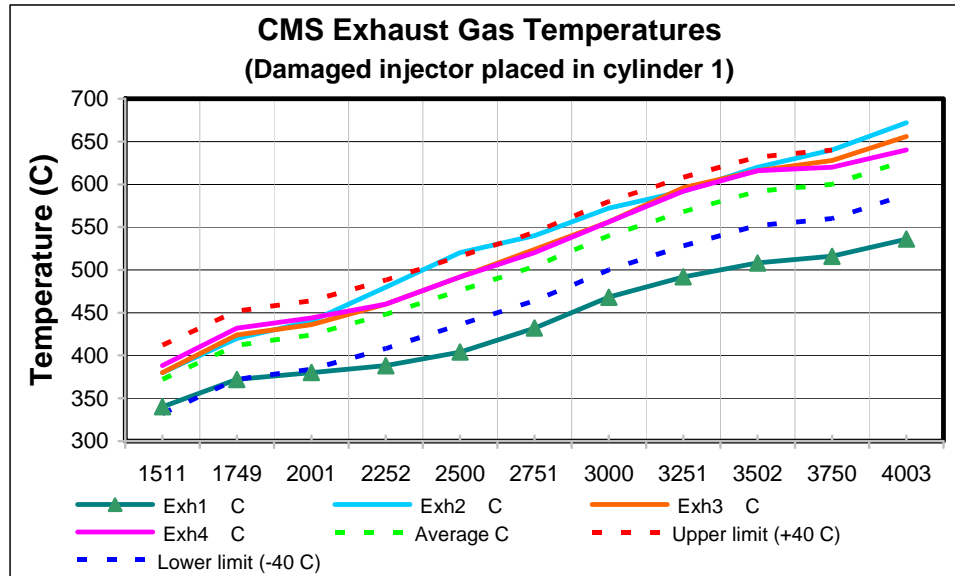


Figure 5-22: Graphic representation of CMS output values for damaged injector in cylinder number 1

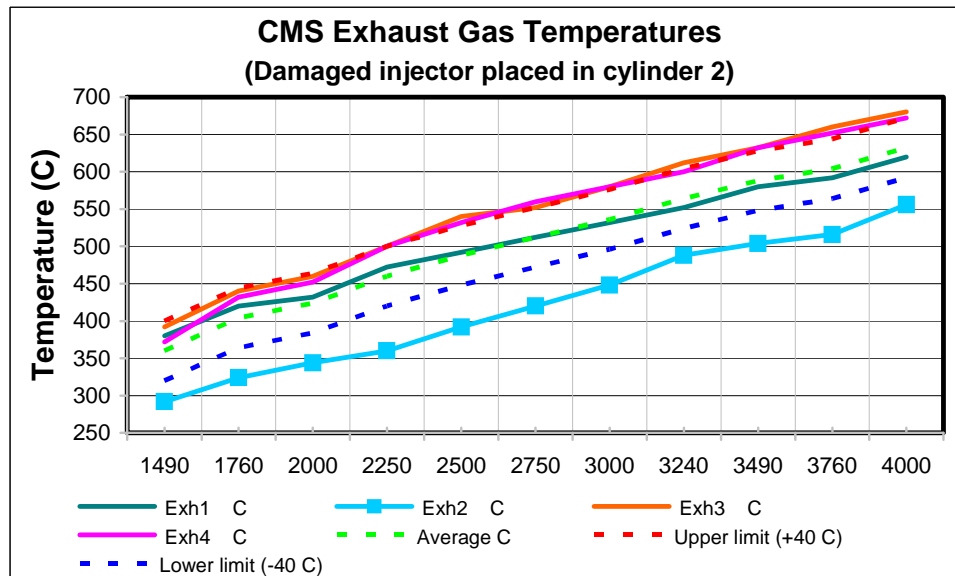


Figure 5-23: Graphic representation of CMS output values for damaged injector in cylinder number 2

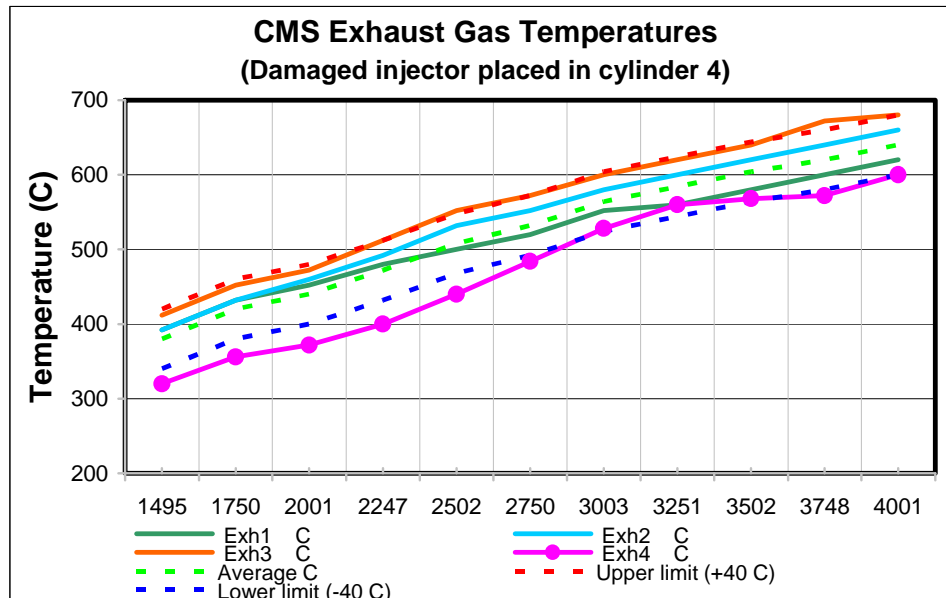


Figure 5-24: Graphic representation of CMS output values for damaged injector in cylinder number 4

5.3.1.1 Discussion

With reference to Figure 5-22 it is interesting to note that the CMS prototype only started registering an alarm condition from 2000 RPM upward as the EGT of cylinder number 1 only began to dip below the lower 40°C limit above this engine speed. A possible explanation for this may be that the injector tip could have been jerked loose within the injector after a few hundred oscillations allowing slightly more complete combustion for a short period before relapsing to seizing again at the higher ‘rev range’.

A similar condition may be observed in Figure 5-24 for the seizing injector in cylinder number 4 where the EGT temperature for this cylinder peaks back into the $\pm 40^\circ\text{C}$ tolerance band between 3000 RPM and 3500 RPM before falling below the lower limit again. It is expected that this ‘bouncing’ of the EGT in a cylinder fitted with a failing injector would be a common occurrence and would progressively become worse as the injector condition deteriorates. The decision to remove this injector would be based on the CMS unit’s fault persistence setting, i.e. the time period for which the EGT temperature falls

outside the set tolerance band for a particular cylinder before the CMS unit sounds the audible alarm.

5.3.2 Results at half load partial fuel delivery

Investigations were also carried out into the effectiveness of the CMS unit at part loads, to represent what would be encountered when a vehicle is being operated below its maximum capacity. The tests were conducted by applying the fuel rack settings necessary at each 250 RPM data point, to attain half the maximum torque figures recorded during the full load, maximum fuel delivery tests. Figure 5-25 shows the EGT temperatures measured for the Ford R2 test engine’s four cylinders with four good injectors at half load.

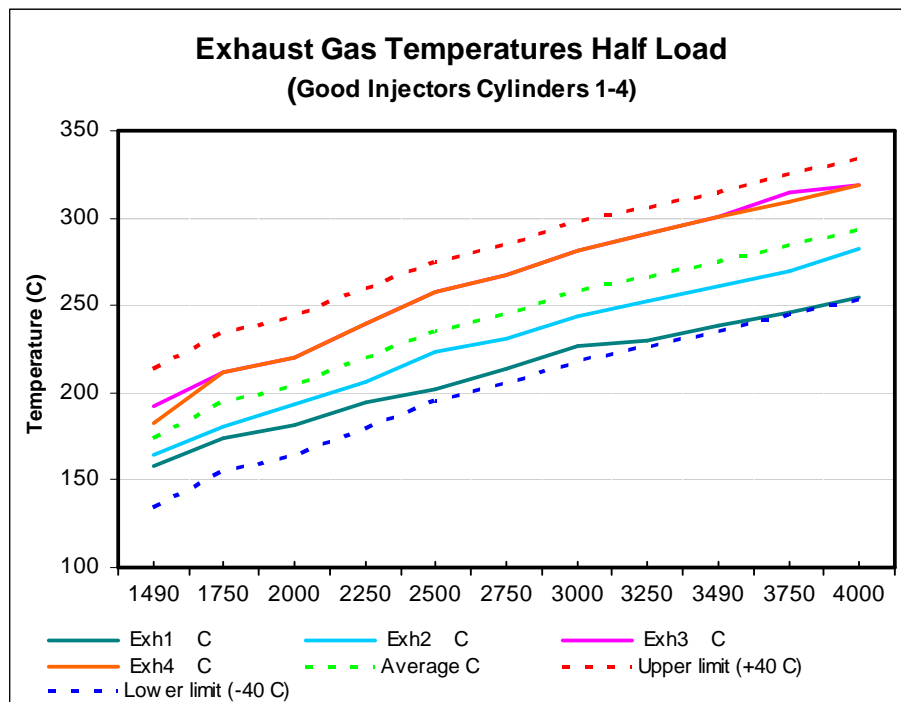


Figure 5-25: Graphic representation of CMS output values for properly functioning injectors at partial load

Again, the $\pm 40^{\circ}\text{C}$ “envelope” is applied about the calculated average to the graph to represent the tolerance band applied by the CMS prototype. It can be

seen that all the cylinder exhaust gas temperatures fall within this tolerance band meaning that the CMS unit will not raise an alarm condition at partial loads.

The experiment was then repeated with the badly scratched injector tip used in the previously discussed tests, inserted into cylinder number 3. The results are depicted in Figure 5-26.

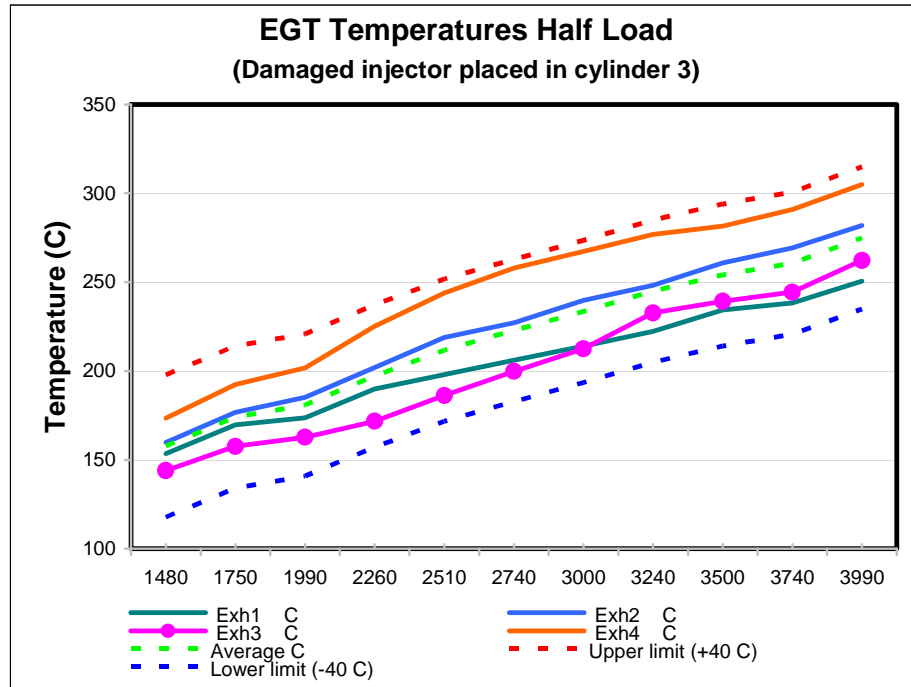


Figure 5-26: Graphic representation of CMS output values for damaged injector in cylinder number 3 at partial load

It is evident that despite the visible drop in EGT for cylinder number 3 when comparing Figure 5-26 to Figure 5-25 the cylinder EGT does not fall below the lower temperature limit setting in the CMS unit.

5.3.2.1 Discussion

For partial loads the CMS unit is not effective in detecting injector malfunction, as the drop in temperature in the offending cylinder is not great enough to fall outside the tolerance band setup in the CMS unit to detect combustion abnormalities at full loads. In order to detect an injector

malfunction at partial loads, the tolerance band would have to be set tighter, but this would potentially result in false alarms at maximum load conditions since this setting is fixed for all loads.

5.3.3 Results for engine rundown

An investigation was also carried out into what happens within the test engine once it is released from load and allowed to ‘run-down’ to idle. This was conducted in an attempt to simulate what would happen under normal vehicle operating conditions when an operator is slowing a vehicle down to a stop. The results are presented in Figure 5-27.

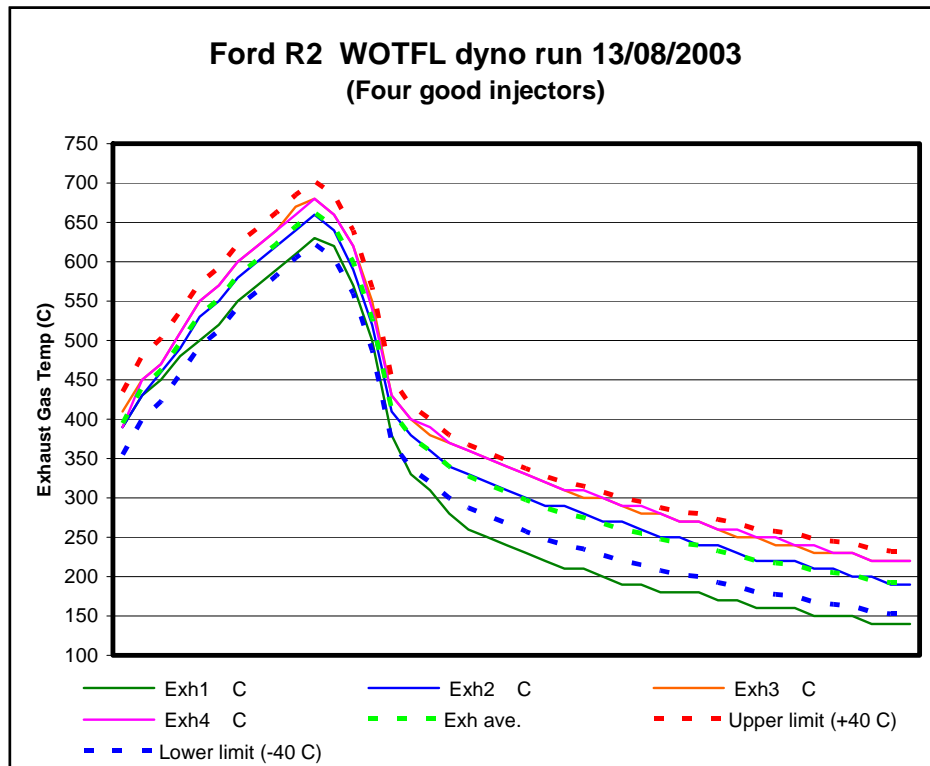


Figure 5-27: EGT results as engine cools down after full load run

The graph represents the engine being loaded to full load and maximum engine speed and then being released from that load and being left to idle for a few minutes. It can be seen that, while under load, all the cylinder exhaust gas

temperatures remain within the preset tolerance band of $\pm 40^{\circ}\text{C}$. Cylinder number 1 however cools down significantly faster than the other cylinders under no load, idle conditions. This results in a false alarm condition of the CMS unit

5.3.3.1 Discussion

The significant deviation in EGT of cylinder number 1 when compared to the other cylinders on ‘run-down’ to idle, may be explained by its proximity to the water pump outlet. It would again, appear that cylinder number 1 benefits the most from coolant flow from the water pump, resulting in its combustion chamber cooling down the quickest. Thus cylinder 1 produces the lowest EGT readings until all the cylinders have stabilised, once more to a common temperature.

A future consideration may be to incorporate the capacity for the CMS unit to store the history of individual cylinder EGTs. This may then also be used in relation to the average calculation conducted by the CMS unit to further fine tune the ability of the unit to detect combustion anomalies and prevent false alarms.

With the limited budget and time scale it was decided not to pursue this avenue further at this stage.

-

6.0 CHAPTER VI – CONCLUSION

6.1 Detecting Combustion Abnormalities within a Diesel Engine

The first goal of this study was to develop a simple, practical method to detect combustion abnormalities within the diesel engine. The practice of monitoring individual cylinder exhaust gas temperatures (EGTs) proved to be an effective way of determining whether potentially destructive combustion abnormalities were taking place within the diesel engine.

By recording these temperatures at certain stages during the engine's operation, taking their average, and comparing each one to this average it is also possible to isolate the location of the combustion abnormality.

This method can practically be implemented on a wide range of diesel engines, particularly as a number of these engines are available, factory fitted, with individual thermocouples for monitoring the exhaust port temperatures. In the absence of this, it is a relatively simple task to drill small holes in the exhaust manifold of an engine and mount thermocouples as close to the exhaust ports as possible.

This method proved to be most effective at full loads and maximum fuel delivery where combustion temperatures are highest and the effects of poor combustion are most noticeable and potentially damaging. The method's accuracy in locating the location of the injector malfunction also increases as the number of cylinders being monitored increases.

6.2 CMS System

The second goal was to develop a small, portable electronic device that makes use of the monitoring technique developed and provides a visual and audible alarm to notify a vehicle operator or technician of a combustion fault within a diesel engine.

A Combustion Monitoring System (CMS) prototype was developed and tested on a small naturally aspirated engine at the University of Pretoria's engine testing facilities. The prototype met its primary goal of detecting simulated combustion abnormalities under a variety of test conditions. Under these conditions, the system proved to be most effective under maximum load conditions with the accuracy of detection increasing with the number of cylinders being monitored.

6.3 System Effectiveness and Limitations

The greatest detractor of a system like this would be unnecessary false alarms. This would be annoying and disruptive to production in an earthmoving or on-road application. It is vital that the installation of non-factory fitted thermocouples be carried out with care to ensure that each sensor is placed as close to the exhaust valve as physically possible and protrudes into the same core exhaust gas flow in each manifold 'out-pipe'.

Setting up the thermocouples so that they all measure similar exhaust gas temperatures is a matter of running the engine a number of times under full load and adjusting the depth to which thermocouples are inserted until similar readings can be acquired from all of the cylinders being measured under full load condition.

This system is ideally suited to engines that have thermocouples factory fitted to the cylinder head exhaust ports, such as the Caterpillar 3512 series engines. This eliminates the potential complications involved with physical space constraints around the exhaust manifold and ensures homogeneous combustion temperature measurement.

Test results indicate that the CMS unit needs to monitor a minimum of three cylinders to provide any type of effective warning. The accuracy with which the CMS system detects a failing injector increases as the number of cylinders being monitored increases. This can be attributed to the statistical nature of the monitoring method. It stands to reason that a greater number of injectors functioning correctly would 'pull up' the calculated average temperature value, causing the offending injector to more readily fall outside the set tolerance band.

As such, monitoring a greater number of cylinders would also increase the CMS unit's ability to detect multiple failing injectors

The effectiveness of the CMS unit is limited to the upper load regions of an engine where exhaust gas temperatures are at their most extreme and any breakdown in combustion is most potentially destructive. This is due to the fact that testing conducted during this study has shown that a cylinder with a malfunctioning injector produces EGT readings that deviate most from the properly functioning ones under full load conditions. Since the CMS prototype unit's tolerance band is fixed for the different load and engine speed conditions during normal engine operation, this may hamper the device's ability to detect a combustion malfunction when the engine is being operated in the lower load and speed regions. A future version of the CMS unit would benefit from added intelligence that would allow it to adjust the tolerance band according to engine speed and/or load. This would however require added sensors to measure engine speed and load.

The Ford R2 engine showed a tendency to cool down the cylinder closest to the water pump faster than the other cylinders. The cooling down of the combustion gases on this cylinder was also much more rapid than on the other cylinders when load was removed from the engine. This caused the CMS unit to go into an alarm condition as described in preceding texts. Due to the large variety of diesel engine configurations it is difficult to predict how the combustion gas temperatures of different engines will behave under operational conditions. This potential pitfall may necessitate incorporating some form of intelligence into a future version of the CMS unit to allow it to stop monitoring when the operator is not accelerating or the engine is not under load.

6.4 Potential Applications

It is envisaged that the monitoring techniques applied in developing the CMS unit may eventually be incorporated into the powerful processing abilities of the modern diesel Engine Control Unit (ECU). These units already monitor a myriad

of different engine parameters and it seems a logical step that, with modern injection systems becoming ever more sensitive to dirt and poor fuel, this parameter be incorporated also.

Incorporating the CMS system into the engine ECU would give the system the computing power necessary for it to statistically calculate the standard deviation temperature limits that would encompass normal injector operation. This would in essence allow the system to ‘learn’ at which limits to set the alarm ‘envelope’. Coupled to the multiple sensors already feeding into the modern engine ECU, it is envisaged that the system would accurately be able to detect combustion anomalies due to injector malfunction for the entire speed and load range of the engine.

In its current form the CMS prototype is a useful tool in sensing combustion related malfunctions within a diesel engine and preventing damage from occurring.

-



ANNEXURE A

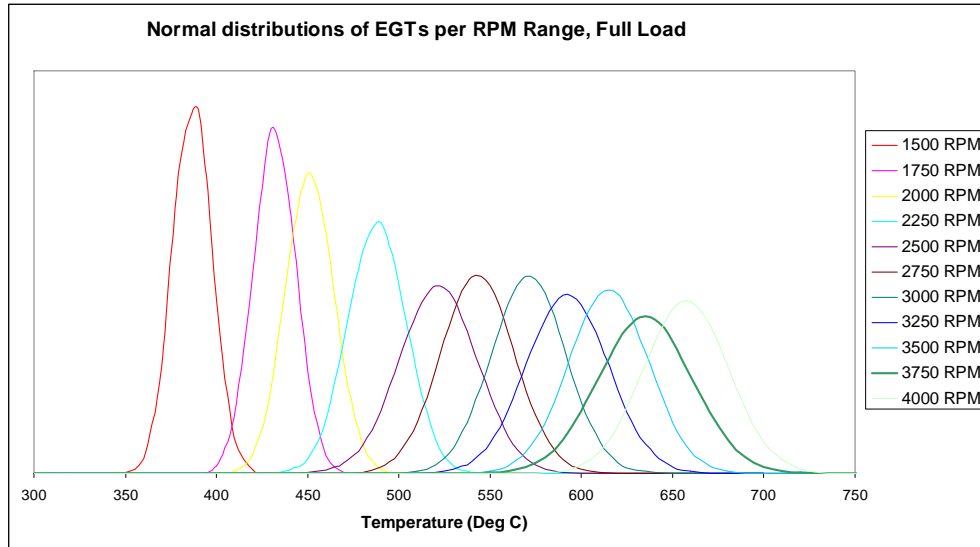


Figure 6-1: Normal distributions at full throttle, throughout RPM range

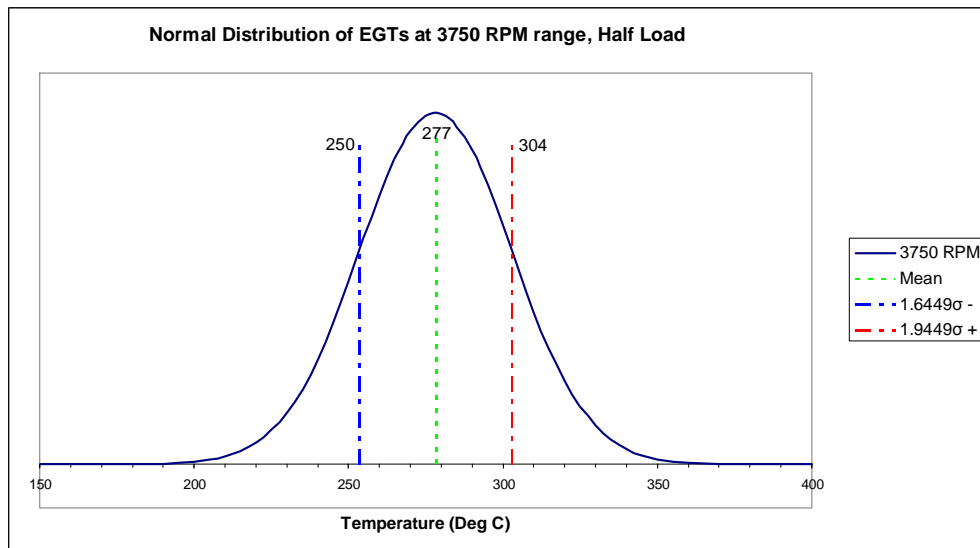


Figure 6-2: Normal distribution at half throttle @ 3 750 RPM

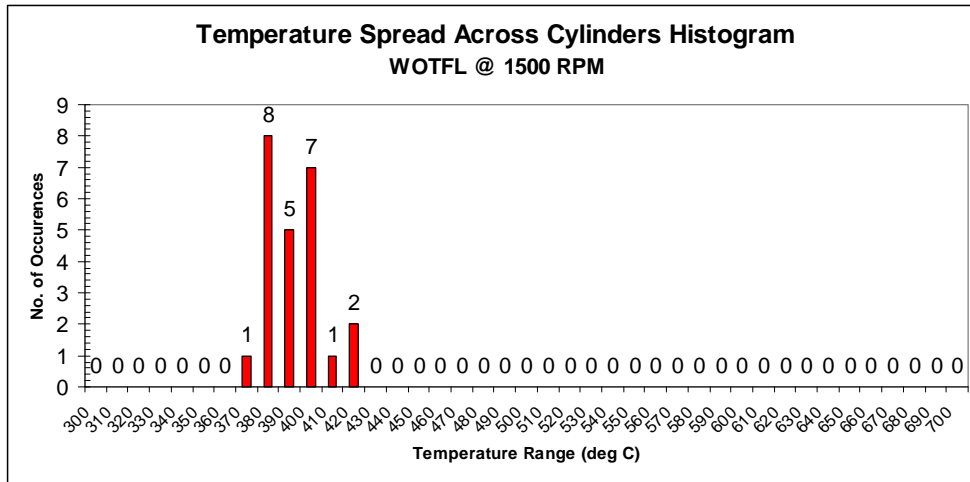


Figure 6-3: Histogram of measured temperature range distribution across all four cylinders for properly functioning injectors at 1500 RPM

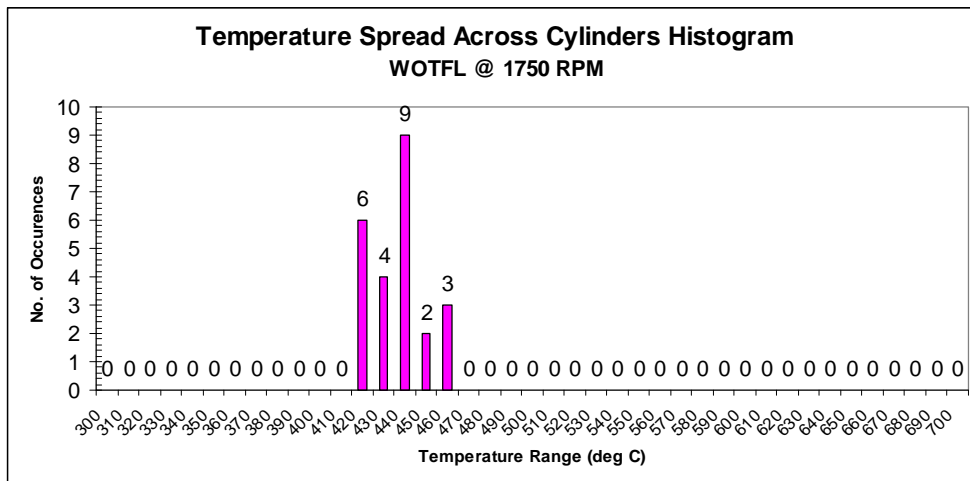


Figure 6-4: Histogram of measured temperature range distribution across all four cylinders for properly functioning injectors at 1750 RPM

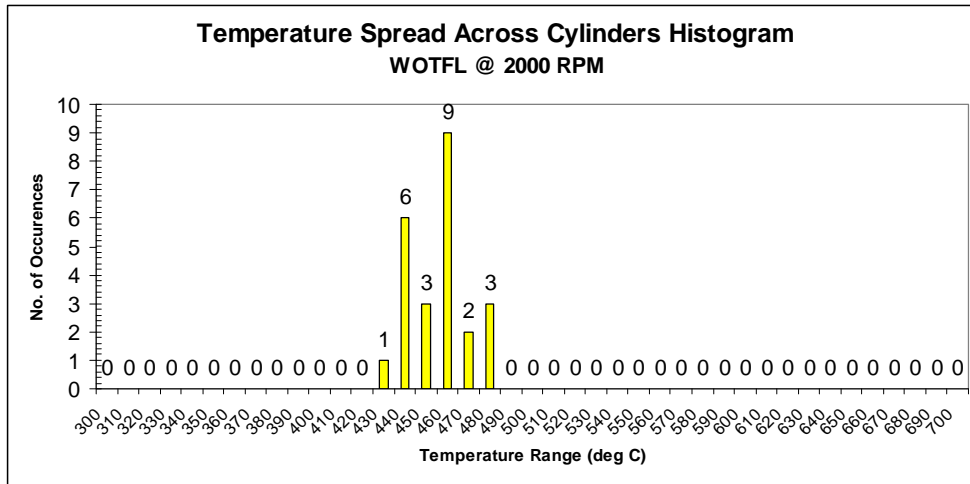


Figure 6-5: Histogram of measured temperature range distribution across all four cylinders for properly functioning injectors at 2000 RPM

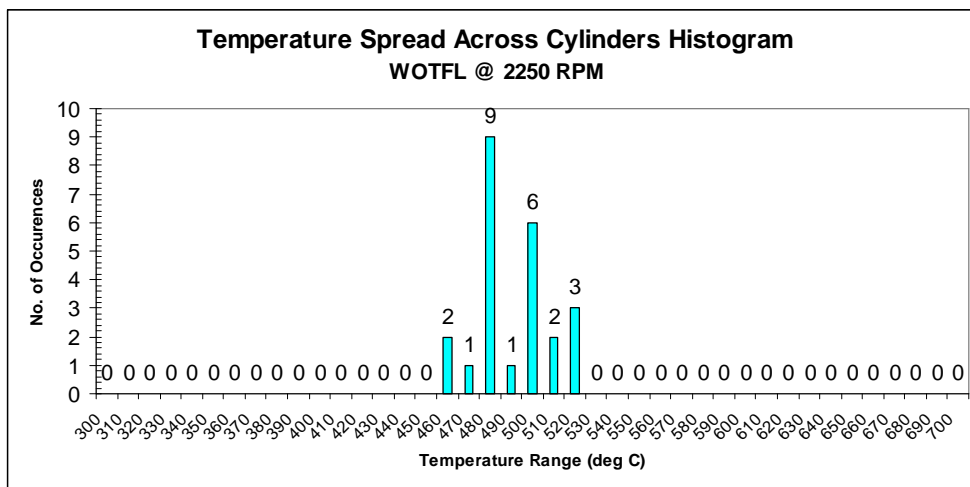


Figure 6-6: Histogram of measured temperature range distribution across all four cylinders for properly functioning injectors at 2250 RPM

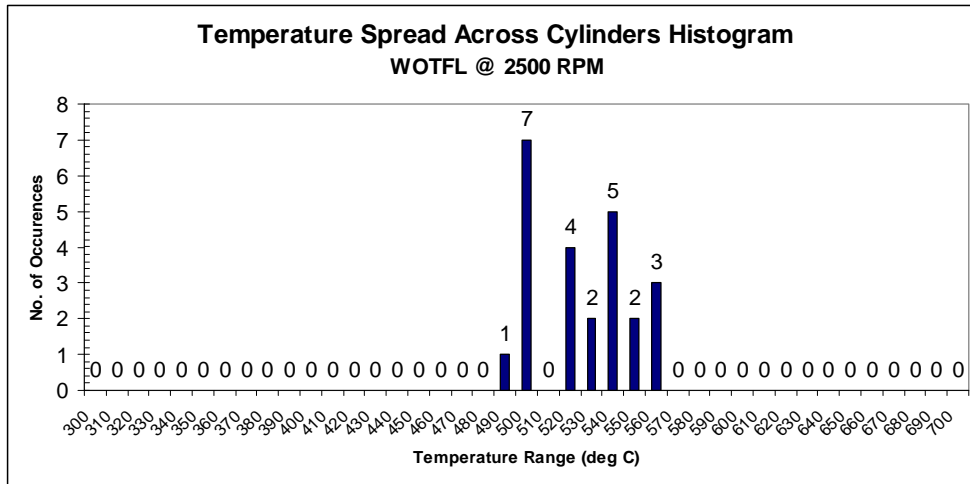


Figure 6-7: Histogram of measured temperature range distribution across all four cylinders for properly functioning injectors at 2500 RPM

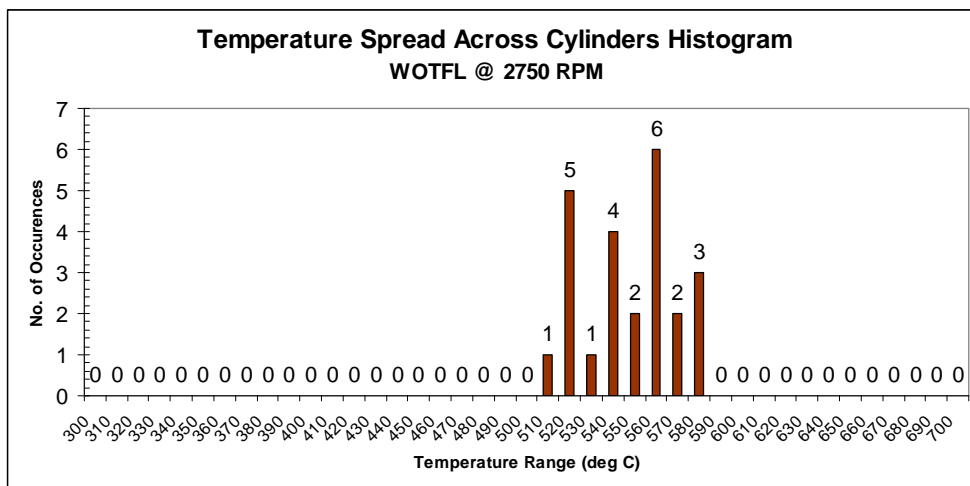


Figure 6-8: Histogram of measured temperature range distribution across all four cylinders for properly functioning injectors at 2750 RPM

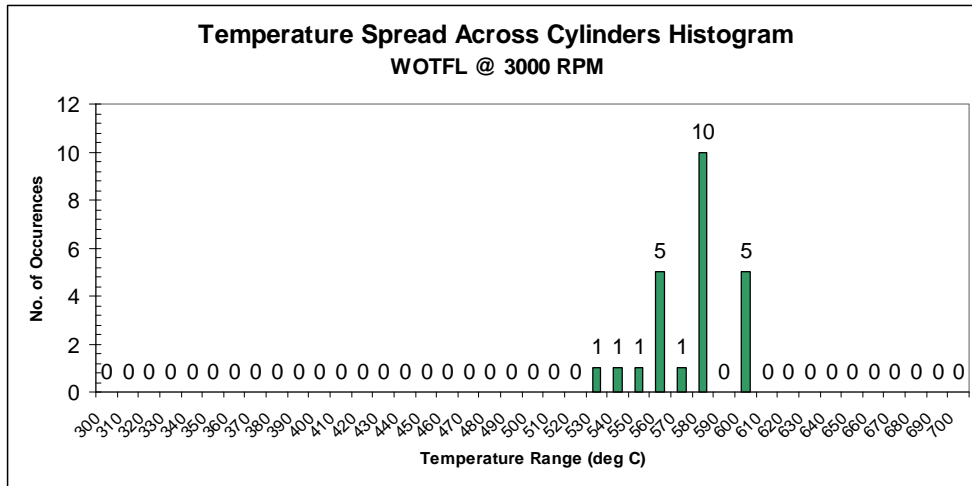


Figure 6-9: Histogram of measured temperature range distribution across all four cylinders for properly functioning injectors at 3000 RPM

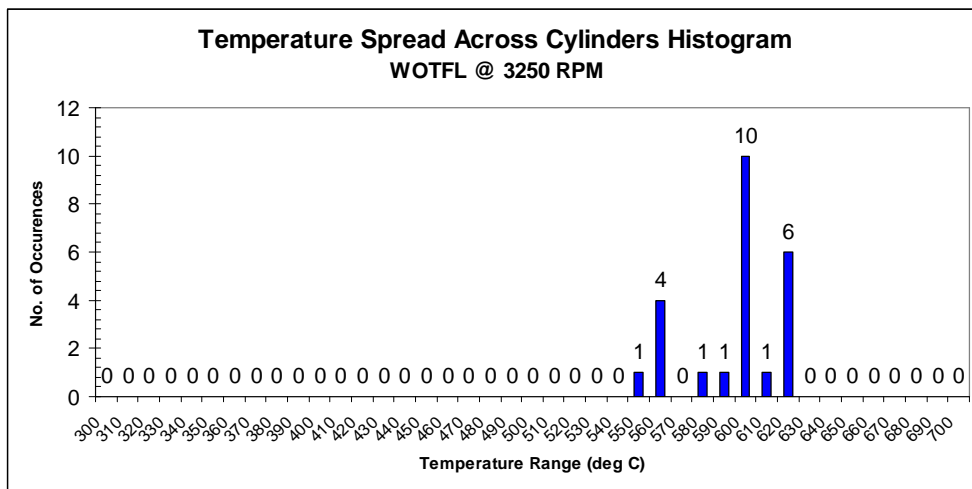


Figure 6-10: Histogram of measured temperature range distribution across all four cylinders for properly functioning injectors at 3250 RPM

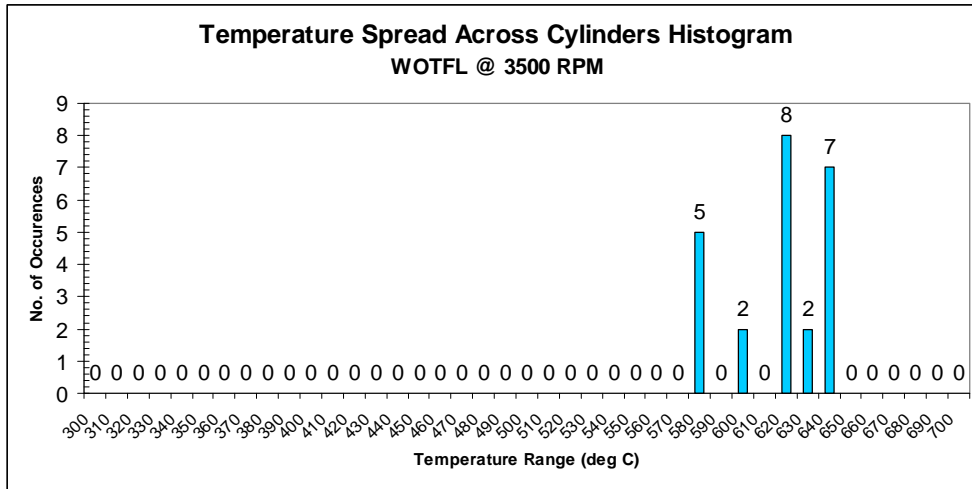


Figure 6-11: Histogram of measured temperature range distribution across all four cylinders for properly functioning injectors at 3500 RPM

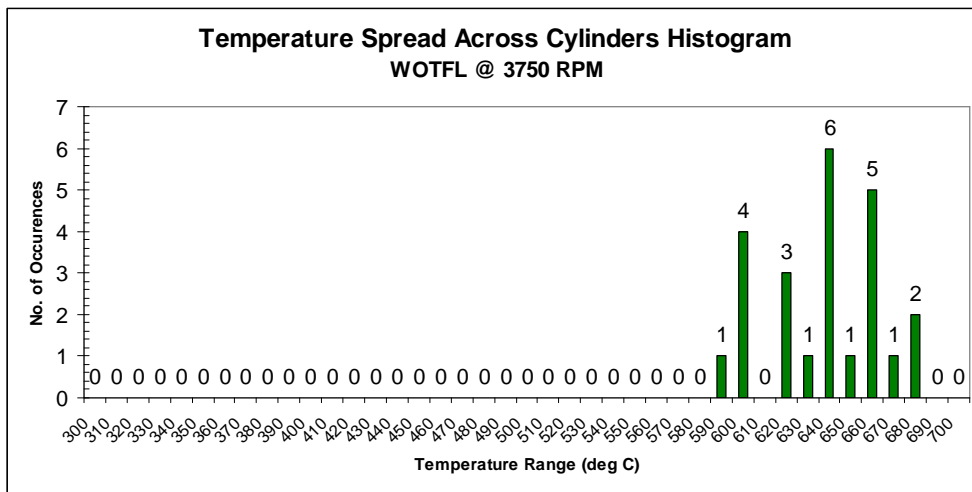


Figure 6-12: Histogram of measured temperature range distribution across all four cylinders for properly functioning injectors at 3750 RPM

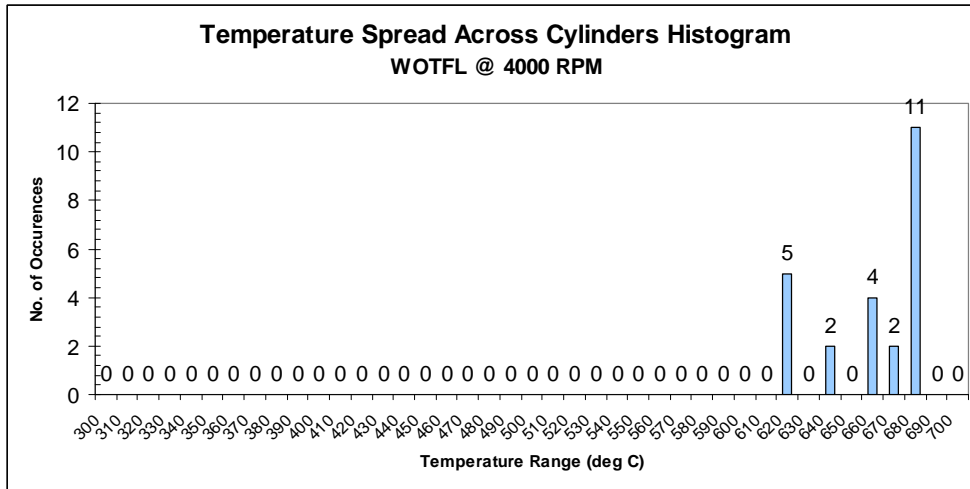
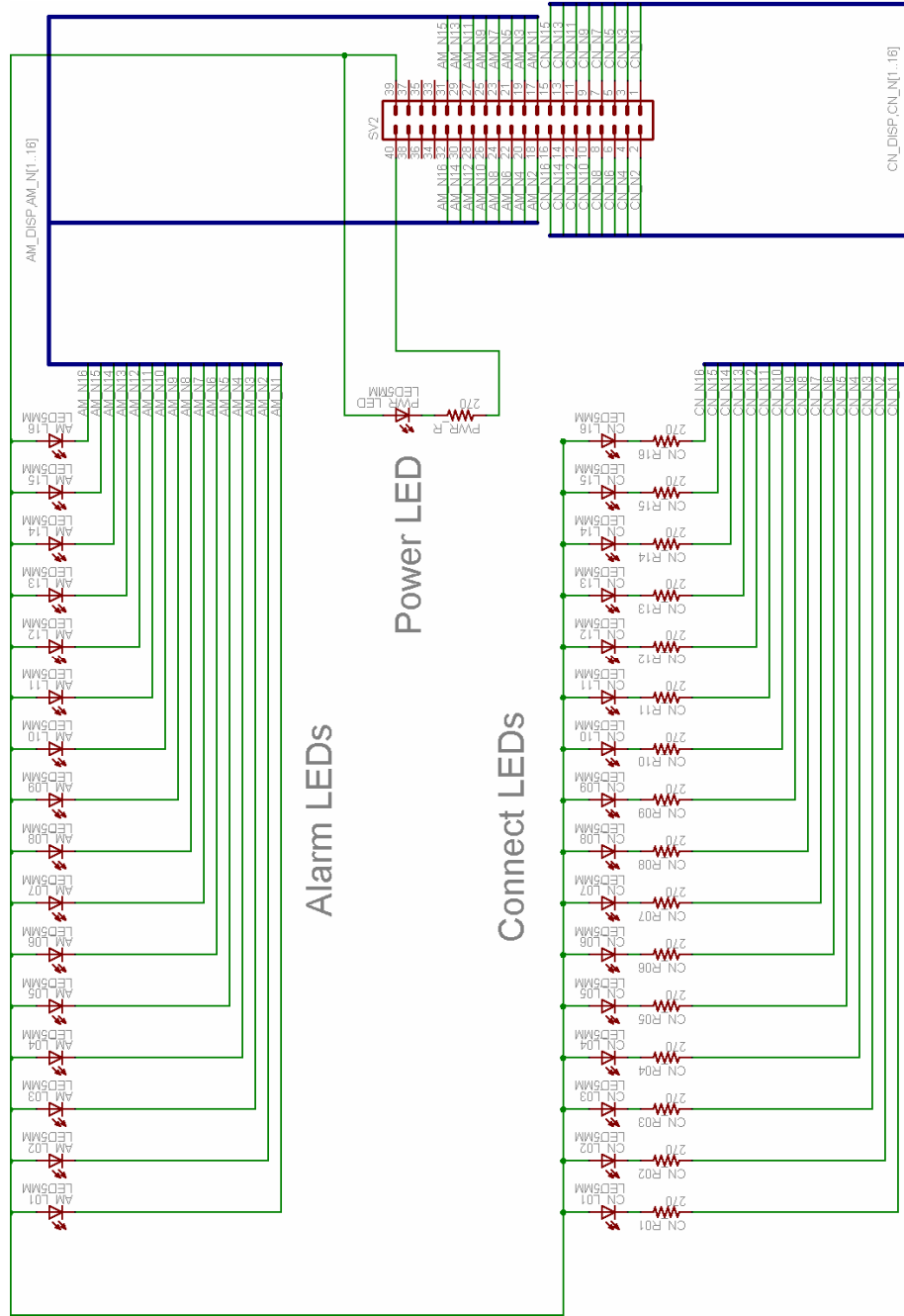


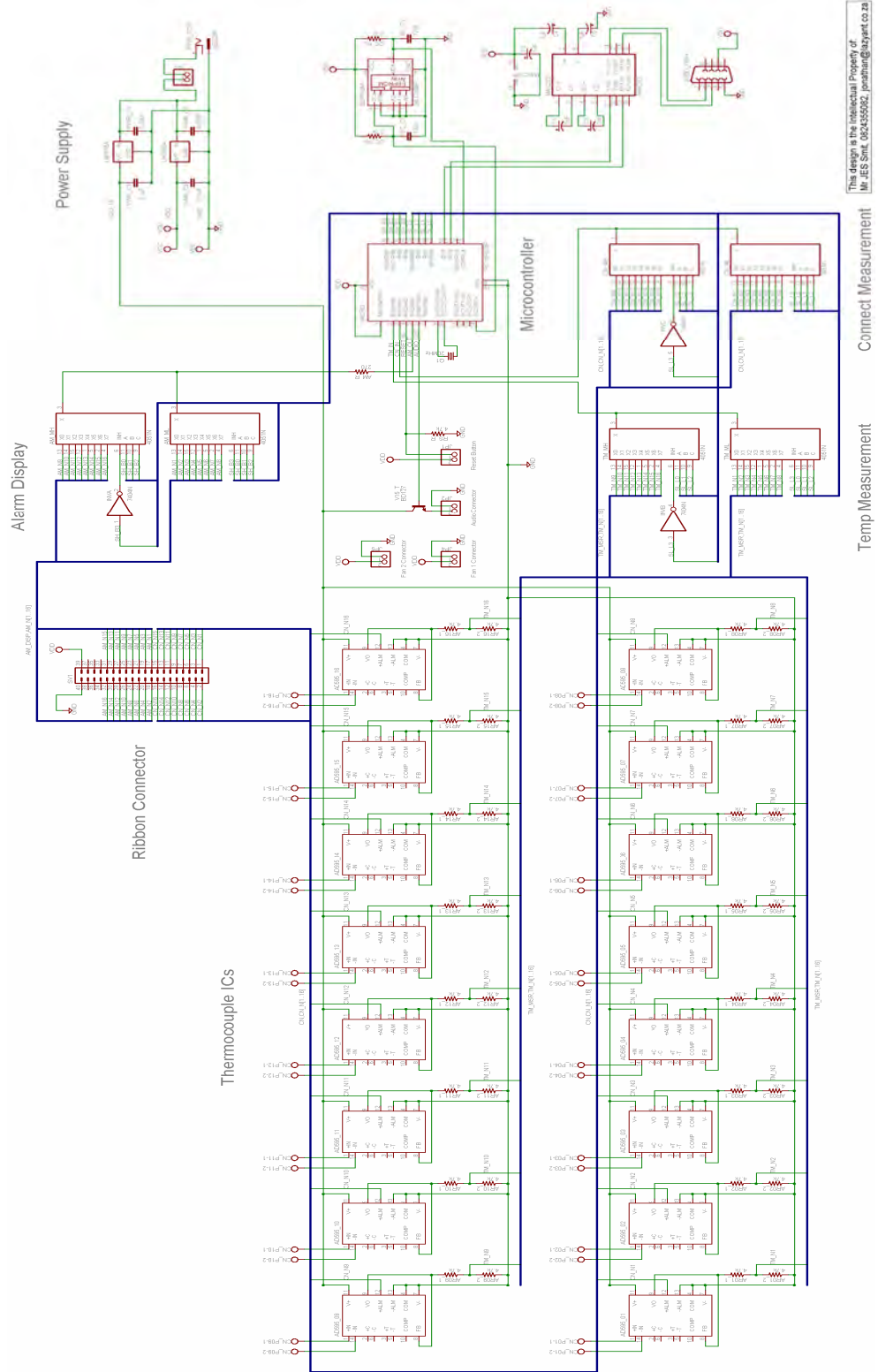
Figure 6-13: Histogram of measured temperature range distribution across all four cylinders for properly functioning injectors at 4000 RPM

ANNEXURE B



This design is the Intellectual Property of:
Mr. JES Smit, 0824355082, jonathan@lazyant.co.za

Figure 6-14: Display circuit board diagram



This design is the Intellectual Property of
Dr. JES Smut. 082455502. jsmut@abgnet.co.za

Figure 6-15: Functional circuit board diagram



ANNEXURE C

Engine Monitor User Manual

Date: 13 August 2003

Contents

1	Connection:.....	2
2	Communications Protocol:.....	5

1 Connection

1. Navigate to *Start -> Programs -> Accessories -> Communications -> HyperTerminal* to start **HyperTerminal**
2. **HyperTerminal** will start loading and display the following window:



Figure 1.1

3. Once **HyperTerminal** has finished loading the following window will open automatically:



Figure 1.2

4. Enter "*Engine Monitor*" into the *Name* field and click **OK**.
5. A window similar to the following will appear:



Figure 1.3

6. Select the COM port you are using to connect to the Engine Monitor by selecting it from the **Connect using:** drop down list and click **OK**. (It is assumed for the rest of this manual that COM1 was selected)
7. A window similar to the following will appear, the title of which indicates which COM port you are using:

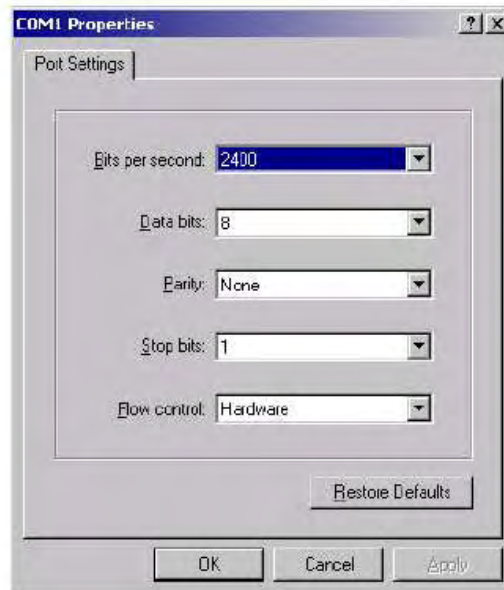


Figure 1.4

8. Using the various drop down boxes on the above window, ensure that the settings are as follows:
 - a. Bits per second - 115200
 - b. Data bits - 8
 - c. Parity - none
 - d. Stop Bits - 1
 - e. Flow control - none
9. Once you have done this, click **OK**.
10. The main HyperTerminal window will now become active.
11. Navigate to *File* -> *Save* to save the connection settings.
12. Navigate to *File* -> *Exit*.
13. If the following window appears, click on the **Yes** button.

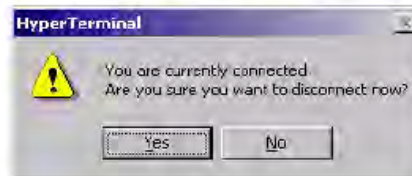


Figure 1.5

14. The settings to connect to the Engine Monitor are now in place and can be accessed without the preceding sequence by navigating to:
Start -> *Programs* -> *Accessories* -> *Communications* -> *HyperTerminal* -> *Engine Monitor.ht*



2 Communications Protocol

The engine monitor conforms to a fairly simple communications protocol described below. All commands are executed by simple typing them in, in the **HyperTerminal** window once connected to the Engine Monitor.

All commands are case insensitive and feedback will be given to the user should the command be successful or not.

Command	Description
V	Displays the current settings of the engine monitor (values).
Sxx	Changes the sample time, where <i>xx</i> is the time between samples given in seconds.
Txx	Changes the tolerance of the Engine Monitor to <i>xx</i> , where <i>xx</i> is the new tolerance value given in degrees. (Note: The value is automatically converted to a multiple of 4 by the monitor)
Pxx	Changes the number of samples for which an alarm condition must persist before it is registered as an actual alarm. <i>xx</i> represents the number of samples.
Oxx	Changes the preference to have the temperature values output as they are read or not, where <i>xx</i> is either <i>00</i> (to disable to output) or <i>01</i> (to enable the output)
Bxxyy	Changes the calibration settings for a thermocouple where <i>xx</i> represents the number of the thermocouple (from 01 to 16) to change, and <i>yy</i> indicates the calibration value. The calibration value is the number to be added to the temperature as displayed by the monitor (ie. it is the degree value to compensate by, divided by 4) to ensure it displays the correct value. eg. to set Thermocouple 01 to read 16 degrees higher than it is, enter: <i>b0104</i>
C	Development: Display which thermocouples are currently connected and which are not (000 = disconnected, 001 = connected)
R	Development: Display the persistence values of all the thermocouples.
A	Development: Display the alarm status of all the thermocouples.
L	Not Yet Implemented: List values stored in external EEPROM

Table 2.1

LIST OF SOURCES QUOTED

- ABRAHAM, R. 2001. Dirt in Diesel. FleetWatch Online.
<http://www.fleetwatch.co.za/supplements/SADiesel/DieselDirtS.htm>, last
referenced 24/02/2001
- BECKWITH, T.G., MARANGONI, R.D., LIENHARD, J.H. 1995. Mechanical
Measurements. 5th Edition, Massachusetts, Addison-Wesley
- BUSCH, R. 2005. Advanced Diesel Common Rail Injection Systems For Future
Emissions Legislation. 10th Diesel Emission Reduction Conference, Robert
Bosch GmbH, [http://www.bosch.co.za/content/language1/Automotive/pdf/
-934584-40-3.pdf](http://www.bosch.co.za/content/language1/Automotive/pdf/-934584-40-3.pdf), last referenced 27/01/2008
- CATERPILLAR INC, 2002. E173 High Exhaust Temperature Warning. SIS
Troubleshooting, Media Number RENR1310-01
- CHEMTRAC SYSTEMS, 2004. Online Catalogue. Chemtrac PC 2400 PS
<http://www.modcon.co.il/chemtrac.htm>
- DENSO, 2006. Diesel Common Rail Systems For Passenger Cars.
[http://www.globaldenso.com/TECHNOLOGY/tec-report/2001/
pdf/T2001_S12-13.pdf](http://www.globaldenso.com/TECHNOLOGY/tec-report/2001/pdf/T2001_S12-13.pdf), last referenced 26/01/2008
- DEPARTMENT OF MINERALS AND ENERGY REPUBLIC OF SOUTH
AFRICA, 4 November 2005. Regulations Regarding Petroleum Products
Specifications And Standards. Government Gazette No. 28191, Vol. 485,
SANS 342
- ESFAHANIAN, MOHSEN. 1994. Fluid-film lubrication with an application to
piston rings. Ph.D. Thesis Ohio State Univ., Columbus, OH.

- GOLDWIN, G., DE BOTTON G., RIVIN, B., SHER, E. 2004. Studying the Relationship between the Vibration Signature and the Combustion Process in Diesel Engines. SAE Technical Paper Series 2004-01-1786
- HEYWOOD, J.B. 1988. Internal Combustion Engine Fundamentals. Int. edition San Francisco: McGraw-Hill
- HUNT, J.D. 2004. "Particularly" Clean. April 2004 Edition, Article, Precision Cleaning Magazine, Columbus, OH.
- KAR, K., ROBERTS, S., STONE, R., OLDFIELD, M., FRENCH, B. 2004. Instantaneous Exhaust Temperature Measurements Using Thermocouple Compensation Techniques. SAE Technical Paper Series 2004-01-1418
- O'CONNELL, M., HALLER, C. 2002. Diesel Engine Condition Based Maintenance. Article, Maintenance Engineering Research, University of Manchester, United Kingdom
- ROTH, K.J., SOBIESIAK, A., ROBERTSON, L., YATES, S. 2002. In-Cylinder Pressure Measurements with Optical Fibre and Piezoelectric Pressure Transducers. SAE Technical Paper Series 2002-01-0745
- SKF INTERNATIONAL.2007. SKF Evolution Online. SKF Article <http://www.evolution.skf.com/zino.aspx?articleID=14959>, last referenced 12/02/2007
- SOUTH AFRICAN NATIONAL STANDARD. SANS 342:2006. Automotive Diesel Fuel. Edition 4. ISBN 0-626-18752-4
- SPIKES, H.A., OLVAR, A.V. 2005. Basics of Mixed Lubrication. Article, Tribology Section, Imperial College of Science, Technology & Medicine, London, United Kingdom

STURGESS, S. 2003 Trucking's Dirty Little Secret. October 2003 Edition,
Article: Heavy Duty Trucking Magazine, South Africa

SUPERFLOW CORPORATION. 1993. SF-901 Instruction Manual. 1st Edition,
Tejon, Colorado Springs, USA

VON WIELLIGH, A.J. 1998. A.J. Von Wielligh & Associates. Failure Reports
and papers delivered at various conferences, University of Pretoria, South
Africa

WALDHAUER, B., SHILLING, U., SCHNAIBEL, S., SZOPA, J. 2004. Piston
Damages, Recognising and Rectifying. 1st Edition, Heilbron, Germany:
MSI Motor Service International

YATES, A. D. B., RABE, T. 2007. The Effect of Diesel Density, Injection
Technology and External Variables on the Acceleration Performance of
Modern Passenger Cars. SAE Technical Paper Series 2007-01-0063

ABSTRACT

INVESTIGATION INTO A SYSTEM THAT CAN DETECT IMPROPER COMBUSTION IN A DIESEL ENGINE BEFORE SIGNIFICANT DAMAGE CAN OCCUR

by

Theo Lawrence Wilcocks

Study leaders: Mr AJ Von Wielligh

& Prof NDL Burger

Degree: Master of Engineering

An alarming number of compression ignition (CI) engines have been failing due to combustion irregularities within their combustion chambers. The need has thus arisen to develop a condition based maintenance technique to warn the machine operator of the start of injection equipment malfunction, hence preventing engine damage and subsequent costly rebuilds or replacements. Laboratory exhaust gas temperature (EGT) testing was conducted, using a Ford R2, 2200 cm³ four cylinder, normally aspirated, diesel engine that was acquired and mounted on the University's SF-901 engine dynamometer. Thermocouples mounted in the exhaust manifold revealed that the effect of an injector, with a tip that has been scratched to such an extent that it seizes within its barrel, is measurable. The associated cylinder EGTs fell below the 'normal operation envelope' thus providing an indication of incomplete combustion. It was also proven that the effects of diluting diesel with illuminating paraffin could be successfully measured.

Two of the Caterpillar range of large, commercial diesel engines, a Cat 3412 and 3512, were made available to the student for monitoring EGTs at the Barloworld Equipment engine test facility in Isando. As a genuine injection equipment malfunction could not be induced on these newly rebuilt customer units, the tests were used to determine the deviation in individual cylinder EGTs during normal machine operation for these engines. From these tests it was concluded that a good starting value for large commercial diesel engines appeared to be a value of 40°C above or below the calculated average value of the cylinder EGTs. This

value appears to hold for engines with conventional MEUI systems but cannot be applied with the same amount of certainty to engines with individual injector control such as the Caterpillar HEUI system.

The second goal was to develop a small, portable electronic device that makes use of the monitoring technique developed and provides a visual and audible alarm to notify a vehicle operator or technician of a combustion fault within a diesel engine. Such a device, named Combustion Monitoring System (CMS) was constructed and successfully tested on the University test bench engine.

It is envisaged that the monitoring techniques applied in developing the CMS unit may eventually be incorporated into the powerful processing abilities of the modern diesel Engine Control Unit (ECU). These units already monitor a myriad of different engine parameters and it seems a logical step that, with modern injection systems becoming ever more sensitive to dirt and poor fuel, this parameter be incorporated also.